



Cite this: *Chem. Soc. Rev.*, 2025, 54, 6412

## Intracellular aggregation of exogenous molecules for biomedical applications

Da-Yong Hou, <sup>†abc</sup> Haoran Wang, <sup>†\*d</sup> Yue-Ze Wang, <sup>ac</sup>  
 Dong-Bing Cheng, <sup>\*e</sup> Ben Zhong Tang <sup>\*cf</sup> and Wanhai Xu <sup>\*a</sup>

Most biomolecules play important roles in aggregated states, as exemplified by proteins and DNA. Inspired by biomacromolecule formation, the exploration of intracellular bioactive materials derived from exogenous molecules has drawn considerable interest. In cells, exogenous molecules may assemble into macromolecules and supermolecules and thus help monitor disease processes or regulate the cell fate, which provides a new approach to disease treatment. The diverse cellular microenvironments (reductive in the cytoplasm, oxidative in mitochondria, and acidic in lysosomes) can be exploited to achieve controllable and precise intracellular aggregation using intelligent molecular design. Moreover, the intracellular polymerization and organelle targeting-triggered aggregation of exogenous molecules can be used for cell fate manipulation. This review deals with the intracellular aggregation of exogenous molecules activated by intracellular stimuli, exogenous stimuli, and organelle targeting and discusses the related molecular mechanisms and biomedical applications, providing guidance for the design of bioactive materials and discovery of theranostic agents.

Received 1st March 2025

DOI: 10.1039/d5cs00141b

[rsc.li/chem-soc-rev](https://rsc.li/chem-soc-rev)

### 1. Introduction

Cells, the basic structural and functional units of life, are heavily reliant on the intricate aggregation of biomolecules within their boundaries to sustain diverse life functions<sup>1</sup> ranging from growth and reproduction to metabolism and communication. The modulation of cell behavior and fate by endogenous biomolecules, such as polysaccharides,<sup>2–5</sup> proteins,<sup>6,7</sup> and nucleic acids,<sup>8–11</sup> has been extensively researched. Given the importance of these biomolecules for regulating cellular processes and determining overall cell health and function,<sup>12</sup> considerable attention has been drawn to their roles in cancer treatment, antiviral therapy, and degenerative neurological disorder management.<sup>13</sup>

The precise control of cellular behavior through the intracellular clustering of exogenous molecules has emerged as a focal point of biomedical research.<sup>14</sup> By introducing foreign molecules into cells and manipulating their aggregation patterns, one can exert fine-tuned control over cellular processes<sup>15</sup> and revolutionize the treatment of diseases and disorders by enabling more targeted and effective interventions.<sup>16</sup> The realization of controllable *in situ* aggregation of biocompatible exogenous molecules inside cells holds promise for creating novel biomaterials and pharmaceuticals specifically designed to interact with and modify cellular processes.<sup>17</sup> Thus, this approach has the potential to advance biomaterial and pharmaceutical sciences and promote the development of new treatments for diverse medical conditions.<sup>18–20</sup>

However, the implementation of the above strategy is hindered by the diversified characteristics of organisms and complexity of the intracellular environment,<sup>21</sup> as well as other constraints.<sup>22,23</sup> The exogenous molecules must be biocompatible, *i.e.*, harmoniously coexist with the cellular machinery without eliciting adverse reactions.<sup>24</sup> Biological barriers, such as cell membranes and intracellular organelles, present physical and chemical obstacles that must be navigated. Furthermore, these molecules should maintain their bioactivity within the cellular environment, as function loss can compromise the intended effects. The conditions causing aggregation are highly specific and must be carefully controlled.<sup>25</sup> Intracellular conditions, including pH, temperature, and the presence of various biomolecules, can profoundly influence the aggregation process.<sup>26</sup>

<sup>a</sup> NHC Key Laboratory of Molecular Probe and Targeted Theranostics, Heilongjiang Key Laboratory of Scientific Research in Urology, Harbin Medical University, Harbin 150001, China. E-mail: xuwanhai@hrbmu.edu.cn

<sup>b</sup> Department of PET-CT/MRI, Harbin Medical University Cancer Hospital, Harbin 150001, China

<sup>c</sup> School of Science and Engineering, Shenzhen Institute of Aggregate Science and Technology, The Chinese University of Hong Kong, Shenzhen (CUHK-Shenzhen), Shenzhen, Guangdong 518172, China. E-mail: tangbenz@cuhk.edu.cn

<sup>d</sup> Faculty of Materials Science, Shenzhen MSU-BIT University, Shenzhen 518115, China. E-mail: wanghr@smbu.edu.cn

<sup>e</sup> School of Chemistry, Chemical Engineering & Life Science, Wuhan University of Technology, No. 122 Lushi Road, Wuhan 430070, China. E-mail: chengdb@whut.edu.cn

<sup>f</sup> Department of Chemistry, Hong Kong Branch of Chinese National Engineering Research Center for Tissue Restoration and Reconstruction, The Hong Kong University of Science and Technology, Hong Kong, China

<sup>†</sup> These authors contributed equally to this work.



Another critical factor is the interference due to intracellular reactive species,<sup>27</sup> including reactive oxygen species (ROS) and reactive nitrogen species, which can disrupt the aggregation process and lead to side reactions or inactive aggregate formation.

The folding of exogenous macromolecules within cells adds another layer of complexity.<sup>28,29</sup> The intricate three-dimensional structure of proteins and other macromolecules is essential for their functions, and achieving the correct fold *in vivo* is a formidable challenge.<sup>30</sup> Despite these challenges, intracellular aggregation has a broad range of applications in cancer therapy, bioimaging, tissue engineering, and other biomedical fields. By artificially regulating cells and tissues through the controlled aggregation of exogenous molecules within the cell, one can unlock new therapeutic strategies, imaging techniques, and tissue regeneration methods.<sup>31–33</sup> This cutting-edge field holds

great promise, motivating researchers to fully tap the potential of intracellular aggregation.<sup>34</sup>

This review deals with the intracellular aggregation of exogenous molecules due to external stimuli or alterations in the cellular microenvironment,<sup>35</sup> discussing the progress in this field and providing a multidisciplinary biomedical perspective (Fig. 1). We examine the related aggregation mechanisms, highlighting key findings, advancements, and limitations. These limitations encompass technical barriers, such as the difficulty in accurately measuring and visualizing aggregation processes at the nano-scale, as well as biological ones, including the dynamic nature of the cellular microenvironment and potential for aggregation to disrupt normal cellular functions.

To facilitate a clearer understanding of the content of this review, Table 1 provides a structured summary of currently reported



**Da-Yong Hou**

*Prof. Da-Yong Hou is an assistant professor at Harbin Medical University Cancer Hospital and deputy director of department of PET-CT/MRI. He got his PhD degree from Harbin Medical University & National Center for Nanoscience and Technology in 2024. His research interest mainly focuses on in vivo self-assembly based biomaterials for tumor diagnosis and treatment. He has published over 20 publications as the first (co-) and corresponding author in international journals including*

*Nat. Commun., Sci. Adv., J. Am. Chem. Soc., Angew. Chem., Int. Ed., Adv. Mater., Sci. Bull., Natl. Sci. Rev., ACS Nano, Biomaterials, and Nano Lett. with over 2000 citations.*



**Haoran Wang**

*Prof. Haoran Wang is currently an Associate Professor at Shenzhen MSU-BIT University. He received BS and PhD degrees from Jilin University in 2016 and 2021, respectively. Following his doctoral studies, he joined Prof. Ben Zhong Tang's group at The Hong Kong University of Science and Technology as a postdoctoral researcher. His research focuses on photochemistry, photophysics, application of aggregation-induced emission materials, and crystal photoactuation. He is member of China Science Writers Association. He has published over 20 publications as the first (co-) and corresponding author in international journals including*

*J. Am. Chem. Soc., Angew. Chem., Int. Ed., Chem. Nat. Commun., and CCS Chem., with over 1200 citations.*



**Yue-Ze Wang**

*Yue-Ze Wang received his BS and master's degree in clinical medicine and surgery from Harbin Medical University (HMU) in 2020 and 2023, respectively. Since then, he has continued his PhD in surgery in Harbin Medical University and co-trained in the Chinese University of Hong Kong (Shenzhen) from 2023 to now, during which he has been engaged in the application research of AIEgens in the diagnosis and treatment of urinary system tumors.*



**Dong-Bing Cheng**

*Prof. Dong-Bing Cheng is a professor at Wuhan University of Technology. He received his PhD degree from Wuhan University in 2015. Then, he worked as a postdoctoral fellow at the National Center for Nanoscience and Technology. His research interests mainly focus on adaptive assembly of medical polymer materials, in particular on the fields of self-assembled nanomaterials and targeted drug delivery system. He has published over 40 publications in international journals including*

*Nat. Commun., J. Am. Chem. Soc., Angew. Chem., Int. Ed., Adv. Mater., and Natl. Sci. Rev. with over 1800 citations.*



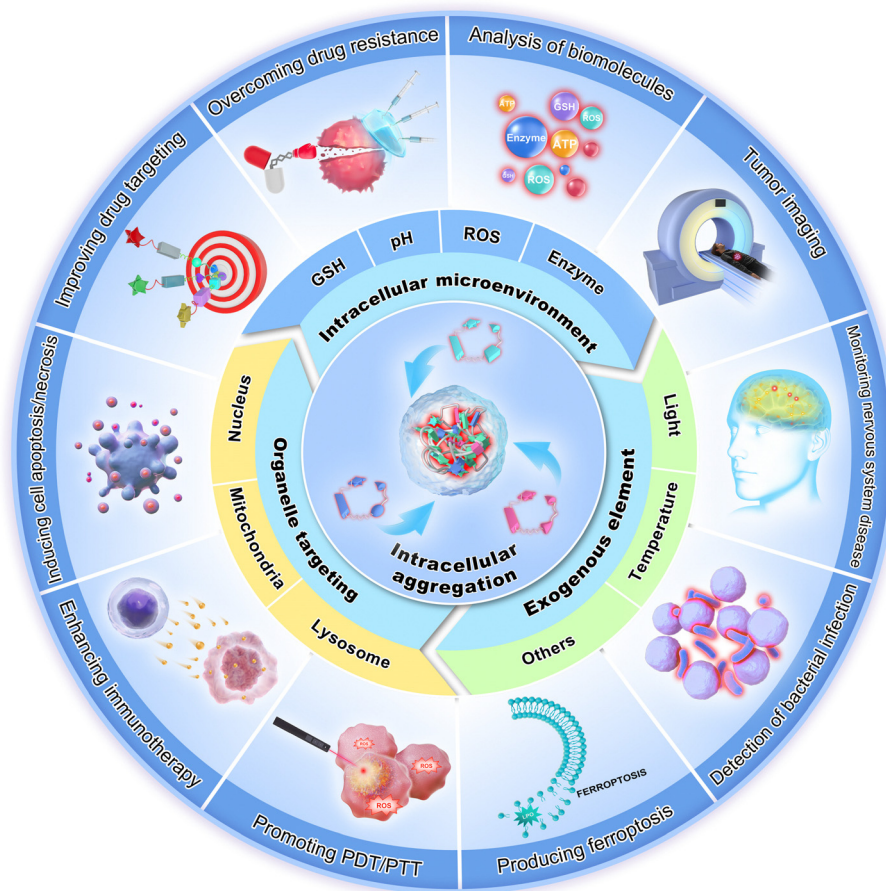


Fig. 1 Intracellular aggregation of exogenous molecules and its biomedical applications.

intracellular aggregation strategies for exogenous molecules. The strategies are systematically categorized based on three key dimensions: mechanism of aggregation (the underlying principles

governing molecular aggregation within cells), molecular design (the structural or chemical features engineered to induce aggregation), and biomedical application (the therapeutic, diagnostic, or



**Ben Zhong Tang**

*Prof. Ben Zhong Tang is currently a Presidential Chair Professor and Dean of School of Science and Engineering at The Chinese University of Hong Kong, Shenzhen (CHUK-Shenzhen). He received BS and PhD degrees from South China University of Technology and Kyoto University in 1982 and 1988, respectively. He was elected to the Chinese Academy of Sciences, Royal Society of Chemistry, World Academy of Sciences for the*

*Advancement of Science in Developing Countries, and Asia-Pacific Artificial Intelligence Association. His research interests include materials science, macromolecular chemistry, and biomedical theranostics. He has over 2000 publications, a citation counts exceeding 220 000, and an h-index of 207.*



**Wanhai Xu**

*Prof. Wanhai Xu is the President of 2nd Affiliated Hospital of Harbin Medical University, the vice president of Harbin Medical University and director of NHC Key Laboratory of Molecular Probe and Targeted Theranostics. His research focuses mainly on the exploration of the mechanisms of urological tumors and precision theranostics. He has published over 50 publications as the corresponding author in international journals including Nat. Commun.,*

*J. Am. Chem. Soc., Angew. Chem., Int. Ed., Adv. Mater., Sci. Bull., Biomaterials, Nano Lett., Bioact. Mater., Eur. J. Nucl. Med. Mol. Imaging, and Natl. Sci. Rev. with over 3000 citations.*



Table 1 Representative intracellular aggregation strategies of exogenous molecule

| Mechanism of aggregation       |   | Molecular design   | Biomedical application  |  |
|--------------------------------|---|--|---|--|
| Intracellular microenvironment | pH  | Schiff base  | Intracellular pH imaging <sup>36</sup>  |  |
|                                |   | Base-pairing DNA   | Cell behavior regulation <sup>37</sup>  |  |
|                                |   | pH-responsive peptide  | Inhibit autophagy <sup>38</sup>   |  |
|                                |   |  | Selective cell death <sup>39</sup>  |  |
|                                |   |  | Increase the anti-prion activity <sup>40</sup>  |  |
|                                |   | ROS  | Phenylboronate  | Monitoring intracellular structural change <sup>41</sup> |
|                                |   |  | Abundant periphery NH <sub>2</sub> groups   | Enhancing antigen presentation <sup>42</sup>             |
|                                |   |  | Liposome-encapsulated spiky nanoparticles   | Phototherapy applications <sup>43</sup>                  |
|                                |   |  | Protonation of CuPc-SO <sub>4</sub>   | Enhance sonodynamic therapy <sup>44</sup>                |
|                                |   |  | Mixed-charge nanoparticles  | Selective death of cancer cells <sup>45</sup>            |
|                                | GSH   | Oligonucleotides   | Chemo-photothermal synergetic therapy <sup>46</sup>                                     |  |
|                                |   | Thio-ketal bond <sup>47</sup>                                    | Selectively inducing apoptosis of cancer cells  |  |
|                                |   | Te-O oxidative polymers <sup>48</sup>                            |   |  |
|                                |   | Organotellurides <sup>49</sup>                                   |   |  |
|                                |   | Aniline dimer derivative   | Phototheranostics of tumor <sup>50</sup>  |  |
| Enzyme                         |   | Y-shaped diacetylene   | Inhibited tumor metastasis <sup>51</sup>  |  |
|                                |   | Thiolated tripeptide   | Intracellular artificial enzyme <sup>52</sup>   |  |
|                                |   | Selenoxide peptide   | Anti-inflammatory treatment <sup>53</sup>   |  |
|                                |   | Thiol-modified oligo ( <i>p</i> -phenylene vinylene)             | Enhancing drug efficacy <sup>54</sup>   |  |
|                                |   | Tz-conjugated assembly precursor                                 | Self-reporting prodrug activation <sup>55</sup>   |  |
|                                |   | GSH-responsive peptide   | Abolish liver tumor growth and metastasis <sup>56</sup>                                 |  |
|                                |   |  | MR imaging of caspase 3/7 <sup>57</sup>   |  |
|                                |   |  | High-efficacy cancer therapy <sup>58–60</sup>   |  |
|                                |   |  | Proteolysis targeting chimera <sup>61</sup>   |  |
|                                |   |  | Enhanced dual-modal imaging and photothermal therapy <sup>62</sup>                      |  |
|                                |   |  | Selective tumor ferroptosis and pyroptosis <sup>63</sup>                                |  |
|                                |   |  | MR contrast of tumor <sup>64</sup>  |  |
|                                |   |  | Self-inflicted apoptosis of cancer cells <sup>65</sup>                                  |  |
|                                |   |  | Enhanced chemotherapy <sup>66</sup>   |  |
|                                |   |  | Selectively enhancing radiosensitivity <sup>67</sup>                                    |  |
|                                |   |  | Overcome drug-resistant cancer cells <sup>68</sup>                                      |  |
|                                |   |  | Enhanced photoacoustic imaging <sup>69</sup>  |  |
|                                |   |  | Quantitative imaging <sup>70</sup>  |  |
|                                |   |  | Chemosensitization <sup>71</sup>  |  |
|                                |   |  | Cancer cell death <sup>72</sup>   |  |
| Exogenous element              | Light   | Protein kinase A (PKA)-responsive phosphorylated polymer         | Cancer immunotherapy <sup>73</sup>  |  |
|                                |   | Matrix metalloproteinase-7 (MMP-7)-responsive peptide derivative | Drug delivery and cancer imaging <sup>74</sup>  |  |
|                                |   | Tyrosinase-catalyzed peptide                                     | Imaging of protease activity <sup>75</sup>  |  |
|                                |   | Caspase-3-responsive peptide derivative                          | Bacterial infection detection <sup>76</sup>   |  |
|                                |   |  | MicroPET tumor imaging <sup>77</sup>  |  |
|                                | Temperature   | Gelatinase-responsive peptide derivative                         | Overcoming multidrug resistance (MDR) <sup>78</sup>                                     |  |
|                                |   | Furin-responsive peptide derivative                              | Sensitive detection and eradication of intracellular bacterial infections <sup>79</sup> |  |
|                                |   |  | Promote the tumor photodynamic therapy <sup>80</sup>                                    |  |
|                                |   | Caspase-1-responsive AIEgen-peptide conjugate                    | Mitochondrial activity modulation <sup>81</sup>   |  |
|                                |   |  | Selective identification and removal of senescent cells <sup>82</sup>                   |  |
| Other                          | Cathepsin B-responsive AIEgen-peptide conjugate       |  |   |  |
|                                | SIRT5-responsive peptide derivative                   |  |   |  |
|                                | β-Galactosidase (β-Gal)-responsive peptide derivative |  |   |  |
|                                |   |  |   |  |
|                                |   |  |   |  |
|                                | Light   | Photochromic arylazopyrazole                                     | Intertubular aggregation of microtubules <sup>83</sup>                                  |  |
|                                |   | Acrylic and methacrylic monomers <sup>84</sup>                   | Modulate cellular function and behaviour  |  |
|                                |   | Tyr-containing proteins <sup>85</sup>                            |   |  |
|                                |   | Photoactivatable prodrug   | Inhibits tumor growth and metastasis <sup>86</sup>                                      |  |
|                                |   | Poly(ethylene glycol) diacrylate                                 | Immunoengineering <sup>87</sup>   |  |
|                                | Temperature   | Poly( <i>N</i> -isopropylacrylamide) (PNIPAM) <sup>88–91</sup>   | Intracellular temperature sensing   |  |
|                                |   | Carbazole-based fluorescent organic nanomaterials <sup>92</sup>  |   |  |
|                                |   | Dispersed fluorescent nanodiamonds <sup>93</sup>                 |   |  |
|                                |   | Poly( <i>N</i> -vinylcaprolactam) (PNVCL) <sup>94</sup>          |   |  |
|                                |   | Polymer-peptide conjugates (PPCs)                                | Deep tumor therapy <sup>95</sup>  |  |
|                                |   | Monitoring tumor therapy <sup>96</sup>                           |   |  |
|                                |   | Mitochondrial temperature sensing <sup>97</sup>                  |   |  |
|                                |   | Photothermal therapy <sup>98</sup>                               |   |  |
|                                |   | Cell imaging and cell killing <sup>99</sup>                      |   |  |
|                                |   | Immuno-chemotherapy <sup>100</sup>                               |   |  |
|                                |   | Enhanced intracellular retention <sup>101</sup>                  |   |  |
|                                |   | Tumor therapy <sup>102</sup>                                     |   |  |
|                                |   | Cancer cell death <sup>103</sup>                                 |   |  |
|                                |   | Ultrasound-guided cell implantation <sup>104,105</sup>           |   |  |
|                                |   |  |   |  |
|                                |   | DNA aptamer  |   |  |
|                                |   | Peptide foldamer   |   |  |
|                                |   | Silica nanoparticles   |   |  |
|                                |   |  |   |  |
|                                |   |  |   |  |



Table 1 (continued)

| Mechanism of aggregation |              | Molecular design  | Biomedical application   |  |
|--------------------------|--------------|---|--|--|
| Organelle targeting      | Mitochondria | Lycobetaine (LBT)<br>Zoledronate  | Modulate mitochondrial connectivity <sup>106</sup><br>Stress macrophage mitochondria <sup>107</sup>  |  |
|                          |              | Cyclometalated platinum(II) compounds <sup>108</sup><br>Host-guest conjugates <sup>109</sup><br>Triphenylphosphonium (TPP) conjugation          | Mitochondria imaging<br><br>Overcome proteolytic degradation <sup>110</sup><br>Controls cancer cell fate <sup>111</sup><br>Treatment of age-related diseases <sup>112</sup><br>Ferroptosis of cancer cells <sup>113</sup><br>Cancer cell apoptosis |  |
|                          | Lysosome     | Mitochondria-targeting nucleopeptide<br>Host-guest conjugates<br>TPP-modified DNA <sup>114,115</sup><br>TPP-modified peptide <sup>116,117</sup> | Mitochondria-targeting nucleopeptide <sup>118</sup><br>DNA nanoparticles<br>DNA-ceria nanocomplex<br>Peptide derivative  | Including cell movement and cell autophagy <sup>37</sup><br>Reducing cell mortality <sup>119</sup><br>Inhibit autophagy <sup>38</sup><br>Triggering apoptosis of cells <sup>120</sup><br>Addressing MDR <sup>121</sup><br>Enhanced antitumor immunity <sup>42,122</sup><br>Cancer cell imaging <sup>123</sup><br>Photothermal therapy <sup>124</sup><br>Addressing MDR <sup>125</sup><br>Augmentation of chemotherapy <sup>126</sup><br>Abolish tumor growth and metastasis <sup>56</sup><br>Antitumor immunity <sup>127</sup><br>Selective killing of tumor cells <sup>128,129</sup><br>Cell sensing and imaging <sup>130</sup> |
|                          |              | Nucleus   | DNA nanoribbons<br>Nanocrystals<br>Drug-silane conjugates<br><br>Drug-peptide conjugates<br>DNA-aptamer<br>Phosphopeptide assemblies<br>Anthracene-guanidine derivative  |  |

imaging-related purposes these strategies serve in biological contexts).

In addressing these limitations, we propose innovative solutions and potential research directions, including the development of advanced imaging techniques to better visualize aggregation processes, utilization of biocompatible materials to minimize cellular function disruption, and exploration of novel strategies to control and manipulate aggregation pathways for therapeutic purposes. By presenting these potential solutions, we aim to stimulate new ways of thinking and foster further advancements in the field of intracellular aggregation research.

## 2. Strategies for the intracellular delivery of exogenous molecules

The intracellular aggregation of molecules can trigger specific biological processes and functions, *e.g.*, the aggregation of amyloid protein fibrils at the lesion site leads to Alzheimer's disease (AD),<sup>131</sup> whereas the aggregation of the tumor suppressor protein p53 in tumor cells is involved in cancer progression.<sup>132</sup> Similarly, certain exogenous molecules, such as small-molecule drugs and macromolecules,<sup>133</sup> can be engineered to aggregate within cells and thus alter their physiological state or achieve a particular function.<sup>134</sup> Usually, the realization of the intracellular aggregation of exogenous molecules is dependent on the pathway of their entry into cells, which is related to the molecular state, *i.e.*, the physicochemical properties of these molecules play a crucial role in determining how and where they enter the cell. The molecular state can influence factors such as molecule size, shape, and charge, which, in turn, affect the ability of exogenous molecules

to traverse the cell membrane.<sup>135</sup> For instance, small uncharged molecules may freely diffuse through the membrane, while larger or charged molecules may require specific transport proteins or other mechanisms to facilitate their entry.

The entry pathway can be influenced by the internal environment of the cell and its regulatory mechanisms.<sup>136,137</sup> Cells have a complex network of signaling pathways and regulatory proteins that control the in- and outward movement of molecules to ensure that only certain molecules enter and are directed to the correct location within the cell.<sup>138</sup> Thus, the realization of intracellular aggregation is a multifaceted process that is heavily influenced by the entry pathway, which is related to the molecular state of the substances involved. Understanding these relationships is crucial for developing effective strategies to manipulate or control intracellular aggregation in biological and medical applications.

### 2.1. Free diffusion

Free diffusion is a process by which exogenous molecules spontaneously and passively permeate through the cell membrane, driven solely by concentration gradients and random molecular motion.<sup>139</sup> The molecules simply diffuse across the phospholipid bilayer of the membrane, moving from higher- to lower-concentration areas until an equilibrium is reached. This intracellular delivery method does not involve active transport proteins or energy-consuming processes and is therefore straightforward but often inefficient.<sup>140</sup> Li *et al.* reported a small molecule that diffused into cells, underwent polymerization catalyzed by intracellular transglutaminase, and subsequently *in situ* aggregated into elastin-like polypeptides (Fig. 2A).<sup>141</sup> Various topological nanostructures were constructed (Fig. 2B and C) and



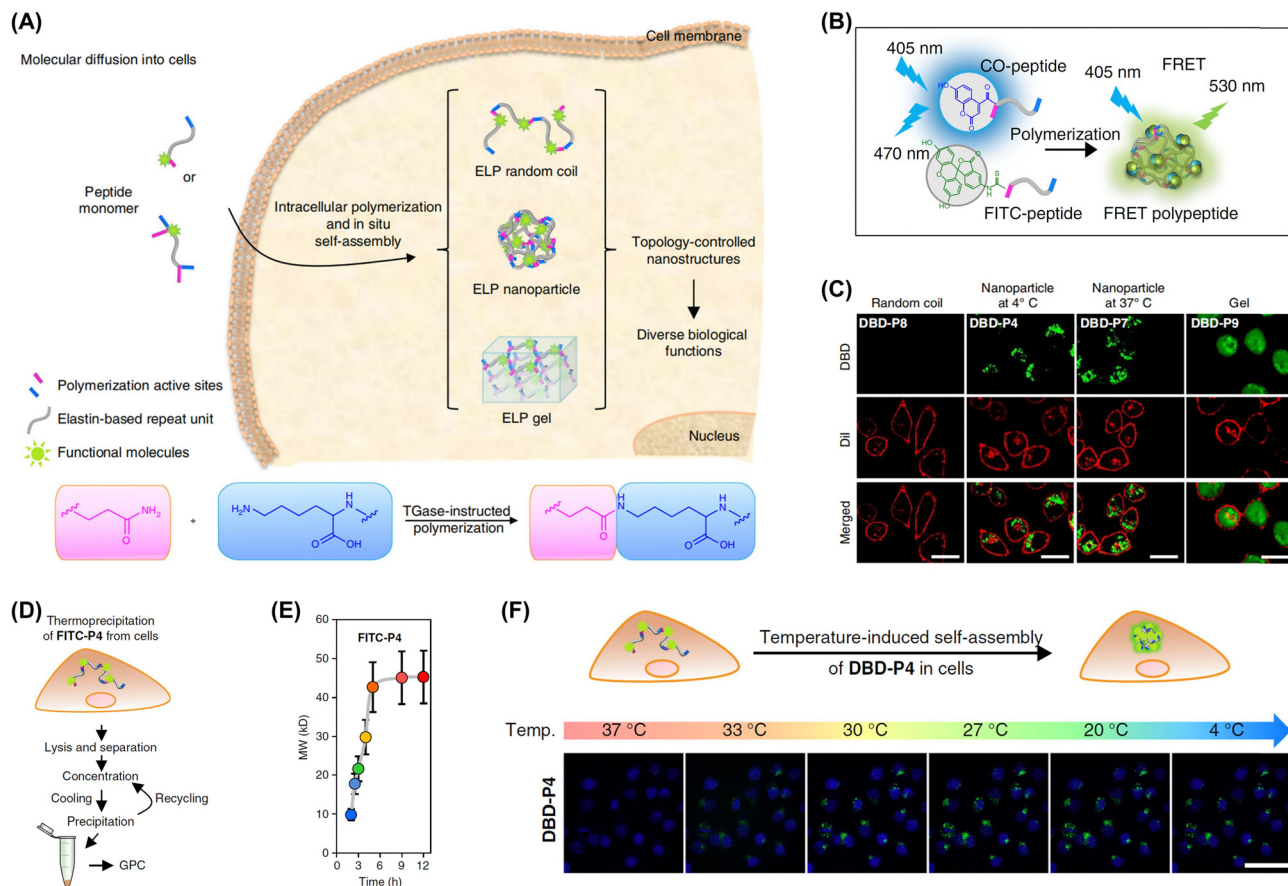


**Fig. 2** (A) Intracellular polymerization catalyzed by TGase and controllable *in situ* nanostructure construction. (B) Intracellular polymerization of peptide monomers by TG2 monitored using fluorescence resonance energy transfer techniques. (C) Confocal images showing the nanostructures (green) formed from P4 at 4 °C and from P7 and P9 at 37 °C. (D) Thermoprecipitation of FITC-P4 from cells. (E) Time-dependent growth of P4 within cells, with the FITC-labeled P4 collected at various time points via thermoprecipitation. (F) Thermodynamic self-assembly of DBD-P4 in HeLa cells during cooling. Adapted with permission from ref. 141. Copyright 2017 Springer Nature.

shown to be substantially cytotoxic despite exhibiting different biological functions (Fig. 2D–F).

## 2.2. Endocytosis

Endocytosis is a fundamental cellular process by which cells internalize extracellular material, including nutrients, signaling molecules, and pathogens,<sup>142</sup> and is characterized by the formation of vesicles that bud off from the plasma membrane and encapsulate extracellular material for delivery into the cell. Exogenous molecules capable of intracellular aggregation typically enter cells through receptor-mediated endocytosis and macropinocytosis. Receptor-mediated endocytosis involves specific interactions between a receptor on the cell surface and its cognate ligand, leading to the internalization of the ligand-receptor complex. This highly specific and regulated form of endocytosis plays a crucial role in the internalization of various exogenous molecules, including nutrients, hormones, growth factors, and antibodies.<sup>143</sup> Macropinocytosis is a form of endocytosis that allows cells to internalize large volumes of extracellular fluid and solutes and is characterized by the formation

of macropinosomes, which are large vesicles derived from the plasma membrane. Macropinocytosis can be used to deliver large molecules, particles, or even cells into the target cell interior. By engineering molecules or particles to trigger macropinocytosis, one can efficiently internalize them while bypassing the traditional barriers of cellular uptake. Xu's group demonstrated that receptor-mediated endocytosis and macropinocytosis are the main endocytic pathways of exogenous molecules (Fig. 3A). Owing to the aggregation of molecules occurring within cells, the intracellular fluorescence intensity of these molecules was significantly higher than that in the control group. This indicates their efficient enrichment inside the cells (Fig. 3B). The intracellular aggregation of molecules was accompanied by a progressive enhancement in fluorescence intensity over the course of laser irradiation, and this phenomenon may be attributed to the laser-mediated escape of these molecules from lysosomes (Fig. 3C). Moreover, the selective aggregation of nanomaterials through endocytosis in cancer cells, which can be realized under the action of tumor-specific enzymes (Fig. 3D and E).<sup>58,144,145</sup>



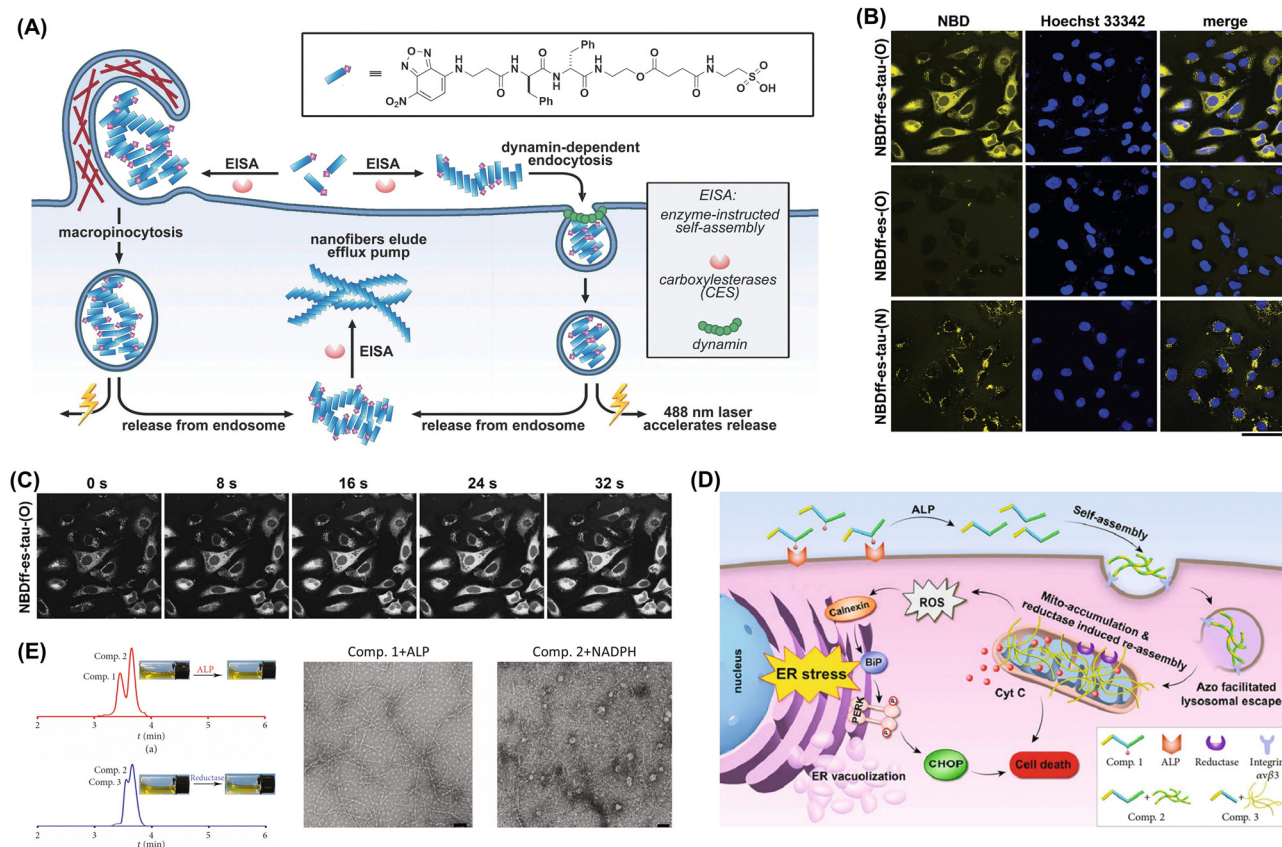


**Fig. 3** (A) Mechanism of endocytic molecular uptake. (B) Images of HeLa cells incubated for 24 h at 37 °C with 500  $\mu$ M NBDff-es-tau-(O), washed three times, and treated with a compound-free live-cell imaging solution. Scale bar: 50  $\mu$ m. (C) Electron microscopy images confirming the endocytosis of NBDff-es-tau-(O) assemblies. Adapted with permission from ref. 145. Copyright 2017 Elsevier BV. (D) Endoplasmic reticulum stress induction through the tandem molecular self-assembly of exogenous molecules. (E) LC spectrum and optical images illustrating the conversion from Comp. 1 to Comp. 3 under the influence of a tumor-specific enzyme. Optical and transmission electron microscopy (TEM) images of the solution formed by adding alkaline phosphatase (ALP) to Comp. 1 (200  $\mu$ M) for 24 h and the precipitate created by adding rat liver microsomes and NADPH to Comp. 2 for 24 h (scale bar: 100 nm). Adapted with permission from ref. 58. Copyright 2019 American Association for the Advancement of Science.

### 3. Intracellular aggregation mechanisms of exogenous molecules

The design and synthesis of exogenous molecules can affect their ability to aggregate within the cell. This aggregation can be achieved by relying on the cellular microenvironment alone without external interventions, as exemplified by the tumor cell microenvironment (ROS, pH, hypoxia, glutathione (GSH), proteases, *etc.*)<sup>146–149</sup> and organelles (lysosomes, mitochondria, endoplasmic reticulum, *etc.*) (Fig. 4). The aggregation of exogenous molecules in cells can also be achieved by exposure to light, ultrasound, heat, and other conditions under artificial control with external interventions.<sup>150,151</sup> Overall, the process and outcome of exogenous molecule polymerization in cells are determined by a combination of factors, including the physical and chemical conditions of the intracellular environment, nature and design of the exogenous molecules, and cell–molecule interactions. Diverse aggregation schemes based on these complex intra- and extracellular conditions have been developed, from the intracellular assembly of peptides, small-molecule aggregation-induced fluorescence emission, and supramolecular host–guest

interactions to the chain-growth and stepwise polymerization of small molecules, to explore the related biomedical prospects, find therapies for major diseases such as cancer, and promote the development of nanobiomedicine.

#### 3.1. Intracellular microenvironment-induced aggregation of exogenous molecules

**3.1.1. pH-induced intracellular aggregation.** Intracellular pH is a critical determinant of the stability and function of various molecules within the cell.<sup>152</sup> pH changes can substantially alter the charge state, solubility, and conformational stability of exogenous molecules.<sup>36,153,154</sup> Moreover, intracellular pH plays a pivotal role in dictating the aggregation behavior of exogenous molecules (*e.g.*, therapeutic agents or imaging probes) introduced into cells.<sup>41,155,156</sup> This process can have important biological implications, influencing the efficacy, toxicity, and overall behavior of the exogenous molecules within the cell. By understanding these pH-induced aggregation processes, one can gain insights into their biological implications and explore their potential applications. The acidic environment of lysosomes is commonly used to achieve the pH-induced intracellular aggregation of



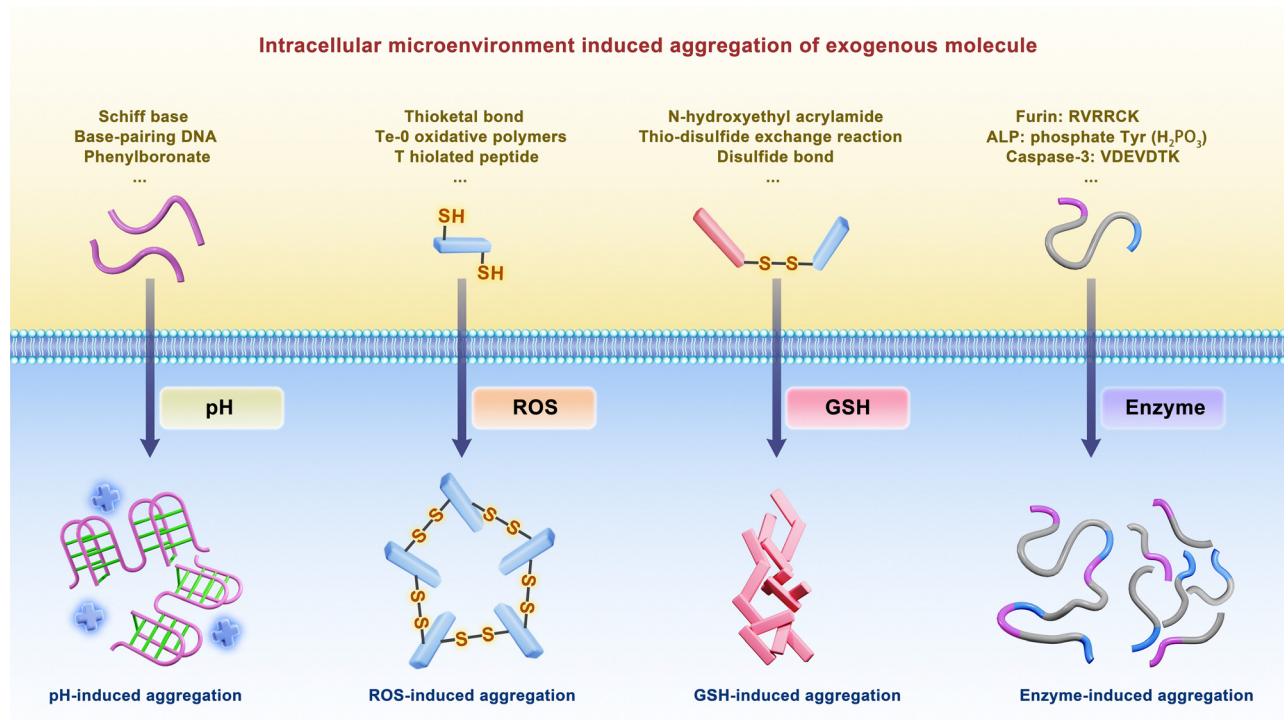


Fig. 4 Intracellular microenvironment-induced aggregation of exogenous molecules.

exogenous molecules. Lysosomes, which are responsible for the breakdown of macromolecules and waste products, maintain a low pH conducive to the aggregation of certain exogenous molecules. By targeting these molecules to lysosomes, one can induce aggregation and thus leverage the natural properties of the lysosomal environment to manipulate the behavior of exogenous molecules within cells.<sup>40,120,157</sup>

Yamamoto *et al.* reported a peptide amphiphile aggregating into entangled nanofibers (hydrogel) in the acidic intracellular environment and used it to induce selective tumor cell death and achieve a high anti-tumor activity (Fig. 5A and B).<sup>39</sup> Lin *et al.* developed a strategy for the pH-responsive intracellular aggregation of inorganic molecules based on the protonation of CuPc-SO<sub>4</sub> and BSA under the acidic intracellular conditions and the resulting interaction weakening, which led to Fe<sup>3+</sup> release and self-aggregation into nanorods (Fig. 5C and D). This acidity-sensitive aggregation was vital for achieving specific accumulation within the tumor microenvironment and thereby enhancing retention and sonodynamic therapy (SDT) efficacy.<sup>44</sup>

pH-responsive intracellular aggregation can not only facilitate the escape of chemotherapeutics from lysosomes but also synergistically augment photothermal therapy (PTT), markedly improving tumor treatment efficacy. Moreover, aggregates formed in the acidic environment of lysosomes can impact cell metabolism, directly regulating cell fate or causing cell death.<sup>37,38,42,46</sup> Borkowska *et al.* developed nanoparticles that featured a blend of positively and negatively charged ligands in precise ratios and targeted lysosomes in cancer cells while demonstrating a negligible cytotoxicity toward normal cells.



Fig. 5 (A) Selective cell death caused by the self-assembly of an intracellular pH-responsive peptide amphiphile. (B) Gelation tests of PBS after 24 h at various pH performed using 0.15 wt% C16-VVAEEE. TEM images of freeze-dried hydrogel and PBS solution at pH 6.8 and 7.4. (C) Acid-responsive aggregation behavior of CuPc-Fe@BSA. (D) TEM images of CuPc-Fe@BSA after variable-duration exposure to media with various pH. Adapted with permission from ref. 44. Copyright 2024 Elsevier BV.

This specificity was attributed to a sequence of pH-responsive aggregation processes. Initially, small clusters prone to endocytosis formed on the cell surface and then transformed into large structured assemblies and crystals inside cancer lysosomes under acidic conditions. These assemblies could not be removed by exocytosis, causing lysosome swelling that progressively compromised lysosomal membrane integrity and ultimately disrupted lysosomal functions and initiated cell death.<sup>45</sup>

**3.1.2. ROS-induced intracellular aggregation.** ROS are generated as the byproducts of normal cellular metabolism or in



response to environmental stressors, such as radiation, pollutants, or toxins. When present at levels exceeding the cellular antioxidant capacity, ROS can interact with various cellular components, including proteins, lipids, and nucleic acids, causing oxidative stress. ROS can also affect the conformations of exogenous molecules, promoting their assembly into larger and often insoluble structures.<sup>158</sup> ROS-induced intracellular aggregation can have profound effects on cell function and viability. For instance, aggregated peptides can impair essential cellular processes, disrupt organelle functions, and even trigger cell death.<sup>47,53,55,159</sup> Wang's group developed an artificial enzyme forming aggregates within cells because of the oxidation of thiol groups in the presence of ROS (Fig. 6A). This process was particularly rapid in tumor cells because of their higher ROS levels, and the deprotonation of the crosslinked artificial enzyme increased its catalytic activity, resulting in typical esterase properties.<sup>52</sup> To further investigate the morphology of intracellular nanoaggregates, intracellular aggregating molecules were modified with ferrocenylmethyl methacrylate (FMMA) and introduced into A549 cells. Biological transmission electron microscopy (bioTEM) observations revealed the *in situ*

formation of spherical nanoparticles within the cells, with diameters of approximately 500 nm, exhibiting a morphology comparable to that observed in aqueous solution. Energy-dispersive spectroscopy analysis of the nanostructures confirmed the presence of iron (Fe) elements, providing evidence that the molecules were capable of undergoing cross-linking reactions within the cells, thereby forming aggregated structures (Fig. 6B). Anticancer drug conjugates, termed OPV-S-Drugs, were synthesized by linking thiol-modified oligo(*p*-phenylene vinylene) with anticancer agents, such as paclitaxel, vincristine, teniposide, tamoxifen, doxorubicin (DOX), and podophyllotoxin, through Michael addition (Fig. 6C).<sup>54</sup> The oxidation of OPV-S-Drugs triggered their intracellular assembly and aggregation into multivalent anticancer drug clusters, preventing drug escape from cancer cells. This aggregation was facilitated by  $\pi$ - $\pi$  stacking and hydrophobic interactions among the OPV backbones, with further stabilization achieved through disulfide bond crosslinking in the presence of ROS (Fig. 6D). This clustering occurred specifically in the cytoplasm of cancer cells with elevated ROS levels, protecting healthy mammalian cells from cytotoxic effects. The above strategy notably reduced

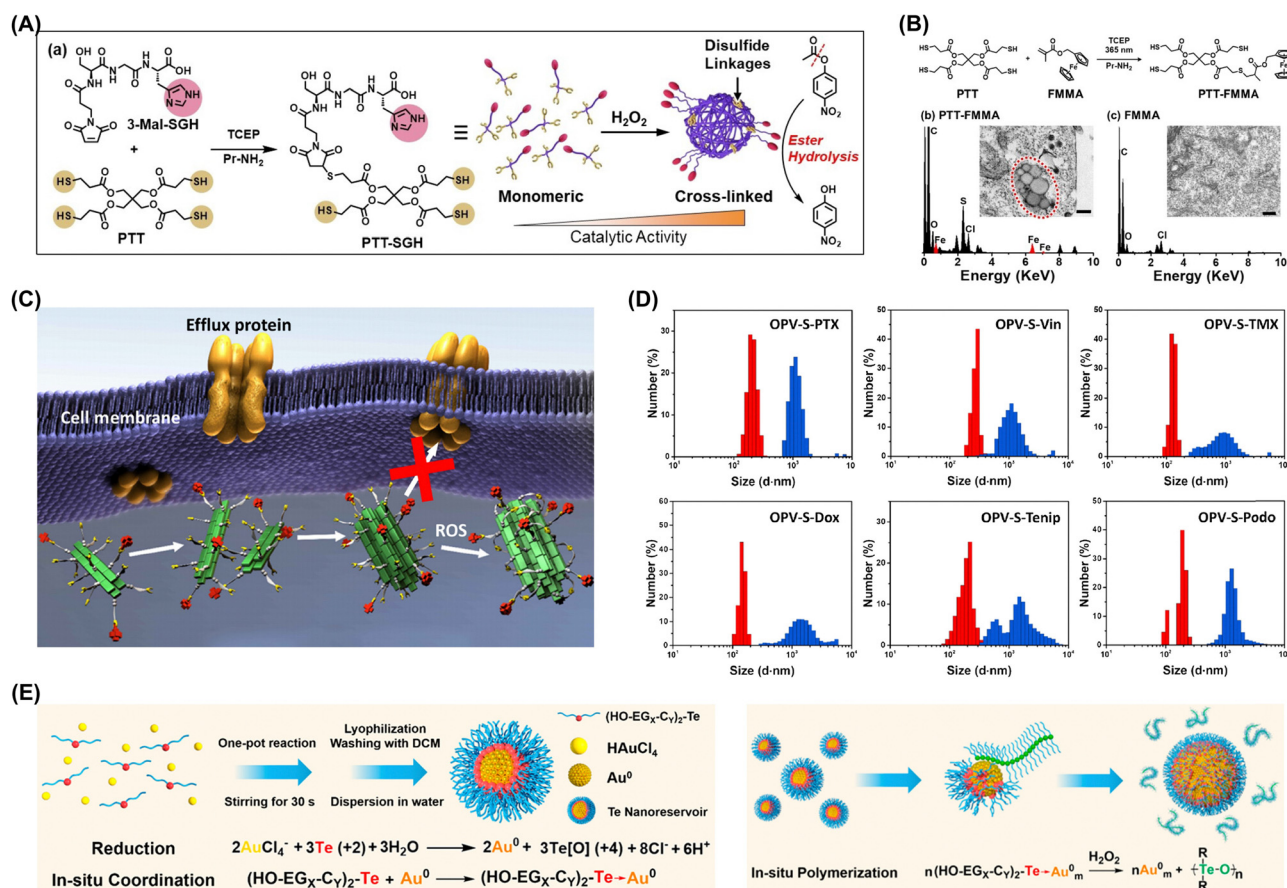


Fig. 6 (A) Overview of artificial enzyme synthesis and thiol group crosslinking under oxidative conditions enhancing ester hydrolysis activity. (B) Synthesis of PTT-FMMA, bio-TEM and energy-dispersive spectra of nanostructures in A549 cells after 24 h of incubation with 100 μM PTT-FMMA or FMMA. Adapted with permission from ref. 52. Copyright 2022 Wiley-VCH. (C) Assembly and aggregation of OPV-S-Drugs in cancer cells. (D) Hydrodynamic diameters of OPV-S-Drugs measured by DLS (red: without H<sub>2</sub>O<sub>2</sub>; blue: with H<sub>2</sub>O<sub>2</sub>). Adapted with permission from ref. 54. Copyright 2019 Chinese Chemical Society. (E) *In situ* polymerization and aggregation processes in cells. Adapted with permission from ref. 48. Copyright 2021 American Chemical Society.



the toxicity of podophyllotoxin to normal cells while maintaining its therapeutic effectiveness.

ROS-induced aggregation is involved in the development and progression of various diseases, including neurodegenerative disorders, cardiovascular diseases, and cancer. Understanding the mechanisms underlying ROS-induced aggregation and developing strategies to mitigate its effects are crucial for advancing therapeutic interventions and improving human health.<sup>50,51</sup> Xu's group developed an oxidative polymerization reaction exploiting the chemical properties of organotellurides and intracellular redox environment. This polymerization occurred within cells without external stimuli and was initiated by intracellular ROS, enabling selective cancer cell targeting (Fig. 6E).<sup>48</sup> The process triggered apoptosis through a self-amplification mechanism, and the polymer products interacted with selenoproteins, disrupting intracellular antioxidant systems and increasing oxidative stress to create a positive feedback loop that further promoted oxidative polymerization and activated ROS-related apoptosis pathways. The same group developed a hyperbranched polymerization process within living cells utilizing the oxidative polymerization of organotellurides in redox environments. The resultant hyperbranched polymers assembled into branched nanostructures capable of efficiently bypassing drug pumps and minimizing drug efflux and thereby enabled sustained treatment through polymerization.<sup>49</sup>

**3.1.3. GSH-induced intracellular aggregation.** The GSH-induced intracellular aggregation of exogenous molecules is a process where GSH, a major intracellular antioxidant, triggers the aggregation of foreign molecules within the cellular environment.<sup>160</sup> This phenomenon can affect the behavior and effectiveness of exogenous molecules (such as drugs, nanoparticles, or other therapeutic agents) entering cells.<sup>56,161,162</sup> The disulfide linkage can stably exist in blood and the extracellular environment but is cleaved at high concentrations of GSH within cells. The elevated GSH concentrations within cancer cells facilitate disulfide bond cleavage and thereby induce intracellular aggregation.<sup>59–62,65,66,163</sup> Gao *et al.* developed NSBSO, a hypertoxic peptide derivative based on L-buthionine-sulfoximine (BSO) and having two main functions, namely the depletion of GSH and suppression of its biosynthesis, targeting ferroptosis and pyroptosis in specific tumors. NSBSO features a hydrophobic segment that enables self-assembly and hydrophilic peptide derivative that contains BSO and inhibits GSH production (Fig. 7A). Upon GSH cleavage, NSBSO transforms from nanoparticles into nanofibers. This species exhibited GSH-dependent cytotoxicity, successfully reducing intracellular GSH levels (Fig. 7B and C).<sup>63</sup>

Magnetic resonance imaging (MRI) is a common diagnostic tool known for its noninvasiveness, soft tissue contrast, high imaging resolution, and lack of ionizing radiation. To improve the sensitivity and specificity of MRI, Liang's group developed a contrast agent that enhanced the detection of early-stage cancer through the aggregation of peptide probes induced by intracellular GSH (Fig. 7D). This smart and controllable intracellular aggregation approach enables the enrichment of low-dose <sup>19</sup>F probes through locally self-assembling and disassembling nanoparticles, thereby avoiding rapid transverse relaxation of

the probes. The designed contrast agent (Fig. 7E) is capable of self-assembling in response to glutathione (GSH) and subsequently disassembling the formed nanoparticles under the action of caspase 3/7 (Fig. 7F). By employing this intelligent strategy, we successfully utilized probe to consecutively detect the activities of GSH and Casp3/7 *in vitro* and within cells. Moreover, under low-dose conditions and with the aid of a 14.1 T magnetic field, we achieved imaging of Casp3/7 activity in cells and zebrafish (Fig. 7G).<sup>57,64</sup>

**3.1.4. Enzyme-induced intracellular aggregation.** The enzyme-induced intracellular aggregation of exogenous molecules involves specific enzymes, which are biological catalysts that are present within the cell and interact with exogenous molecules, *i.e.*, substances that are foreign or nonnative to the usual cell environment.<sup>164</sup> This interaction leads to the aggregation, or clustering, of these molecules<sup>70,71,73,165</sup> and can originate from enzymatic activities such as hydrolysis, oxidation, or reduction, which alter the chemical properties of the exogenous molecules to make them more prone to interact with each other.<sup>67,72,75,82</sup> Enzymes catalyze these reactions, lowering the activation energy of aggregation. The significance of the enzyme-induced intracellular aggregation of exogenous molecules depends on the context and can be beneficial, as exemplified by the breakdown and elimination of harmful substances or formation of essential cellular structures.

In certain cases, enzyme-induced intracellular aggregation can generate toxic aggregates inducing the death of tumor cells. Li *et al.* used enzyme-instructed self-assembly to develop intracellular supramolecular structures markedly increasing the effectiveness of cisplatin against drug-resistant ovarian cancer cells (Fig. 8A).<sup>68</sup> The synthesized small peptide precursors acted as substrates for carboxylesterase, which cleaved the pre-installed ester bond to afford peptides spontaneously forming nanofibers in aqueous environments. At optimal concentrations, these peptide precursors were nontoxic to cells and effectively enhanced cisplatin activity against drug-resistant ovarian cancer cells. Wang's group developed a caspase-3/7-triggered intracellular aggregation system, integrating imaging probes and therapeutic agents. When this system was applied to mouse models, intracellular aggregation enhanced drug accumulation within solid tumors because of the recognition-induced self-assembly effect (Fig. 8B and C).<sup>74</sup>

Understanding the mechanisms and outcomes of the enzyme-induced intracellular aggregation of exogenous molecules is crucial for various fields, including toxicology, pharmacology, and biotechnology. By studying these interactions, one can gain insights into how cells process and respond to foreign substances and develop strategies to manipulate or effectively utilize aggregation events. Wu *et al.* designed a near-infrared (NIR) probe for the photoacoustic imaging of alkaline phosphatase (ALP) activity. Under the catalytic action of ALP, the probe can undergo efficient hydrolysis, followed by self-assembly to form nanoparticles. The formed nanoparticles exhibit a 6.4-fold enhancement in the photoacoustic (PA) signal at 795 nm. *In vivo* tumor photoacoustic imaging results demonstrate that, compared to the ALP inhibitor-treated control



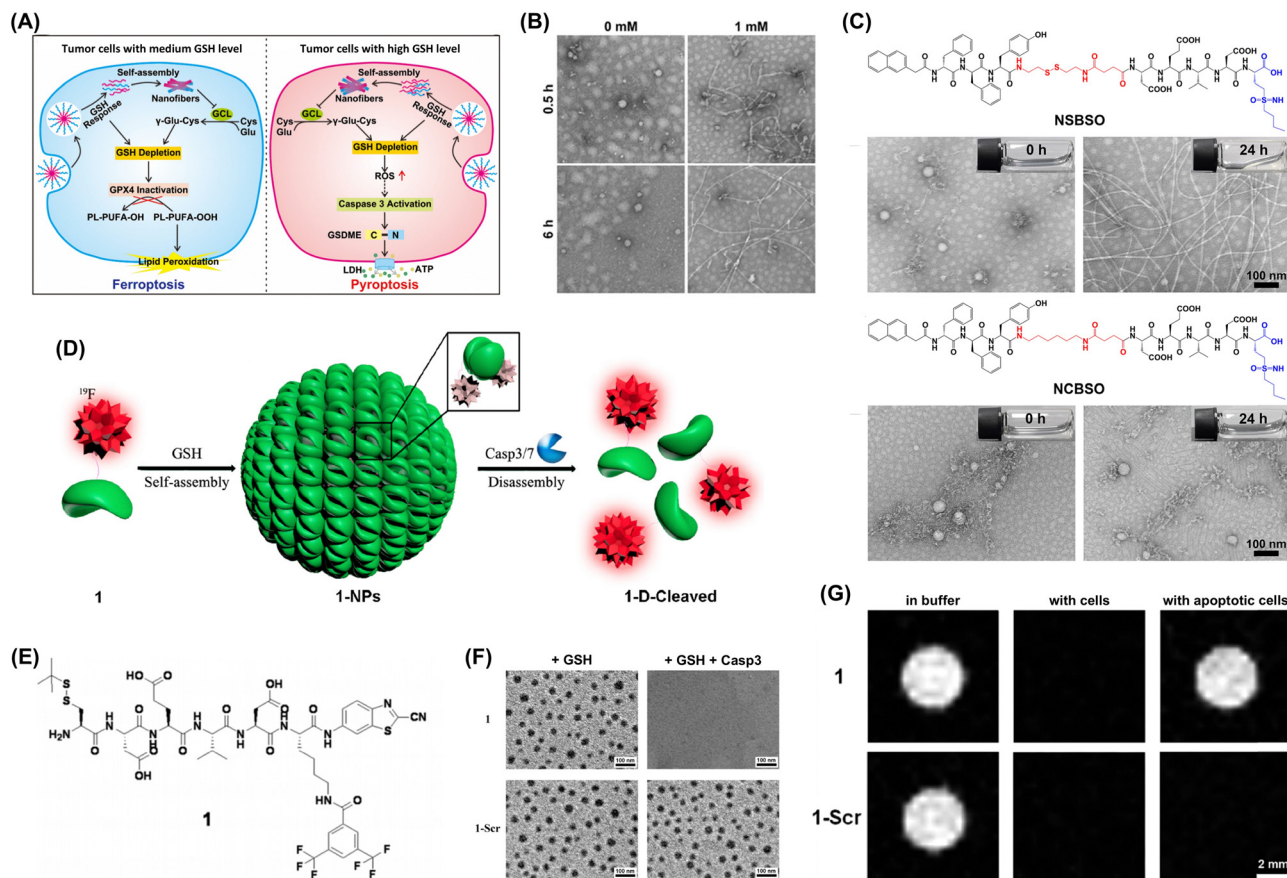


Fig. 7 (A) GSH-responsive intracellular reassembly of NSBSO selectively inducing ferroptosis or pyroptosis in tumor cells based on intracellular GSH levels. (B) TEM images of NSBSO obtained after 6 h exposure to 0 and 1 mM GSH at 37 °C. (C) Molecular structures of NSBSO and NCBSO and optical and TEM images acquired after 24 h exposure to 10 mM GSH at 37 °C. Adapted with permission from ref. 63. Copyright 2022 Springer Nature. (D) GSH-controlled self-assembly turning  $^{19}\text{F}$  NMR signals off and Casp3/7-controlled disassembly turning them on. (E) Chemical structures of the peptide probe. (F) TEM images of 1-NPs (top) and 1-Ser-NPs (bottom) following 30 min exposure to 2 mM GSH and subsequent incubation with Casp3. (G)  $^{19}\text{F}$  MRI of 1 (top) and 1-Ser (bottom) in RIPA lysis buffer and cell lysate incubated with HepG2 cells and apoptotic HepG2 cells. Adapted with permission from ref. 57. Copyright 2015 American Chemical Society.

group, the tumor photoacoustic contrast in the experimental group increases by 2.3-fold at 4 hours post-probe injection (Fig. 8D).<sup>69</sup> Chen *et al.* reported two precursor molecules capable of synthesizing hybrid gallium-68 nanoparticles in furin-overexpressing cancer cells and enhancing microPET tumor imaging in mice. *In vivo* experimental results revealed that when these two molecules were co-injected, the radiotracer exhibited the longest retention time in the bloodstream, the highest radioactivity in tumor regions, and the most pronounced enhancement in microPET tumor imaging within mice (Fig. 8E).<sup>77</sup> Liu *et al.* developed an enzyme-mediated aggregation-induced emission luminogen (AIEgen), promoting its accumulation and retention within tumors and thus enabling extended imaging and enhanced tumor growth inhibition (Fig. 8F).<sup>80</sup> Upon the action of tumor-specific cathepsin proteases, the cleavage of the peptide triggers a condensation polymerization reaction between the exposed cysteine residue and the 2-cyanobenzothiazole group. This reaction facilitates AIEgen accumulation at the tumor site, amplifying the fluorescence signal. Enzyme-catalyzed polymerization disrupts actin

architecture, altering cell motility and suppressing proliferation. Furthermore, the AIEgen's inherent photosensitization combined with tumoral accumulation markedly boosts *in vivo* PDT antitumor efficacy upon light exposure.

### 3.2. Exogenous stimuli-induced aggregation of exogenous molecules

Exogenous molecules may undergo aggregation in response to physical, chemical, or biological interactions prompted by exogenous stimuli. Such aggregation phenomena can have important implications in various fields, including biology, chemistry, and materials science, where understanding and controlling the behavior of exogenous molecules is crucial for the development of novel technologies and applications.

**3.2.1. Light-induced aggregation.** Intracellular exogenous molecules exposed to light can undergo aggregation to form larger assemblies with unique chemical or biological properties. The mechanism behind light-induced aggregation is multifaceted.<sup>85,86,166</sup> Light can act as an energy source, exciting the electrons within exogenous molecules to higher energy



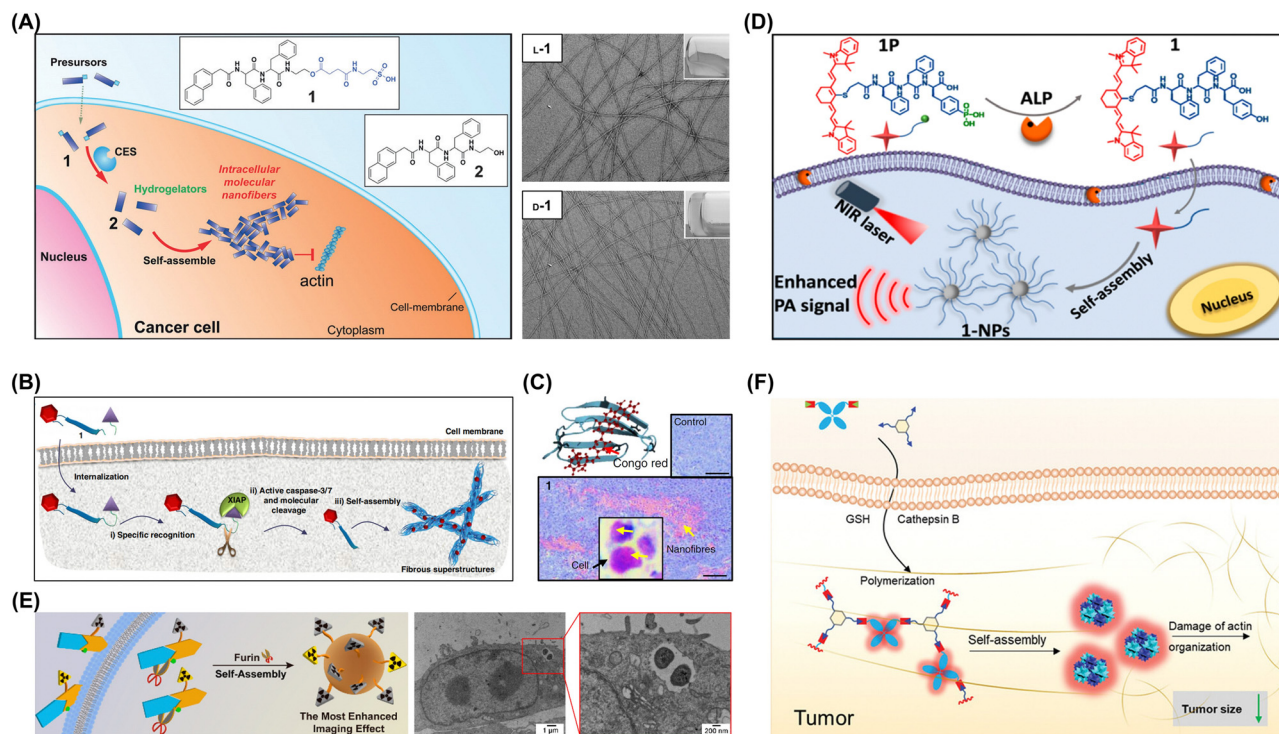


**Fig. 8** (A) Enzymatic transformation of precursor 1 by carboxylesterase to hydrogelator 2 for intracellular self-assembly. Adapted with permission from ref. 68. Copyright 2015 Wiley-VCH. (B) Mechanism of specific recognition, molecular cleavage, and *in situ* self-assembly leading to  $\beta$ -sheet nanostructures enhancing accumulation in tumor tissue. (C) Light microscopy images of Congo red-stained tumor sections with yellow arrows indicating nanofibers. Adapted with permission from ref. 74. Copyright 2019 Springer Nature. (D) ALP-triggered self-assembly of near-infrared (NIR) nanoprobes for the enhanced photoacoustic imaging of tumors. Adapted with permission from ref. 69. Copyright 2018 American Chemical Society. (E) Intracellular synthesis of hybrid gallium-68 nanoparticles in cancer cells for enhanced microPET imaging. Adapted with permission from ref. 77. Copyright 2021 American Chemical Society. (F) Enzyme-mediated intracellular reduction and condensation of peptides affording aggregation-induced emission luminogen (AIEgen)-based nanostructures enhancing fluorescence and tumor treatment efficacy. Adapted with permission from ref. 80. Copyright 2021 Wiley-VCH.

states and thus facilitating interactions with neighboring molecules and aggregation. Moreover, energy transfer between molecules (*i.e.*, the absorption of energy by one molecule followed by transfer to another molecule) can trigger aggregation in the recipient molecule. Charge distribution changes within molecules upon light exposure can also contribute to aggregation by altering intermolecular forces. Geng *et al.* proposed a strategy involving the direct synthesis of unnatural polymers within cells *via* free-radical photopolymerization, utilizing various biocompatible acrylic and methacrylic monomers (Fig. 9A).<sup>84</sup> This method offers a versatile platform for the manipulation, monitoring, and regulation of cellular behavior and enables the *in situ* generation of macromolecules capable of altering cellular motility. The above approach enables cell labeling by generating fluorescent polymers for comprehensive tracking studies and the formation of various nanostructures within cells (Fig. 9B). Ferrocenylmethyl methacrylate (FMMA) was employed in this study. After co-incubating HeLa cells with the initiator, TEM observations revealed the *in situ* formation of spherical nanoparticles within the cells, encompassing both the cytoplasm and nucleus, with diameters ranging approximately from 50–70 nm. These nanoparticles exhibited dimensions comparable to those of the poly(FMMA) aggregates

observed in PBS. In contrast, no such nanostructures were formed in the control groups. This outcome further substantiates the occurrence of polymerization reactions and subsequent *in situ* aggregation within the cells (Fig. 9C). Liu's group integrated naturally occurring microtubules with synthetically designed macrocyclic receptors and photoregulated the configuration of the microtubule self-assembly through host-guest interactions between a paclitaxel-modified  $\beta$ -cyclodextrin and photochromic arylazopyrazole (Fig. 9D).<sup>83</sup> The supramolecular aggregation of microtubules within a cellular milieu can strongly alter cell morphology and induce cell death. This supramolecular strategy, grounded in the secondary complexation of PTX-AAP with PTX-CD, offers a straightforward means to reversibly manipulate the intertubular aggregation patterns of microtubules, offering novel insights into the treatment of diseases associated with aberrant protein aggregation. This small-molecule-induced reversible aggregation of microtubules disrupts pathological aggregation pathways by competing for shared nucleation sites or altering cellular trafficking of aggregation-prone proteins. This approach exemplifies how strategies targeting one protein system can inform therapeutic design for others, given the conserved biophysical principles governing aggregation.



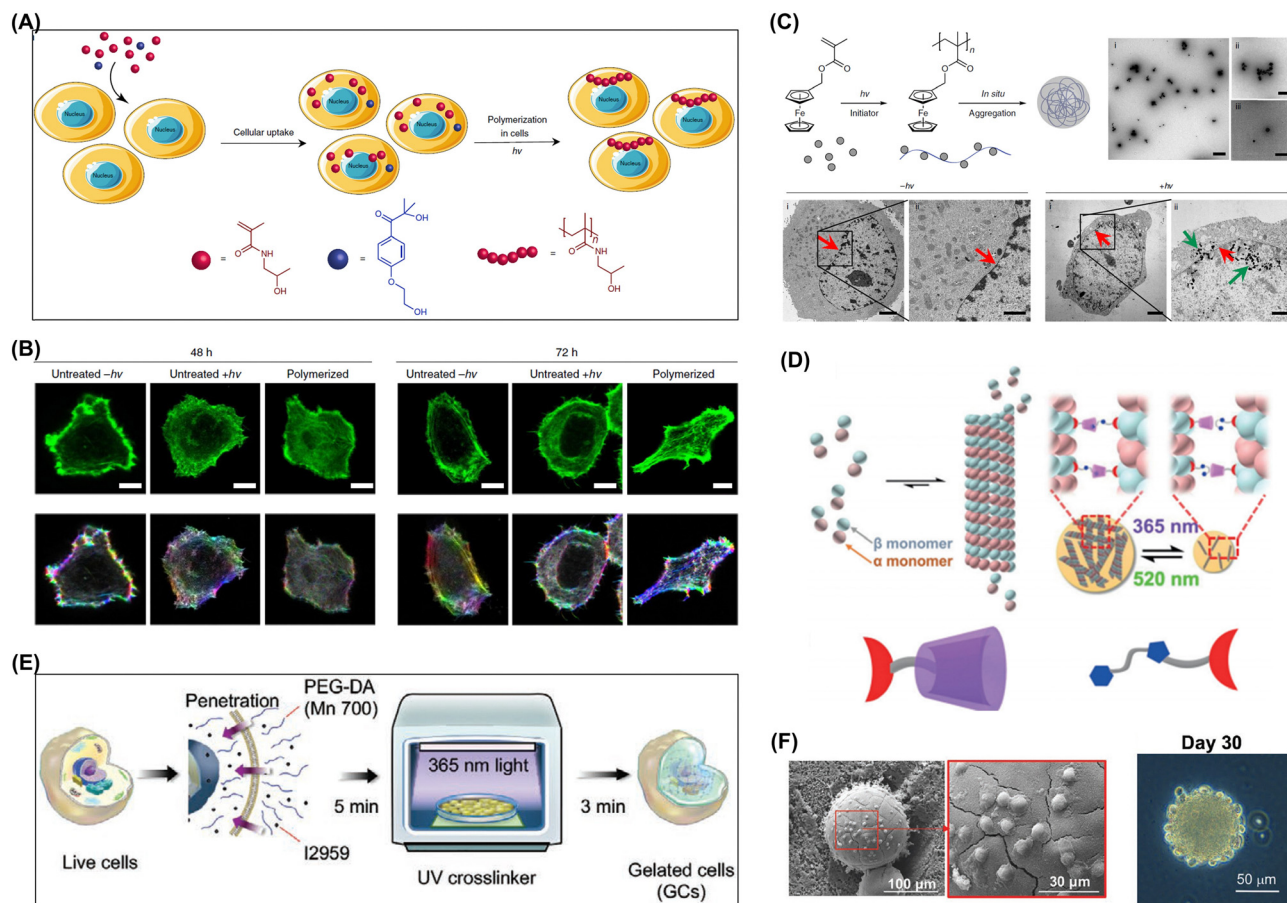


**Fig. 9** (A) Strategy for 365 nm illumination-induced polymerization within living cells using HPMA as a monomer and irgacure 2959 as an initiator. (B) Comparison of untreated cells and polymerized cells with actin filament staining (F-actin) after 48 and 72 h; scale bar: 10  $\mu\text{m}$ . (C) Polymerization of FMMA in HeLa cells. Adapted with permission from ref. 84. Copyright 2019 Springer Nature. (D) Molecular structures of a paclitaxel-modified cyclodextrin ternary supramolecular assembly. Adapted with permission from ref. 83. Copyright 2018 Wiley-VCH. (E) Illustration of G-DC preparation through the direct permeation of hydrogel monomers and photoinitiators into cells. (F) Cryo-SEM images revealing the topographical features of GC-MPs, which maintained stability and structural integrity over 30 days. Adapted with permission from ref. 87. Copyright 2021 Wiley-VCH.

Several factors influence the extent and nature of light-induced aggregation.<sup>167</sup> The intensity, wavelength, and duration of light exposure strongly affect the aggregation degree. The chemical structure of exogenous molecules, including their functional groups and charge distributions, plays a pivotal role in determining their aggregation behavior. Moreover, the solvent environment, such as polarity, viscosity, and the presence of ions or other solutes, can markedly affect the aggregation process. Intracellular hydrogelation was swiftly achieved with minimal disruption to cellular morphology and surface antigen presentation by directly permeating dendritic cells with poly(ethylene glycol) diacrylate hydrogel monomers and using ultraviolet-activated radical polymerization (Fig. 9E). This process resulted in highly durable and adaptable cell-gel hybrid structures enabling the exchange of peptide antigens. These structures could be preserved through freezing and lyophilization and functionalized with cytokine-releasing carriers to modulate T-cell activity (Fig. 9F).<sup>87</sup>

**3.2.2. Temperature-induced aggregation.** When cells are exposed to stressful conditions, such as heat shock, certain

cellular proteins aggregate to form large structures known as stress granules, which can be disrupted as the cell and its protein components recover. Although protein aggregation and the formation of stress granules are correlated, they are independent processes. In some cases, protein aggregation occurs without the formation of stress granules, representing an intrinsic protein aggregation phenomenon within cells. When cells are exposed to high nonlethal temperatures, some exogenous molecules can also aggregate within them. This aggregation seems to reflect the cellular response to stress, and the accumulation of intracellular aggregates is not prevented during their formation. For some temperature-sensitive molecules, when the cells return to normal temperatures, these aggregates can be completely reversed and dissociated, and the molecules regain their monomeric state.<sup>88,89,95</sup>

More often than not, under the influence of temperature, exogenous molecules form stable aggregates within cells. These aggregates can not only persist within cells and be used for cellular imaging but also strongly affect normal cell functioning.<sup>92–94,97</sup> MacKay *et al.* introduced a platform capable of reversibly assembling genetically engineered protein microdomains in living cells within



minutes. Similar to the human protein tropoelastin, these protein polymers experienced a phase transition that generated a secondary aqueous phase above a certain threshold temperature (Fig. 10A).<sup>168</sup> By varying the molecular weight and hydrophobicity of these polymers, the authors made the assembly occur at or near physiological temperatures (Fig. 10B).

The temperature-sensitive properties of molecules are often used to achieve the aggregation of materials within cells. Poly(*N*-isopropylacrylamide) is a prominent temperature-sensitive polymer because of its unique lower critical solution temperature.<sup>90,91</sup> This characteristic enables rapid phase transitions at physiological temperatures, which subsequently trigger aggregation within cellular environments. Qiao *et al.* used poly(*N*-isopropylacrylamide) to create functional nanoaggregates for the *in vivo* sensing and monitoring of cellular physiological processes (Fig. 10C).<sup>96,169</sup> This strategy involved designing thermosensitive polymer-peptide conjugates (PPCs) forming nanoaggregates within cells because of their isothermal phase transition behavior. The phase transition characteristics of PPCs were studied by analyzing various critical parameters, including chain length, hydrophilicity, grafted peptide ratio, and concentration. In response to specific intracellular stimuli, the PPCs underwent customized changes and formed nanoaggregates with long-term retention properties.

**3.2.3. Other strategies for inducing aggregation.** Other methods of inducing exogenous molecule aggregation within cells include the use of click reactions and specific interactions with intracellular molecules.<sup>100,102,104,106,170</sup> Owing to their energetically favorable nature, high specificity, universal chemical transformation format, and single product formation, click

reactions find numerous biological applications and are particularly well suited for inducing the intracellular aggregation of exogenous molecules.<sup>171</sup>

Yin *et al.* developed a nanohybrid capable of capturing, converting, and utilizing the excess copper found in tumor cells.<sup>98</sup> This approach provided dual therapeutic effects, inducing photothermal damage to primary tumors and inhibiting metastasis *via* copper deficiency. The nanohybrid consisted of gold nanoparticles (AuNPs) comodified with 3-azidopropylamine, 4-ethynylaniline, and *N*-aminoethyl-*N'*-benzoylthiourea (BTU). During therapy, BTU selectively chelated copper after endocytosis, diminishing intracellular copper levels and thus suppressing vascularization and tumor migration. Concurrently, BTU converted copper to cuprous ions, facilitating a click reaction between the azido and alkynyl groups on the AuNP surface and resulting in on-demand AuNP aggregation (Fig. 11A and B). Being unnatural to living cells, click reactions hold promise for advancing biological research.

Tang *et al.* introduced a “lab-in-cell” concept using a novel spontaneous amino-yne click polymerization.<sup>99</sup> This method involved the spontaneous polymerization of a carbonyl-activated terminal diyne with a tetraphenylethene (TPE)-containing primary diamine within cells, resulting in a polymer with a weight-average molecular weight of 7300 Da. By leveraging the *in vivo* amino-yne click polymerization and aggregation-induced emission properties of TPE, the authors achieved a “turn-on” capability for cell imaging (Fig. 11C).

Specific interactions with intracellular molecules can induce their aggregation, which helps regulate intracellular molecule

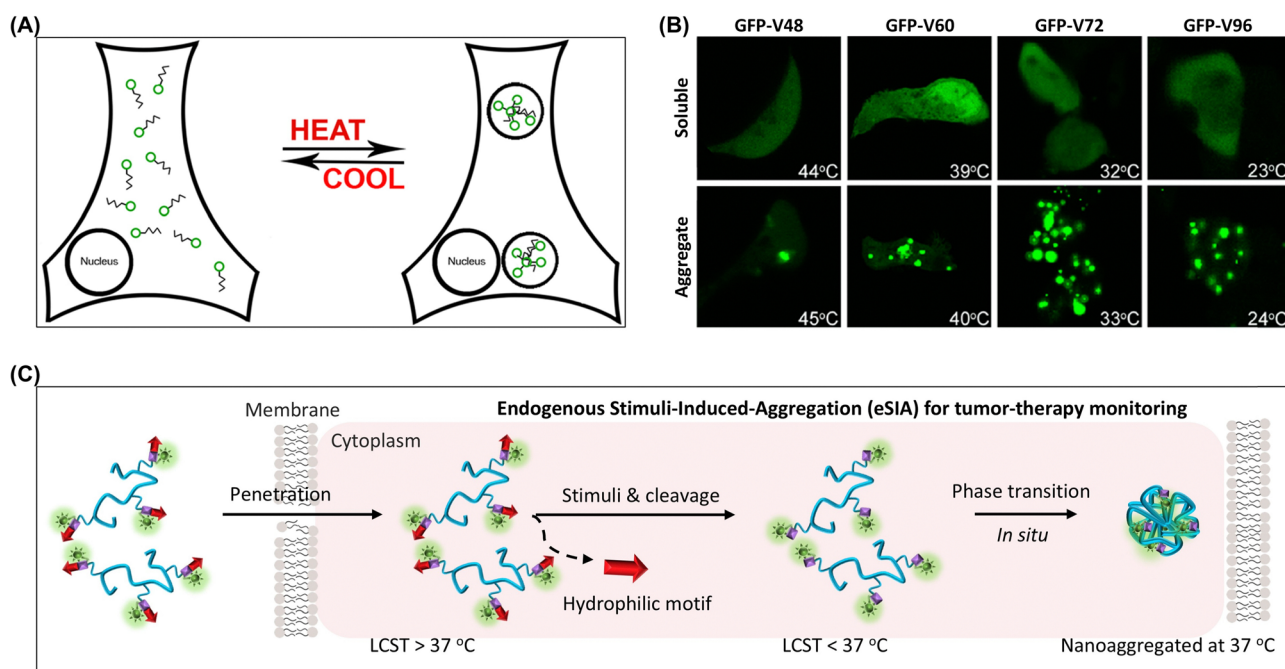


**Fig. 10** (A) Schematic of triggered microdomain assembly in living cells showing the solubility of GFP-ELPs in the cytosol prior to heating. (B) Illustration of polymer phase separation in a valine library of elastin-like polypeptides. Adapted with permission from ref. 168. Copyright 2012 American Chemical Society. (C) Stimuli-instructed construction of controllable nanoaggregates for monitoring tumor therapy responses. Adapted with permission from ref. 96. Copyright 2017 American Chemical Society.



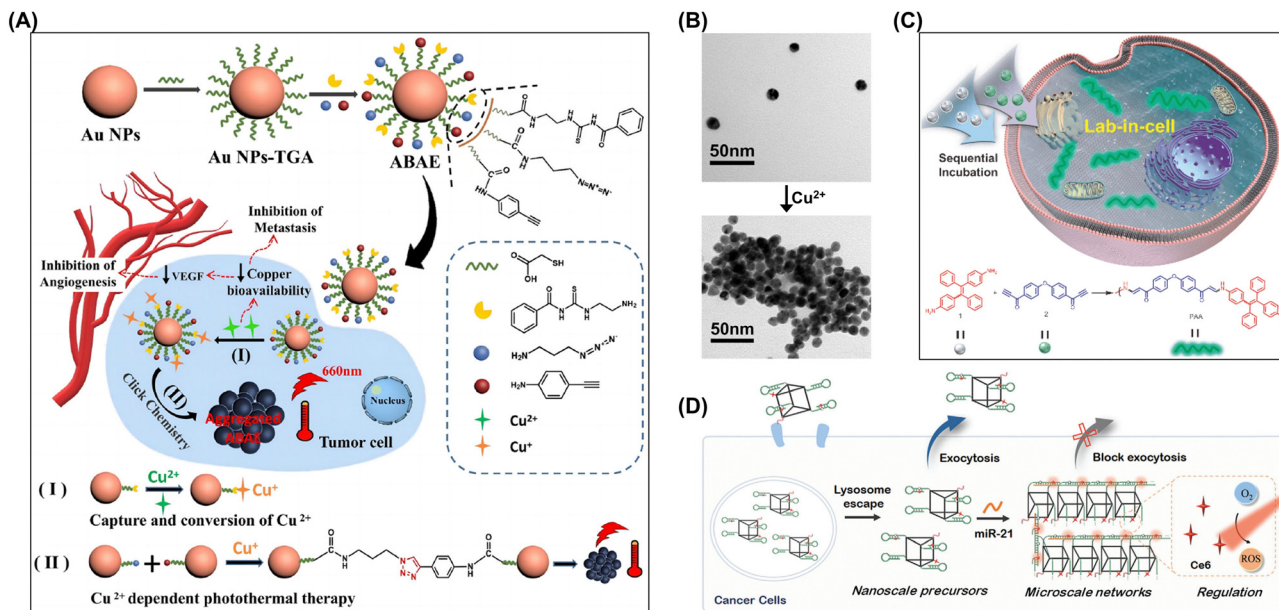


**Fig. 11** (A) Synthesis and therapeutic mechanism of ABAE nanoparticles, which target overexpressed copper in tumor cells for primary tumor elimination and metastasis inhibition through copper capture, state conversion, and cuprous ion-induced photothermal therapy. Adapted with permission from ref. 98. Copyright 2023 Wiley-VCH. (B) TEM images of ABAE nanoparticles before and after  $\text{Cu}^{2+}$  chelation. (C) Intracellular spontaneous amino-yne click polymerization and synthesis of poly( $\beta$ -aminoacrylate). Adapted with permission from ref. 99. Copyright 2023 Science China Press. (D) Self-assembly of DNA hyperbranched aggregates in cancer cells mediated by microRNA-21. Adapted with permission from ref. 101. Copyright 2024 Wiley-VCH.

concentrations and enhance biomolecule activity.<sup>103,105,107,172</sup> Li *et al.* used a DNA framework along with the hybridization chain reaction (HCR) to achieve the targeted assembly of hyperbranched aggregates within cancer cells.<sup>101</sup> HCR is known for its signal amplification and linear extension features, enabling the precise triggering of precursor morphological transformations by minimal amounts of endogenous microRNA-21. The confined spatial environment of the framework and varied orientations of hairpins sped up the hyperbranched network assembly, and the produced micrometer-sized aggregates demonstrated improved intracellular retention capabilities (Fig. 11D).

### 3.3. Organelle targeting-induced aggregation of exogenous molecules

The rapid progress in biotechnology and nanoscience has drawn attention to methods of precisely manipulating the localization and function of exogenous molecules within cells. Organelles serve as highly specialized structural and functional units within cells, undertaking a variety of biochemical reactions and material transport tasks. Achieving the precise regulation of their functions through the induction of exogenous molecule aggregation on specific organelles is a promising strategy. Molecular recognition mechanisms can be used to direct exogenous molecules (such as drugs, nanoparticles, and proteins) to specific organelles and induce their aggregation thereon to regulate organelle functions. Organelle (mitochondria, lysosomes, nuclei, *etc.*) targeting-induced aggregation has enabled remarkable progress in targeted therapies (Fig. 12).<sup>173</sup>

**3.3.1. Mitochondria targeting-induced aggregation.** Mitochondria are the energy factories of cells, playing a crucial role

in cellular growth, development, and metabolism.<sup>174</sup> These organelles are not only responsible for generating adenosine triphosphate (ATP) and thus providing energy but also participate in the regulation of cell apoptosis, signal transduction, calcium-ion homeostasis, and other biological processes.<sup>175</sup> Specific molecular recognition mechanisms can be used to direct exogenous molecules to mitochondria and thus induce aggregation on their surface or within their interior.<sup>108,109,111,116</sup> This aggregation not only enhances the interaction between exogenous molecules and mitochondria but also enables the precise regulation of mitochondrial functions.<sup>110,112,114,115</sup> For instance, by making therapeutically active molecules aggregate on mitochondria, one can effectively inhibit the growth and proliferation of tumor cells (Fig. 13A and B).<sup>118</sup> Ryu's group demonstrated that the self-assembly of a peptide amphiphile within mitochondria is an effective strategy for influencing cellular fate (Fig. 13C).<sup>117</sup> Specifically, a phenylalanine dipeptide modified with a mitochondria-targeting (triphenylphosphonium) moiety (Mito-FF) preferentially accumulated in mitochondria at concentrations sufficient for fibrous nanostructure formation. These nanostructures were visualized using confocal laser scanning microscopy and transmission electron microscopy (Fig. 13D). The Mito-FF fibrils induced mitochondrial dysfunction by disrupting the membrane and thus activated apoptosis.

The high levels of hydrogen peroxide near mitochondria enable mitochondria-targeted aggregates to effectively catalyze the Fenton reaction and thus generate considerable amounts of ROS, which enhance the ability of these aggregates to kill tumor cells.<sup>176</sup> Yang *et al.* showed that host-guest complexation is an



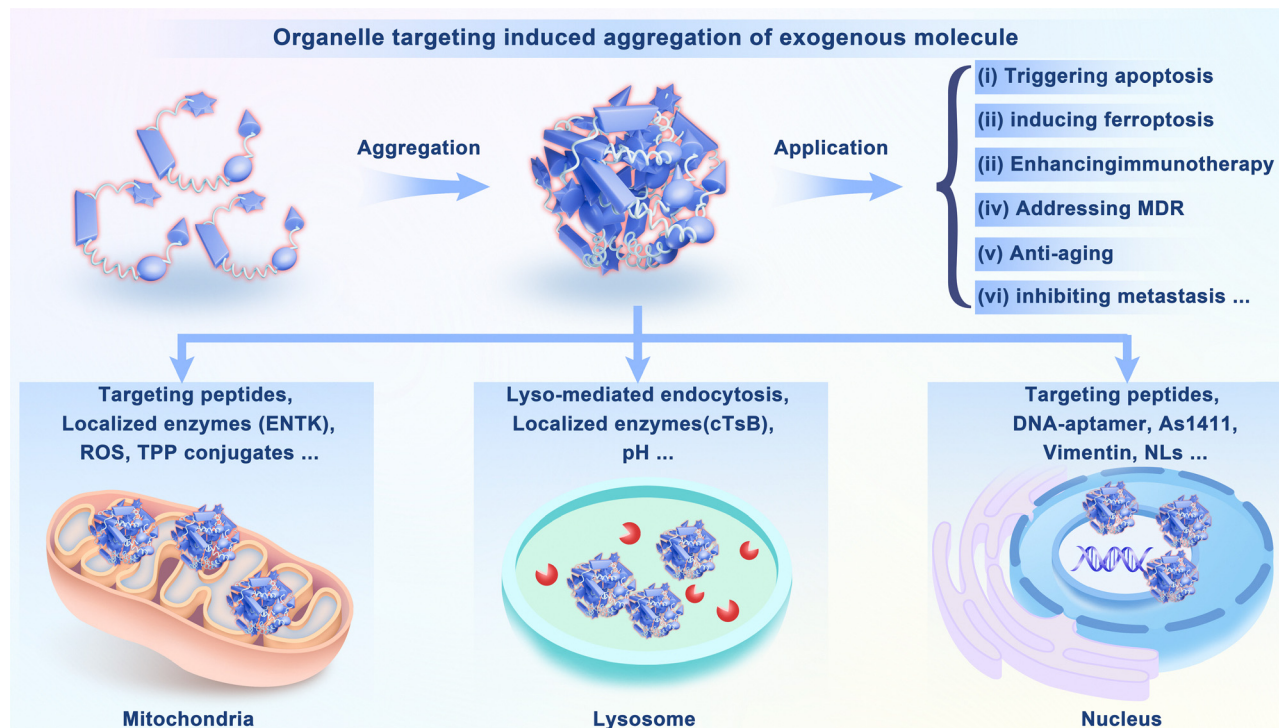


Fig. 12 Organelle targeting-induced aggregation of exogenous molecules.

effective strategy for modulating the enzymatic self-assembly of peptides. This complexation inhibited the enzymatic kinetics of peptide assemblies on the cell surface, promoting their internalization. Once internalized, the complex dissociated in the acidic environment of lysosomes to release the peptides, which then self-assembled within mitochondria. The buildup of these assemblies induced ferroptosis in cancer cells, leading to cell death both *in vitro* and in tumor-bearing mouse models (Fig. 13E).<sup>113</sup>

**3.3.2. Lysosome targeting-induced aggregation.** Lysosomes are cellular organelles containing hydrolytic enzymes capable of breaking down and digesting intracellular biological macromolecules (such as proteins, nucleic acids, and polysaccharides) and senescent or damaged organelles. In certain scenarios, exogenous molecules may be degraded by the hydrolytic enzymes within lysosomes to release small-molecule fragments or products. In other cases, exogenous molecules may aggregate within lysosomes because of specific interactions to form larger complexes or aggregates.<sup>38,121,122,125,126,177</sup> Lysosome-targeting aggregation typically refers to the process of directing specific molecules or drugs to lysosomes to achieve aggregation therein. Huang *et al.* programmed the intracellular clustering of spiky nanoparticles (SNPs) by encapsulating them within anionic liposomes using frame-guided self-assembly (Fig. 14A).<sup>43</sup> The resulting liposome-encapsulated SNPs (lipo-SNPs) exhibited an enhanced lysosome-induced aggregation behavior while maintaining an excellent monodispersity even in acidic or protein-rich environments (Fig. 14B). The photothermal conversion efficiency of lipo-SNP clusters exceeded that of individual lipo-SNPs 15-fold (Fig. 14C). Additionally, upon accumulation in

lysosomes, the cell-killing efficiency of lipo-SNPs increased from 12% to 45% at a concentration of  $24 \mu\text{g mL}^{-1}$ , and clustering increased 2.4-fold.

The aggregation of exogenous molecules within lysosomes is not only closely related to the metabolic and regulatory mechanisms within cells but may also impact their normal physiological functions. The aggregation of certain exogenous molecules may interfere with the normal functioning of lysosomes, leading to abnormal degradation or the accumulation of intracellular biomacromolecules and thus triggering cell damage or disease. The aggregation of exogenous molecules within lysosomes can also be used to develop new principles and methods of treating certain diseases.<sup>123,124,178</sup> Yang's group developed a dynamic assembly system using a DNA-ceria nanocomplex for the intracellular *in situ* construction of artificial peroxisomes (APs) (Fig. 14D).<sup>119</sup> These nanocomplexes were created with branched DNA featuring an i-motif structure that responded to acidic lysosomal conditions and enabled the transformation from a nanocomplex to bulk-scale APs (Fig. 14E). The initial nanoscale size promoted cellular uptake, while the bulk scale of the APs enhanced retention within the cell. The APs demonstrated enzyme-like catalytic activities, scavenging ROS through the decomposition of  $\text{H}_2\text{O}_2$  into  $\text{O}_2$  and  $\text{H}_2\text{O}$ . Luo *et al.* reported a low-generation lysine dendrimer (SPR-G2) that underwent bioorthogonal *in situ* polymerization in response to intracellular GSH within mouse breast cancer cells to afford large assemblies (Fig. 14F).<sup>42</sup> These assemblies interacted with lysosomes, causing their expansion and enhancing lysosomal membrane permeabilization (Fig. 14G). This, in turn, upregulated major histocompatibility complex class I on the tumor cell surfaces



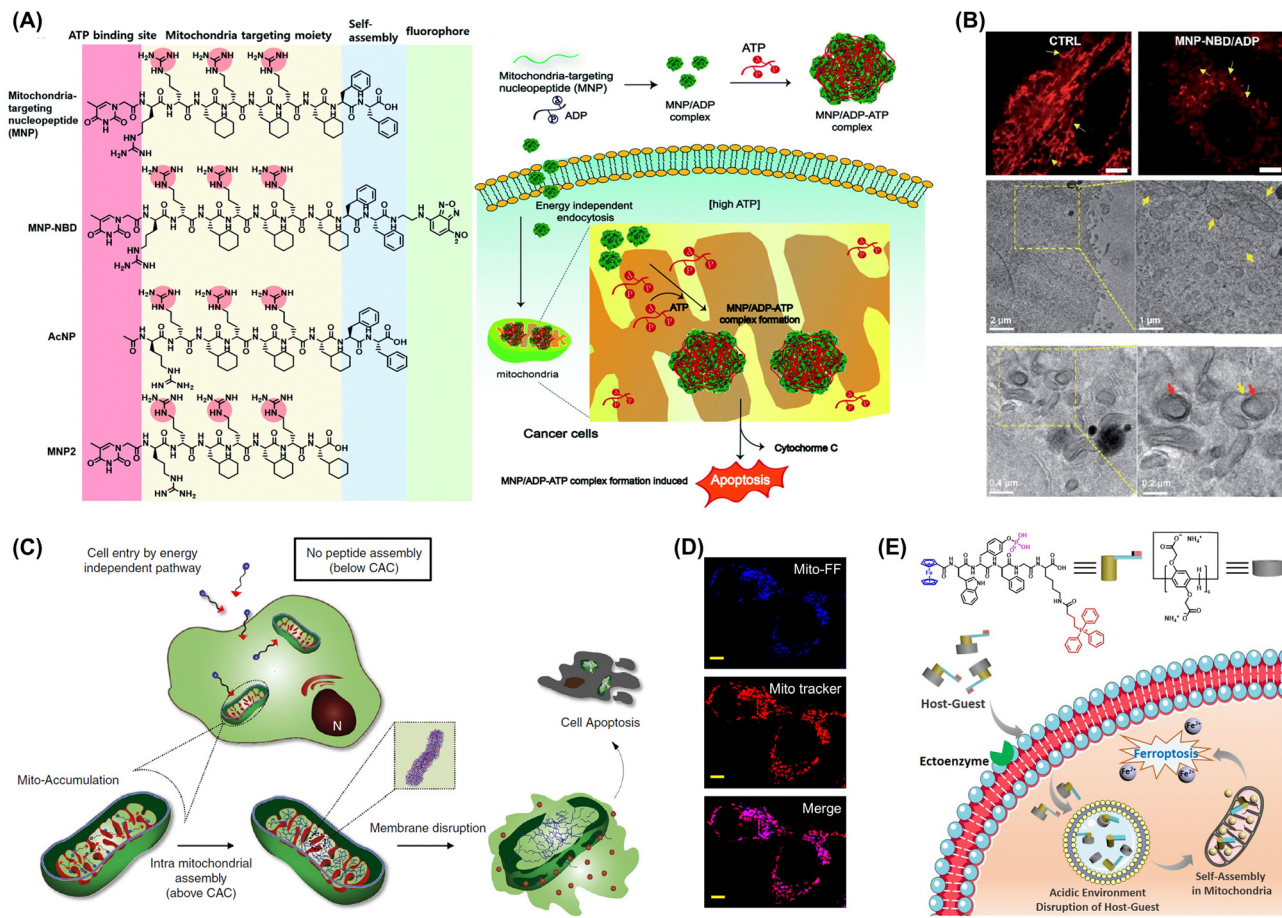


Fig. 13 (A) Trapping of adenosine triphosphate (ATP) within the mitochondria of cancer cells facilitated by MNP interacting with adenosine diphosphate (ADP) to trigger cell apoptosis. (B) TEM images of control cells and those exposed to the MNP/ADP complex for 4 h at a concentration of 50 mM. Adapted with permission from ref. 118. Copyright 2022 Royal Society of Chemistry. (C) Intramitochondrial formation of Mito-FF. (D) Mitochondrial colocalization of Mito-FF assessed using MitoTracker Red FM. Notable accumulation within the mitochondria is observed (scale bar: 5  $\mu$ m). Adapted with permission from ref. 117. Copyright 2017 Springer Nature. (E) (i) Assemblies generated *via* host-guest interactions between Fc-TPP1 and WP6 molecules and (ii) nanostructures resulting from the enzyme-mediated self-assembly of these host-guest complexes. Adapted with permission from ref. 113. Copyright 2022 American Chemical Society.

and resulted in tumor cell death. Furthermore, the therapeutic efficacy of camptothecin, a chemotherapeutic, was enhanced by conjugating it to SPR-G2.

**3.3.3. Nucleus targeting-induced aggregation.** The nucleus, as the core cellular structure, is not only the storage and replication center for genetic information but also a vital regulatory hub for activities such as cell metabolism, growth, differentiation, and apoptosis. As the storage and regulatory center for genetic information, the nucleus possesses a high specificity and sensitivity. Materials acting on the nucleus can precisely regulate gene expression and cellular life activities, thereby achieving precise treatment. Nucleus targeting-induced molecular aggregation enables the delivery of drug molecules with specific pharmacological effects to the nucleus to regulate or treat specific targets (such as DNA, RNA, and proteins) within the same.<sup>127</sup> Xu's group demonstrated the formation of intranuclear nanoribbons through the dephosphorylation of leucine-rich L- or D-phosphopeptides catalyzed by ALP, selectively targeting osteosarcoma cells (Fig. 15A).<sup>128,130</sup> In the presence of ALP,

the peptides underwent dephosphorylation to form micelles that subsequently formed nanoribbons (Fig. 15B). These peptide assemblies aggregated on cell membranes, entered cells *via* endocytosis, and accumulated within nuclei, especially in nucleoli (Fig. 15C). Proteomic analysis showed that these assemblies interacted with histone proteins. The peptides effectively induced osteosarcoma cell death while showing no toxicity to normal cells. Additionally, repeated exposure enhanced the sensitivity of cancer cells rather than promoting their resistance.

Zhan *et al.* developed a peptide conjugate (HpYss) incorporating 10-hydroxycamptothecin (HCPT) to mimic the transformation of artificial extracellular vesicles for targeted liver cancer therapy (Fig. 15D). This conjugate underwent sequential self-assembly triggered by extracellular ALP and intracellular GSH, leading to a morphological change from nanoparticles to nanofibers. An experimental phase diagram was created to illustrate the effects of varying ALP and GSH levels on self-assembly. Within HepG2 cells, HpYss formed dynamically transforming organelle-mimetic structures facilitating the efficient delivery of



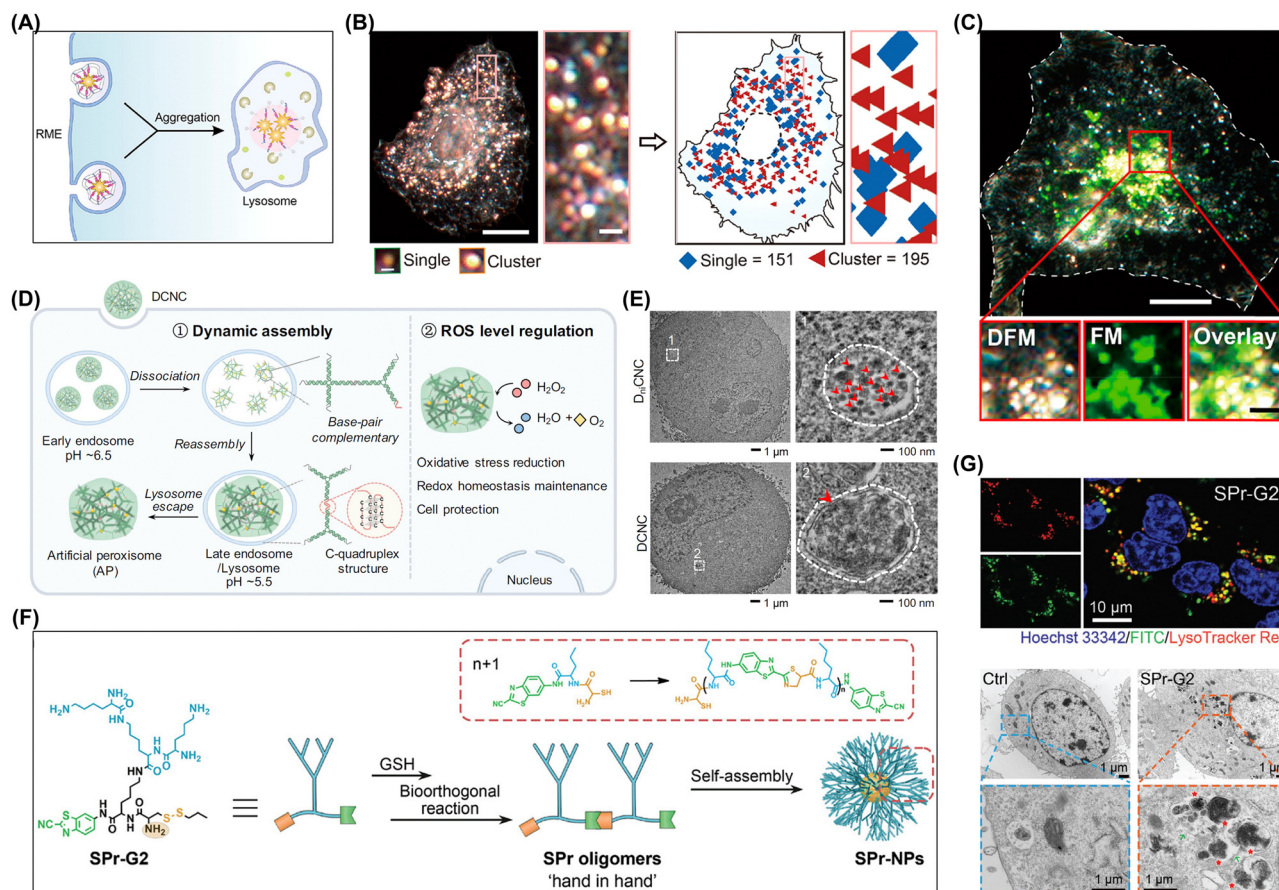


**Fig. 14** (A) Aggregation of lipo-SNPs induced by intracellular lysosome targeting during cellular uptake. (B) Left: Representative DFM images; right: corresponding pseudoimages obtained using the CBA method. Scale bars: 10  $\mu\text{m}$ , 1  $\mu\text{m}$  (enlarged), and 500 nm (bottom). (C) DFM-FM images revealing the colocalization of lipo-SNPs (bright yellow) alongside lysosomes (green), with scale bars measuring 10 and 2  $\mu\text{m}$  (insets). Adapted with permission from ref. 43. Copyright 2024 American Chemical Society. (D) Assembly of DCNC into artificial peroxisomes under acidic conditions within lysosomes. (E) Representative TEM images and a partial enlargement of MCF-7 cells treated with DnCNC and DCNC for 6 h. Adapted with permission from ref. 119. Copyright 2022 Springer Nature. (F) Plausible mechanism of aggregation induced by intracellular lysosome targeting and representative bio-TEM images of 4T1 cells treated with PBS or SPR-G2 ( $200 \times 10^{-6}$  M) for 3 h. Adapted with permission from ref. 42. Copyright 2022 Springer Nature.

HCPT to the nucleus. The transition from extracellular nanoparticles (50–100 nm) to intracellular nanofibers (4–9 nm wide) was found to be essential for effective nuclear delivery.<sup>56</sup> The nucleus targeting-induced aggregation of exogenous molecule features broad application prospects and challenges. Continuous in-depth research and technological innovation are expected to expand the scope of applications in disease treatment, gene editing, and other fields.<sup>129,179</sup>

## 4. Biomedical applications of intracellular aggregation

Intracellular molecular aggregation has broad biomedical application prospects, revealing the microscopic mechanisms of life activities while providing new insights for disease diagnosis and treatment. Endogenous biomolecular aggregation represents certain normal cellular processes, such as the formation of biomolecular condensates, which is an efficient means of organization and regulation developed by cells during

their evolution. These condensates function as small intracellular communities concentrating proteins or other biomolecules to perform specific tasks. Molecular aggregation facilitates gene expression processes by increasing the opportunities for intermolecular binding and thereby promotes gene expression.

By designing exogenous molecules to achieve precise and controllable aggregation within organisms, one can exploit the properties of molecular aggregates to further advance disease diagnosis and treatment. For example, exogenous molecules capable of aggregation-induced emission (AIE) and having specific targeting capabilities can be designed to aggregate within specific cells or tissues and thus enable precise disease localization and imaging. Additionally, by regulating the aggregation state of exogenous molecules within cells, one can achieve therapeutic effects. The aggregated molecules can also serve as tools for screening drugs or treatment methods. By observing aggregation state changes, one can assess the impact of drugs or treatment methods on cells or tissues and thereby screen out potentially effective drugs or therapies. Furthermore,



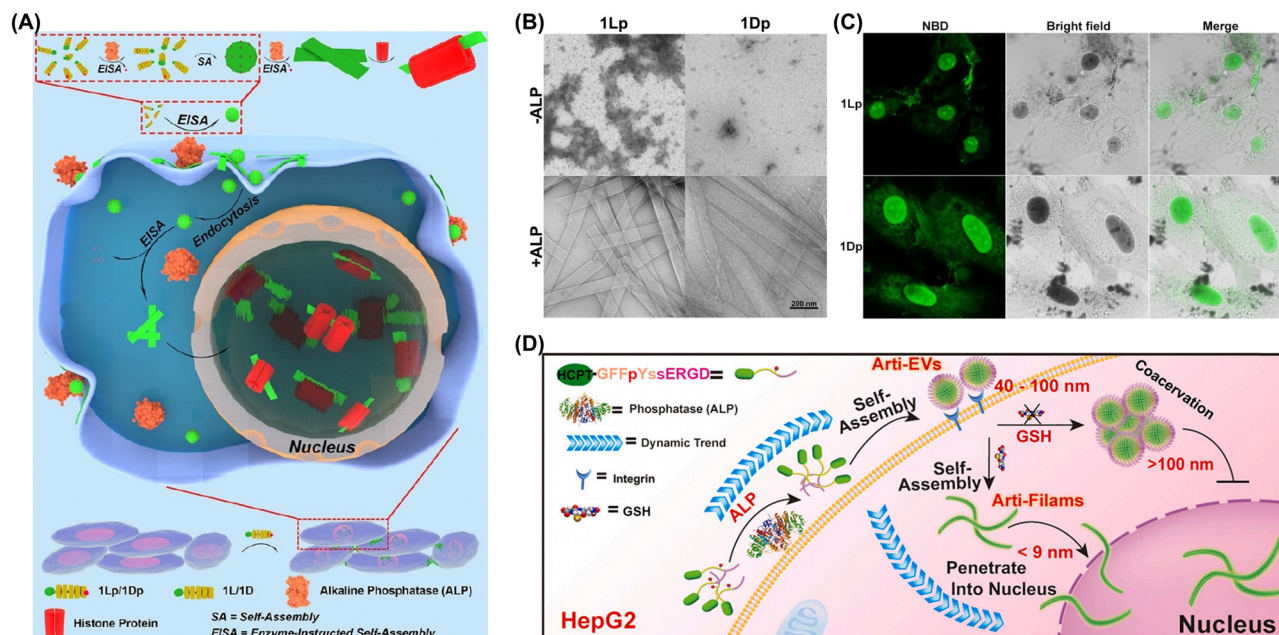


Fig. 15 (A) Enzyme-instructed self-assembly involving 1Lp or 1Dp and leading to the formation of intranuclear assemblies. Following cellular entry, the micelle transforms into nanoribbons through ALP-catalyzed dephosphorylation and subsequently coassembles with histone proteins within the cell nuclei. (B) TEM images of 1Lp and 1Dp at a concentration of 200  $\mu\text{M}$  in PBS, along with the resulting 1L and 1D, obtained 24 h after ALP addition. (C) CLSM images of SJS-A-1 cells treated with 1Lp or 1Dp at 200  $\mu\text{M}$  for 4 h. Adapted with permission from ref. 128. Copyright 2022 Wiley-VCH. (D) Proposed self-adaptive mechanism of membrane-to-nucleus delivery via an organelle-mimicking cascade process. Adapted with permission from ref. 56. Copyright 2022 KeAi Communications Co.

molecular aggregation can be used to construct biosensors or bioreactors for monitoring environmental changes within organisms or producing specific biological products.

#### 4.1. Exploration of life processes

**4.1.1. Biomolecule analysis.** Biomolecules, including enzymes, ATP, GSH, and ROS, play crucial roles in life activities and not only participate in the basic metabolic processes of cells but are also closely related to health status and disease progression.<sup>180–183</sup> By detecting and analyzing changes in the levels, structures, and functions of these biomolecules, one can predict the risk and progression of the related diseases and obtain important information for early disease diagnosis and treatment.<sup>184–187</sup> Numerous studies have reported biomolecule-responsive intracellular aggregation strategies enabling precise biomolecule detection.<sup>188–193</sup> By specifically recognizing biomolecules, these strategies can induce or alter the aggregation state of certain markers or signaling molecules and thereby achieve target molecule detection.

Xu *et al.* used driving primer-triggered polymerization-mediated metastable assembly to construct a well-structured metastable DNA nanostructure solely comprising two hairpin probes (HAPs), which is an important development in assembly techniques (Fig. 16A).<sup>194</sup> The characteristics and functions of this nanostructure were examined using atomic force microscopy and gel electrophoresis. Despite existing in a metastable state, the structure exhibited a considerable stability at physiological temperatures. This assembly technique could be modified for the *in situ* imaging of microRNA-21 within cancer cells

by tagging one of the hairpin probes with a fluorophore and quencher. In contrast to the conventional fluorescence probe-based *in situ* hybridization method, this DNA nanoassembly markedly improved imaging effectiveness within cancer cells and provided a sensitive indication of microRNA-21 expression levels, as revealed by confocal imaging (Fig. 16B).

Selectivity and specificity, as well as the stability and controllability of aggregation mechanisms and the efficiency and accuracy of signal amplification, are crucial factors.<sup>196–200</sup> Consequently, future research should further optimize and refine these strategies to enhance detection sensitivity and accuracy.<sup>201</sup> To achieve this goal, researchers need to delve deeper into the underlying principles of these strategies, exploring innovative approaches to improve their performance. This may involve refining the design of selective and specific recognition elements, enhancing the stability and predictability of aggregation processes, and optimizing signal amplification techniques to minimize noise and errors.<sup>202–209</sup> By concentrating on these aspects, one can improve detection technologies and realize more precise and dependable outcomes across diverse domains, including biomedicine, environmental monitoring, and food safety.<sup>210–212</sup> Liu's group developed a targeted light-up probe for intracellular thiol imaging in cells expressing integrin  $\alpha\text{v}\beta3$  (Fig. 16C).<sup>195</sup> This probe was carefully engineered using a highly soluble targeted cyclic RGD (cRGD) peptide containing five aspartic acid residues (referred to as D5), a TPE fluorogen for fluorescence, and a thiol-reactive disulfide linker cleavable under certain conditions. The related emission spectra revealed a positive correlation between GSH concentration and fluorescence intensity,



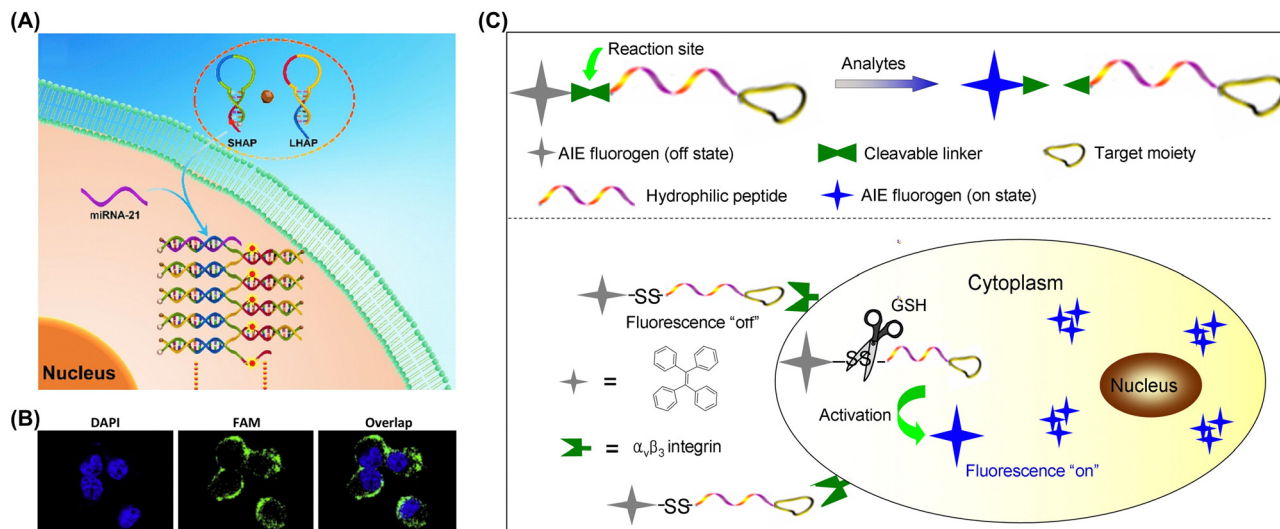


Fig. 16 (A) DNA nanoassembly triggered by microRNA-21 designed for the *in situ* visualization of miRNAs within cells. (B) *In situ* images of microRNA-21 within MCF-7 cells acquired using a mixture of SHAP and LHAP in the absence (upper panel) and presence (lower panel) of polymerase. Adapted with permission from ref. 194. Copyright 2017 Elsevier BV. (C) General strategy for probe design focusing on the cRGD-targeted imaging of intracellular thiols via  $\alpha_v\beta_3$  integrin-mediated cellular uptake, which leads to disulfide bond cleavage and subsequent fluorescence activation. Adapted with permission from ref. 195. Copyright 2014 Royal Society of Chemistry.

which was ascribed to the increase in the quantity of TPE aggregates forming in aqueous environments with elevated GSH concentrations. The probe was suitable for live cell imaging.

**4.1.2. Tumor imaging.** Exogenous molecular intracellular accumulation can be used for tumor imaging.<sup>213–217</sup> This technique is based on the principles of molecular imaging and relies on the aggregation characteristics of exogenous molecules (such as fluorescent molecules and radioactive tracers) within cells to visualize, describe, and measure biological processes in tumor tissues.<sup>218–220</sup> In tumor imaging, exogenous molecules are designed to specifically bind to tumor cells or tumor-related biomolecules.<sup>221–223</sup> When these molecules enter tumor tissues, they accumulate within tumor cells to generate visible imaging signals. This accumulation is usually due to the specific biomarkers or metabolic characteristics of tumor cells, which allow exogenous molecules to bind to and accumulate inside them. Exogenous molecular intracellular accumulation has broad prospects for applications in tumor imaging, including early tumor detection, localization, staging, and treatment monitoring.<sup>224,225</sup> However, this technology faces certain challenges, such as low probe specificity, sensitivity, and stability, as well as the insufficient resolution and high cost of imaging equipment. To improve imaging effectiveness, researchers are continuously exploring new probe materials and imaging methods and optimizing existing imaging technologies. Liang's group designed a small-molecule probe, Cys(StBu)-Lys(Ru(bpy)<sub>3</sub><sup>2+</sup>)-CBT, which self-assembled into nanoparticles (1-NPs) within cells and exhibited persistent unquenched phosphorescence (Fig. 17A).<sup>226</sup> This property enabled the long-term monitoring of biothiol activity in live HepG2 cells and tumors (Fig. 17B).

Moreover, Liang group further leveraged the biocompatible condensation reaction to craft a "smart" contrast agent, VC-Gd-CBT, which is responsive to CTSB and based on gadolinium

(Gd) (Fig. 17C).<sup>226</sup> This agent can autonomously assemble into larger Gd-laden nanoparticles within cells, facilitated by glutathione reduction and CTSB cleavage (Fig. 17D). This transformation amplifies the T2-weighted magnetic resonance (MR) contrast for imaging of tumors. Ye *et al.* designed a small-molecule probe labeled with fluorine-18, and this probe was crafted using a biocompatible CBT-Cys condensation reaction and cleverly adorned with a  $\gamma$ -glutamate ( $\gamma$ -Glu) substrate, which is recognizable by gamma-glutamyltransferase (GGT) (Fig. 17E).<sup>220</sup> This innovation aims to enhance PET imaging for detecting GGT levels in tumors of living nude mice.

**4.1.3. Monitoring of nervous system diseases.** As a monitoring method, the intracellular aggregation of exogenous molecules is not commonly used in the diagnosis and research of neurological diseases. However, biomarkers play a crucial role in the monitoring of neurological diseases. Neurological diseases often manifest as subtle symptoms in their early stages, and biomarkers can help detect abnormalities before symptoms appear or when they are mild, enabling early diagnosis.

Liang's group developed a NIR AIEgen (Ac-Trp-Glu-His-Asp-Cys(StBu)-Pra(QMT)-CBT (QMT-CBT)) reacting through a CBT-Cys click reaction upon caspase-1 activation (Fig. 18A).<sup>229</sup> This reaction formed cyclic dimers, which then aggregated into nanoparticles. This dual aggregation process activated the AIE signal, improving the AD imaging capability. Molecular dynamics simulations indicated that QMT within the QMT-NPs stacked more tightly than in the single aggregates of the control compound. The dual aggregation enhanced fluorescence intensity 1.9-, 1.7-, and 1.4-fold compared with single aggregation states *in vitro*, within cells, and in a living AD mouse model, respectively (Fig. 18B and C).

Changes in amyloid-beta ( $A\beta$ ) and tau protein levels in the cerebrospinal fluid can occur years before clinical symptoms of AD appear. Fu *et al.* developed a strategy for the rational design



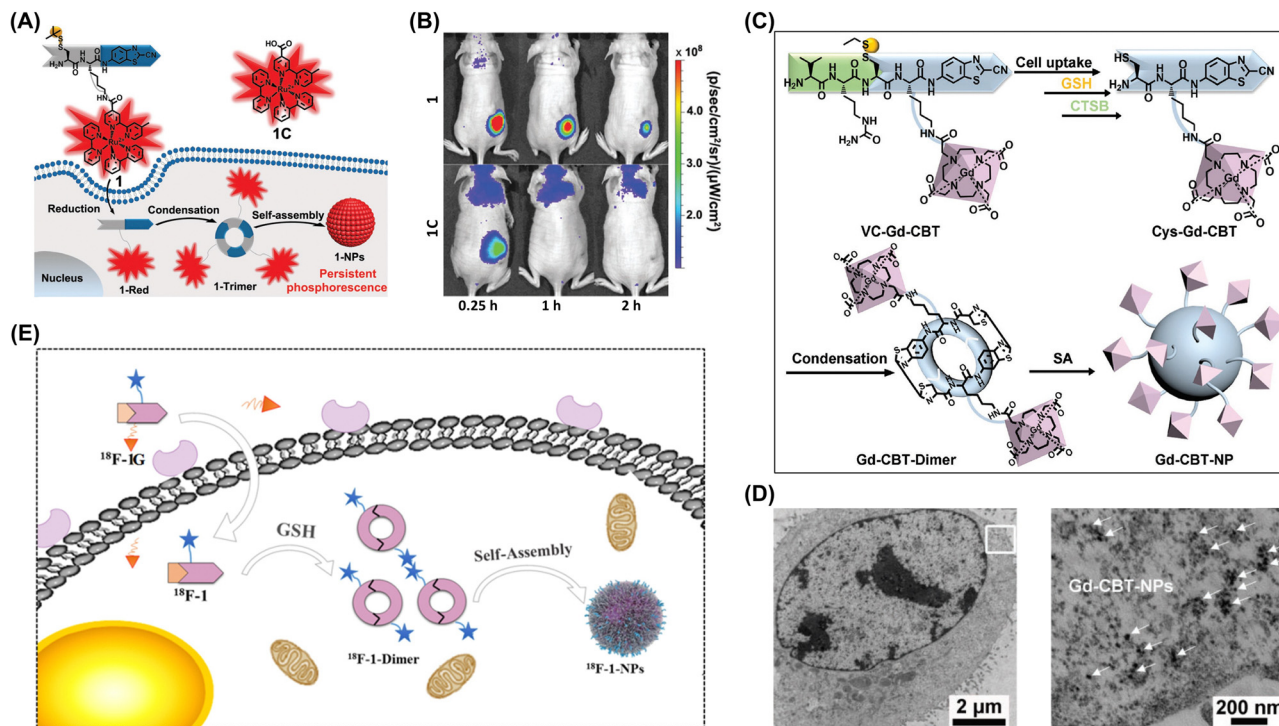


**Fig. 17** (A) Chemical structures of **1** and **1C** and cartoon illustrating the intracellular reduction-controlled condensation of **1** resulting in the self-assembly of **1-NPs** for tumor imaging with persistent phosphorescence. (B) Time-course phosphorescence images of nude mice xenografted with HepG2 tumor cells acquired at 0.25, 1, 2, 4, 12, and 24 h after probe injection. Adapted with permission from ref. 226. Copyright 2018 Royal Society of Chemistry. (C) CTSB-acquid intracellular formation of Gd-CBT-NPs aimed at enhancing T2-weighted magnetic resonance imaging at 9.4 T. (D) TEM image of MDA-MB-231 cells treated with 300  $\mu\text{M}$  VC-Gd-CBT for 8 h. Adapted with permission from ref. 227. Copyright 2023 Wiley-VCH. (E) Reduction-induced self-assembly of a  $\gamma$ -glutamyltransferase (GGT)-targeted probe into nanoparticles for *in vivo* PET imaging. Adapted with permission from ref. 228. Copyright 2020 American Chemical Society.

of NIR AIE-active probes specifically targeting A $\beta$  plaques (Fig. 18D).<sup>230</sup> The authors incorporated a lipophilic  $\pi$ -conjugated thiophene bridge to shift the emission wavelength into the NIR range and improve blood-brain barrier permeability. The QM-FN-SO<sub>3</sub> probe successfully addressed the AIE challenge of balancing lipophilicity with aggregation in aqueous environments, enabling the high-fidelity detection of A $\beta$  plaques *in vivo* with an exceptional binding affinity. This probe is a superior alternative to commercial probes, such as ThT or ThS (Fig. 18E). The dosage and safety of exogenous molecules should be controlled to prevent unnecessary nervous system damage, and monitoring results should be interpreted alongside other biomarkers and clinical manifestations for a comprehensive assessment.

**4.1.4. Detection of bacterial infections.** Bacteria trigger a series of biochemical reactions within infected cells.<sup>231</sup> Exogenous molecules can be designed to aggregate under bacterial infection conditions.<sup>232</sup> This aggregation can be detected through optical, magnetic, or other physical means, indirectly indicating the presence of bacterial infections. Such molecules may exhibit high specificity and sensitivity, accurately reflecting the bacterial infection status.<sup>79,233,234</sup> The aggregation of exogenous molecules within cells can be combined with other technologies, such as gene editing and single-cell sequencing, to achieve a deeper understanding of bacterial infections and more precise treatment. Dai *et al.* created an AIEgen with

metabolic labeling and *in situ* photodynamic scavenging capabilities *via* click chemistry. This AIEgen rapidly and selectively labeled live *Mycobacterium tuberculosis* within 10 min by integrating into cytoderm peptidoglycan biosynthesis (Fig. 19A)<sup>235</sup> and enabled a 50-fold increase in tuberculosis detection sensitivity compared with traditional acid-fast bacilli methods. The AIEgen also achieved efficient labeling of intracellular *Bacillus Calmette Guerin*, while the control group failed to produce similar results, indicating that the AIEgen holds promise as a potential reagent for clinical detection of intracellular *Mycobacterium tuberculosis* and diagnosis of latent tuberculosis infection (Fig. 19B).

The intracellular invasion and persistence of *Staphylococcus aureus* within phagocytic cells contribute to the challenges in treating *S. aureus* infections and potential for developing antibiotic resistance.<sup>76,237</sup> Identifying phagocytic cells infected by *S. aureus* is crucial for guiding antibiotic therapy and mitigating drug resistance. Wang's group reported a peptide-chlorophyll photoacoustic probe that utilized the activation of caspase-1 enzymes in immune cells in response to infected sites and was subsequently cleaved and assembled to enable the imaging of bacterial infection sites (Fig. 19C).<sup>236</sup> Once the probe entered macrophages through receptor-mediated endocytosis, caspase-1 enzymes were activated and cleaved the probe. Owing to the change in the hydrophilic and hydrophobic properties, the



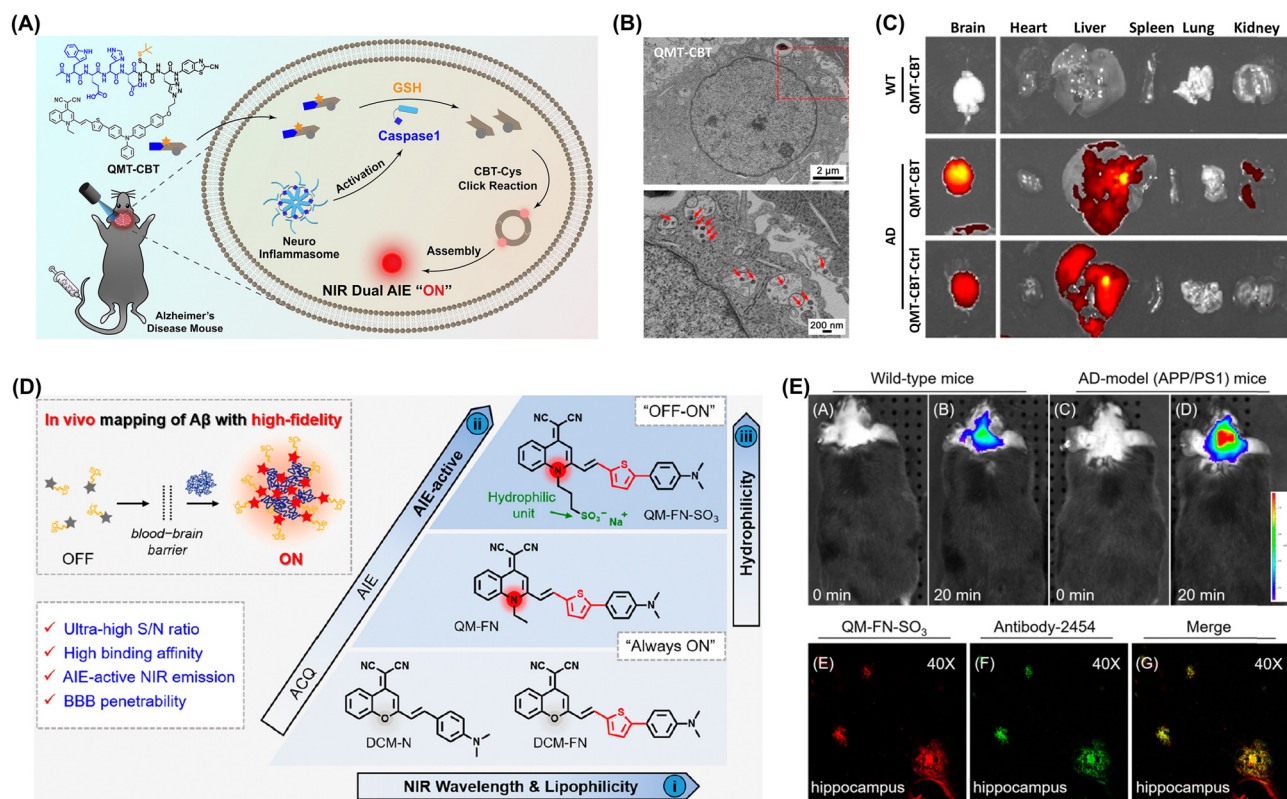


**Fig. 18** (A) Caspase-1-instructed dual aggregations of QMT-CBT activating NIR fluorescence and enhancing Alzheimer's disease (AD) imaging. (B) Bio-TEM images of  $A\beta_{25-35}$ -treated PC12 cells incubated with 10  $\mu\text{M}$  QMT-CBT for 1 h. (C) Ex vivo fluorescence images displaying the brain and major organs of WT and AD mice. Adapted with permission from ref. 229. Copyright 2023 American Chemical Society. (D) Step-by-step strategy used to overcome the limitations of commercial ThT and leading to the development of ultrasensitive off-on NIR probes. (E) In vivo mapping illustrating  $A\beta$  deposition in an AD model (APP/PS1 transgenic) mouse. Comparison of fluorescence images acquired 20 min after the intravenous injection of QM-FN-SO<sub>3</sub> into wild-type and APP/PS1 mice. Adapted with permission from ref. 230. Copyright 2019 American Chemical Society.

cleaved substrate molecules aggregated and assembled through hydrophobic interactions, achieving a good photoacoustic imaging effect and enabling the detection of intracellularly hidden bacteria (Fig. 19D). This method is effective for detecting early-stage infections and assessing treatment efficacy in later stages. Additionally, photosensitizers can be used to effectively kill intracellular host-associated bacteria and thus reduce the emergence of resistant strains and recurrent infections.

## 4.2. Regulation of cell fate

### 4.2.1. Drug resistance mitigation.

Drug resistance considerably complicates cancer treatment, as cancer cells can overexpress drug efflux pumps to expel low-molecular-weight chemotherapeutics and thus reduce their in-cell levels and, hence, therapeutic efficacy.<sup>78,238</sup> This problem can be addressed through the use of intracellular aggregated drug reservoirs to control the formation and dissociation of aggregates and thus retain anticancer drugs within cancer cells.<sup>125,126</sup> Intracellular aggregation enhances the rapid recruitment and long-term retention of drugs, enabling sustained effective doses that improve therapeutic outcomes.<sup>239,240</sup>

Intracellular biomolecular aggregates can be used as drug reservoirs to extend the residence time of drugs in drug-resistant cancer cells. Du *et al.* developed a tripeptide, phenylalanine-phenylalanine-tyrosine (Phe-Phe-Tyr or FFY), that underwent

oxidation and spontaneously assembled into nanoparticles strongly interfering with microtubules and effectively reversing drug resistance in melanoma (Fig. 20A).<sup>241</sup> In the presence of tyrosinase, FFY was converted into a melanin-like dimer (mFFY), which self-assembled into mFFY assemblies. These assemblies inhibited tubulin self-polymerization, resulting in a notable G2/M cell cycle arrest (13.9% higher compared with the control) (Fig. 20B).

*In vivo* experiments showed that the peritumoral injections of FFY reduced resistant melanoma tumor volumes by 87.4% compared with controls. Wang *et al.* demonstrated that nucleopeptide assemblies can selectively capture ATP in complex environments, such as serum and cytosol (Fig. 20C).<sup>242</sup> These assemblies preferentially sequester ATP over adenosine diphosphate (ADP), and enzymes that convert ATP and ADP influence the nanostructures formed by nucleopeptides and nucleotides. The nucleopeptides efficiently sequester ATP within cells to decelerate efflux pumps in multidrug-resistant cancer cells and thus enhance the effectiveness of DOX (Fig. 20D).

### 4.2.2. Drug targeting improvement.

The intracellular aggregation of exogenous molecules is an effective strategy for the enhancement of drug targeting.<sup>243-246</sup> Specific molecular design can endow drugs or their carriers with the ability to aggregate within cells and thereby improve the ability of drugs



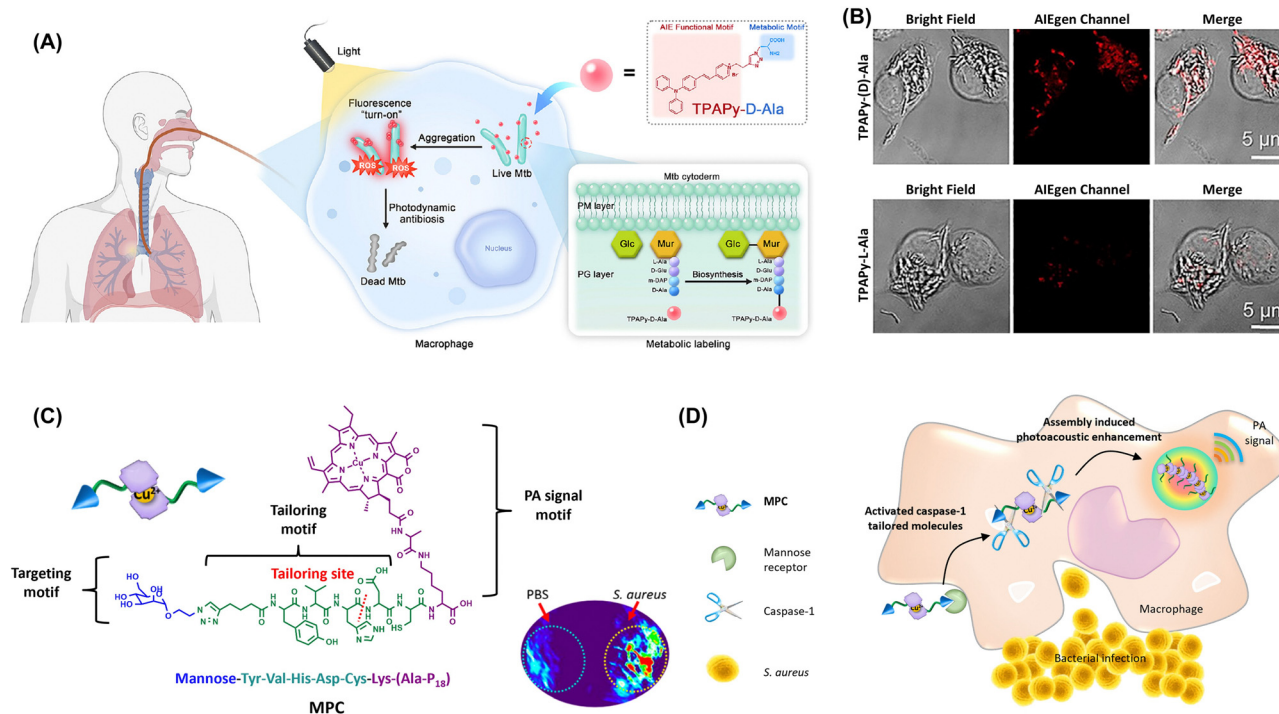


**Fig. 19** (A) Peptidoglycan metabolic labeling AI-Egen (TPAPy-D-Ala) for rapid and precise *Mycobacterium tuberculosis* diagnosis and *in situ* elimination in macrophage cells. (B) Labeling of intracellular BCG with TPAPy-D-Ala. Adapted with permission from ref. 235. Copyright 2023 Cell Press. (C) Macrophage chemotaxis-instructed detection of *Staphylococcus aureus* infection *in vivo* and the molecular component of the probe (MPC). (D) MPC is actively targeted to the mannose receptor of the macrophage cell. Under the pathogen-associated molecular patterns, the activated caspase-1 inside the macrophage cells specifically tailors MPC to induce self-assembly and retention. Adapted with permission from ref. 236. Copyright 2018 American Chemical Society.

to specifically recognize and bind to target cells or tissues.<sup>247,248</sup> Molecular aggregation increases the local concentration of drugs or their carriers within the target cells or tissues.<sup>249–252</sup> Additionally, aggregated drugs may have longer half-lives and therefore be less susceptible to rapid elimination and exert their effects for a longer time. By carefully designing the structure and properties of aggregated molecules, one can achieve targeted recognition and binding to specific cells or tissues and thus reduce damage to nontarget tissues. Gao *et al.* used legumain to induce the aggregation of AuNPs and thus enhance the retention of chemotherapeutics in brain tumors (Fig. 21A).<sup>253</sup> This method improved AuNP retention within glioma cells *in vitro* and *in vivo* (Fig. 21B) by preventing the exocytosis of these nanoparticles and minimizing their return to the bloodstream. Additionally, conjugating DOX to AuNPs-A&C *via* a pH-sensitive linker enhanced glioma treatment efficacy. To address the poor solubility, limited cellular uptake, and inadequate cell selectivity of macromolecules, Du *et al.* used a chemical modification strategy based on enzyme-instructed self-assembly (Fig. 21C).<sup>254</sup> By targeting protoporphyrin IX (PpIX) and its metal complex (Zn-PpIX) for modification, this approach combined enzymatic transformation with molecular self-assembly to improve solubility and enhance intracellular uptake in cancer cells.

Despite the potential of the intracellular aggregation of exogenous molecules for enhancing drug targeting, this strategy faces certain challenges, as exemplified by the need to (i)

precisely control the size, shape, and stability of molecular aggregates; (ii) avoid toxicity or damage to cells caused by aggregated drugs; and (iii) further optimize the mechanisms and conditions for drug release.<sup>255–258</sup> Yu's group introduced a GSH-responsive *in situ* self-sorting peptide assembly system targeting multiple organelles within cancer cells to induce their combinatorial dysfunction and death (Fig. 21D).<sup>259</sup> This system utilized two peptides derived from lipid-inspired peptide interdigitating amphiphiles (E3C16E6) and peptide bola-amphiphiles (EVMSeO). The unique organization patterns of these peptides enabled GSH-induced self-sorting into isolated nanofibrils within cells facilitated by the cleavage of disulfide-linked hydrophilic domains or reduction of selenoxide groups. The self-sorting behavior of these peptide assemblies within HeLa cells was characterized using super-resolution structured illumination microscopy (Fig. 21E). With the continuous development of biotechnology, nanotechnology, and materials science, these challenges will be overcome, and the application of exogenous intracellular molecular aggregation in drug targeting will become more extensive and thorough. The use of the intracellular aggregation of exogenous molecules to enhance drug targeting is an innovative and promising strategy. By precisely designing and optimizing the structure and properties of molecular aggregates, one can realize specific recognition and binding to target cells or tissues and thereby improve drug efficacy and safety.



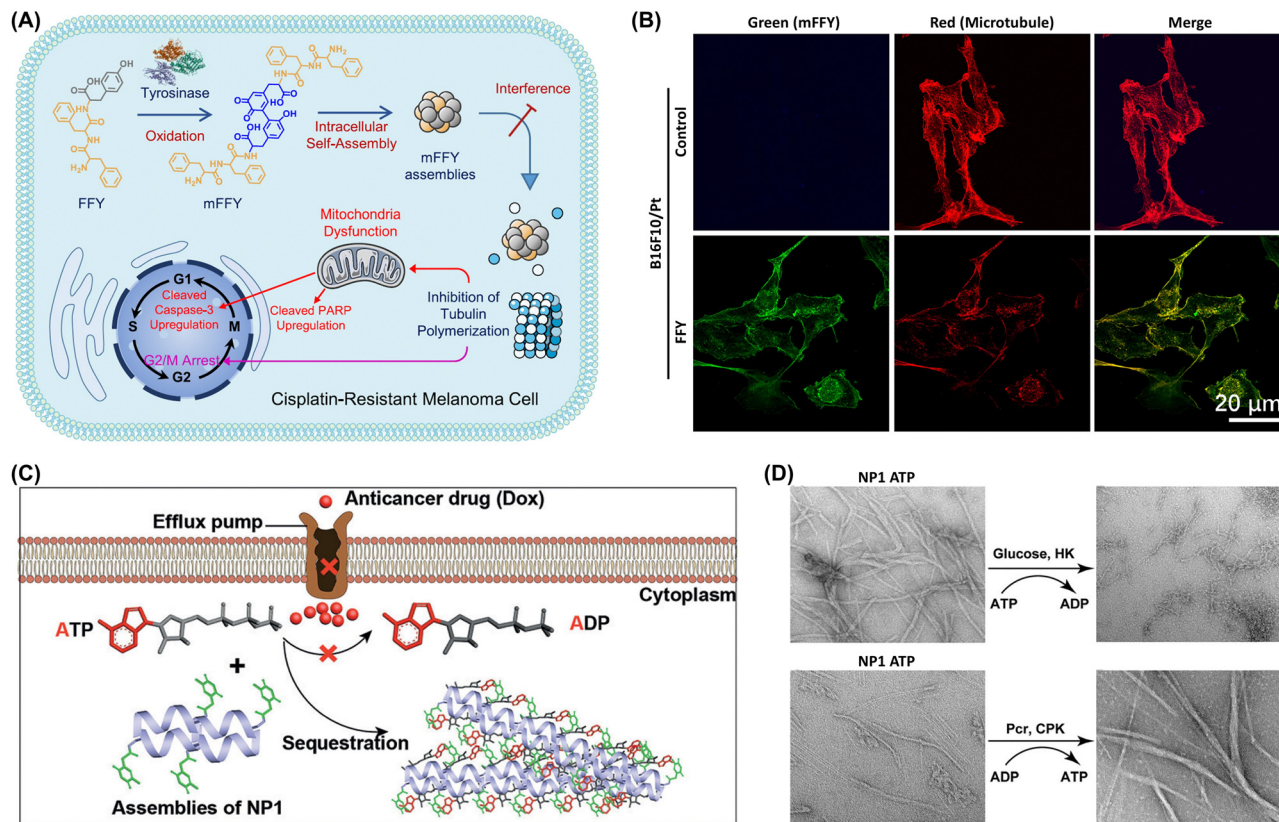


Fig. 20 (A) Tyrosinase-induced tripeptide assemblies and their apoptotic effects on cisplatin-resistant melanoma cells. (B) Intracellular localization of green (mFFY) and red (microtubule) fluorescence signals after 24 h of treatment. Adapted with permission from ref. 241. Copyright 2022 American Chemical Society. (C) Proposed mechanism of ATP sequestration by NP1 assemblies in multidrug-resistant cells leading to the deceleration of drug efflux and drug efficacy enhancement. (D) NP1 assemblies with ATP formed in the presence of glucose. Adapted with permission from ref. 242. Copyright 2018 Wiley-VCH.

**4.2.3. Cell apoptosis/necrosis induction.** Cell necrosis, a pathological sequence involving irreversible cell damage and eventual demise, is triggered by a multitude of factors, including hypoxia, physical insults, chemical exposure, biological agents, and immune reactions. This process is characterized by the swelling of organelles, plasma membrane disruption, and eventual cell lysis, leading to the leakage of cellular contents into the surrounding tissue and its subsequent injury. The abnormal accumulation of exogenous molecules within cells can exert profound effects on cellular architecture and functionality.<sup>260,261</sup> Specifically, such accumulation may alter the plasma membrane structure, enhancing its permeability and potentially causing rupture, as well as impair the normal functioning of organelles, *e.g.*, mitochondria and the endoplasmic reticulum. Moreover, the accumulation of exogenous molecules can disrupt the normal apoptotic pathway, preventing cells from undergoing programmed death and redirecting them toward necrosis.<sup>262</sup>

Guo *et al.* used heterogeneous peptide–protein assembly to selectively phosphorylate proteins and thereby activate the necroptotic signaling pathway and facilitate cell necroptosis (Fig. 22A).<sup>263</sup> Inspired by natural necrosome structures formed by receptor-interacting protein kinases (RIPKs) 1 and 3, the authors designed kinase-biomimetic peptides using natural or *D*-amino acids or by connecting *D*-amino acids in a retro-inverso

(DRI) configuration. These peptides self-assembled into nanofibrils and accelerated the assembly of PR3 when mixed with the same. The DRI–PR1 peptide exhibited a strong binding affinity for the RIPK3 protein, showing a specific cytotoxicity toward colon cancer cells overexpressing RIPK3 (Fig. 22B). Mechanistic studies indicated that RIPK1-biomimetic peptides enhanced the phosphorylation of RIPK3, activating the necroptotic signaling pathway responsible for cell death while not substantially increasing inflammatory cytokine secretion (Fig. 22C).

The aggregation of exogenous molecules within cells may trigger signaling pathways closely related to apoptosis regulation.<sup>218,265,266</sup> For instance, certain exogenous molecules can activate the caspase pathway and thus initiate apoptosis. The aggregation of exogenous molecules may also impact the function of organelles such as mitochondria and the endoplasmic reticulum, which play crucial roles in apoptosis. Damage to mitochondria can trigger the onset of apoptosis.<sup>267,268</sup> The abovementioned aggregation may also affect cell cycle progression. By interfering with the regulatory mechanisms of the cell cycle, exogenous molecules can induce apoptosis at specific stages. In cancer treatment, the effective inhibition of tumor growth and spreading can be achieved by inducing apoptosis in tumor cells.

Wang's group developed a self-assembled scaffold using a cyclic peptide recognizing the membrane protein EGFR and



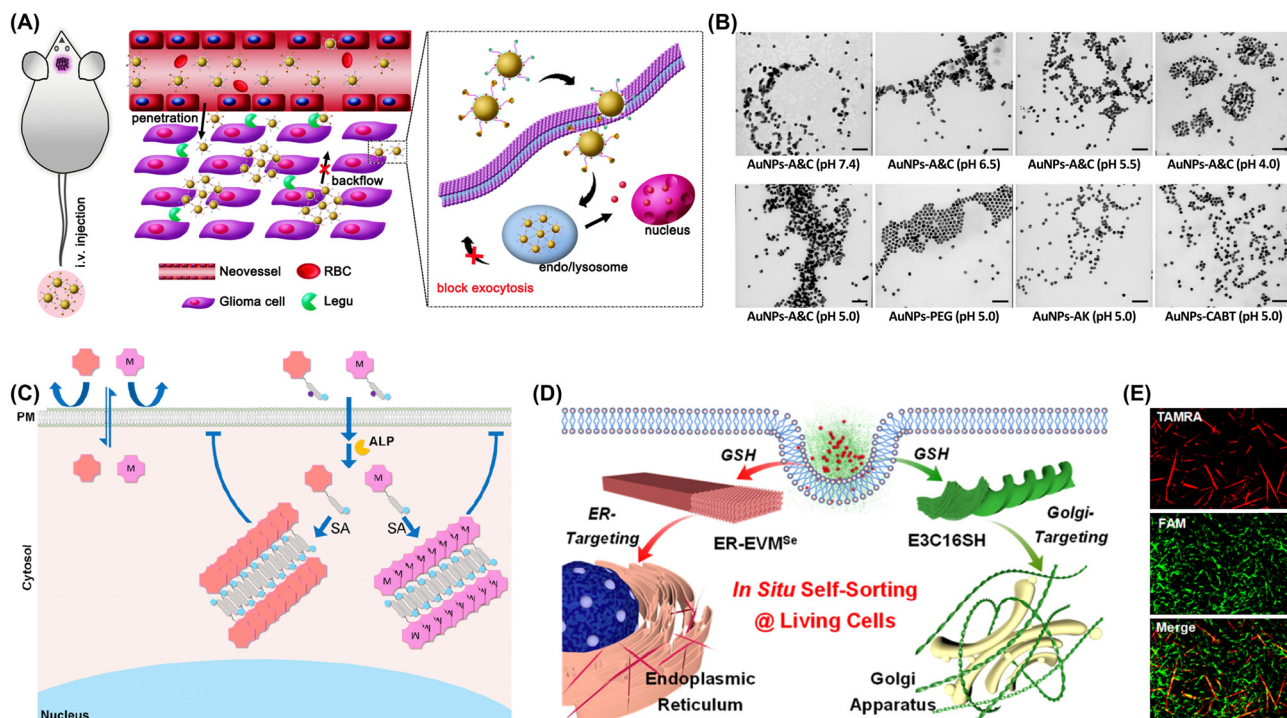


Fig. 21 (A) *In vivo* behavior of AuNPs-doxorubicin-A $\beta$ C following intravenous injection (increased accumulation is highlighted). (B) TEM images of AuNPs-A $\beta$ C incubated with legumain at various pH for 12 h and those of control nanoparticles incubated at pH 5.0 for the same duration. Scale bar: 100 nm. Adapted with permission from ref. 253. Copyright 2016 American Chemical Society. (C) Immobilization of macromolecules or macromolecule-metal complexes within the cytosol. Adapted with permission from ref. 254. Copyright 2022 American Chemical Society. (D) *In situ* self-sorting peptide assemblies within living cells. (E) SIM images of mixed E3C16 (0.5 mM) and EVMSe (0.5 mM), with FAM-E3C16 (1  $\mu$ M) and TAMRA-EVMSe (1  $\mu$ M) as fluorescence probes, viewed under channel I (FAM), channel II (TAMRA), or merged channels. Adapted with permission from ref. 259. Copyright 2022 American Chemical Society.

disrupting its signaling pathway through multivalent interactions driven by assembly-induced aggregation (Fig. 22D).<sup>264</sup> Upon introduction to cells, PAD-1 oligomers targeted and bound to overexpressed EGFR on cancer cell membranes, effectively inhibiting its function. This binding triggered endocytosis, leading to the accumulation of PAD-1 and EGFR within lysosomes. Inside the lysosomes, PAD-1 and EGFR formed nanofibers to induce lysosomal membrane permeabilization (LMP) (Fig. 22E). This permeabilization disrupted EGFR homeostasis and halted the downstream signaling vital for cancer cell survival while leading to the release of protein aggregates that induce endoplasmic reticulum stress and ultimately resulting in the selective apoptosis or necrosis of cancer cells.

**4.2.4. Immunotherapy enhancement.** Immunotherapy is an effective cancer treatment that leverages the natural capabilities of the immune system by activating, enhancing, or improving the patient's immune response to inhibit or kill tumor cells. This method typically involves multiple mechanisms, including boosting the activity and proliferation of immune cells and enhancing their ability to recognize tumor cells. Exogenous molecules (such as antibodies and peptides) that can specifically recognize tumor cells can accumulate within the same to trigger an immune response.<sup>269–271</sup> Some exogenous molecules may possess immunogenicity, that is, stimulate the immune system to produce an immune response

against tumor cells. After these molecules accumulate within tumor cells, they may increase the immunogenicity of the same and make them more susceptible to recognition and attack by the immune system.<sup>272</sup> Chen's group introduced a cancer vaccine leveraging mRNA compartmentalization through a multimodule DNA nanostructure (MMDNS) assembly designed to enhance mRNA translation efficiency (Fig. 23A).<sup>273</sup> This MMDNS compartment facilitated the localization of mRNA and relevant reaction molecules *in situ* and was constructed *via* a programmable DNA HCR-based strategy, integrating antigen-coded mRNA, CpG oligodeoxynucleotides (ODNs), acid-responsive DNA sequences, and aptamers targeting dendritic cells. In acidic lysosomal environments, the MMDNS assembled into microscale aggregates enhancing the adjuvant efficacy of CpG oligodeoxynucleotides. These aggregates subsequently escaped into the cytoplasm, creating a compartment supporting the efficient translation of nearby mRNA transcripts by localizing necessary reaction molecules and thereby increased the efficiency of the immune response.

The intracellular aggregation of exogenous molecules provides a novel approach to tumor immunotherapy. However, further research and exploration are required to ensure the effectiveness and safety of this strategy. In particular, efficient, specific, and low-toxicity exogenous molecules should be identified to guarantee treatment safety and efficacy. Precise immune response regulation is also needed to avoid autoimmune



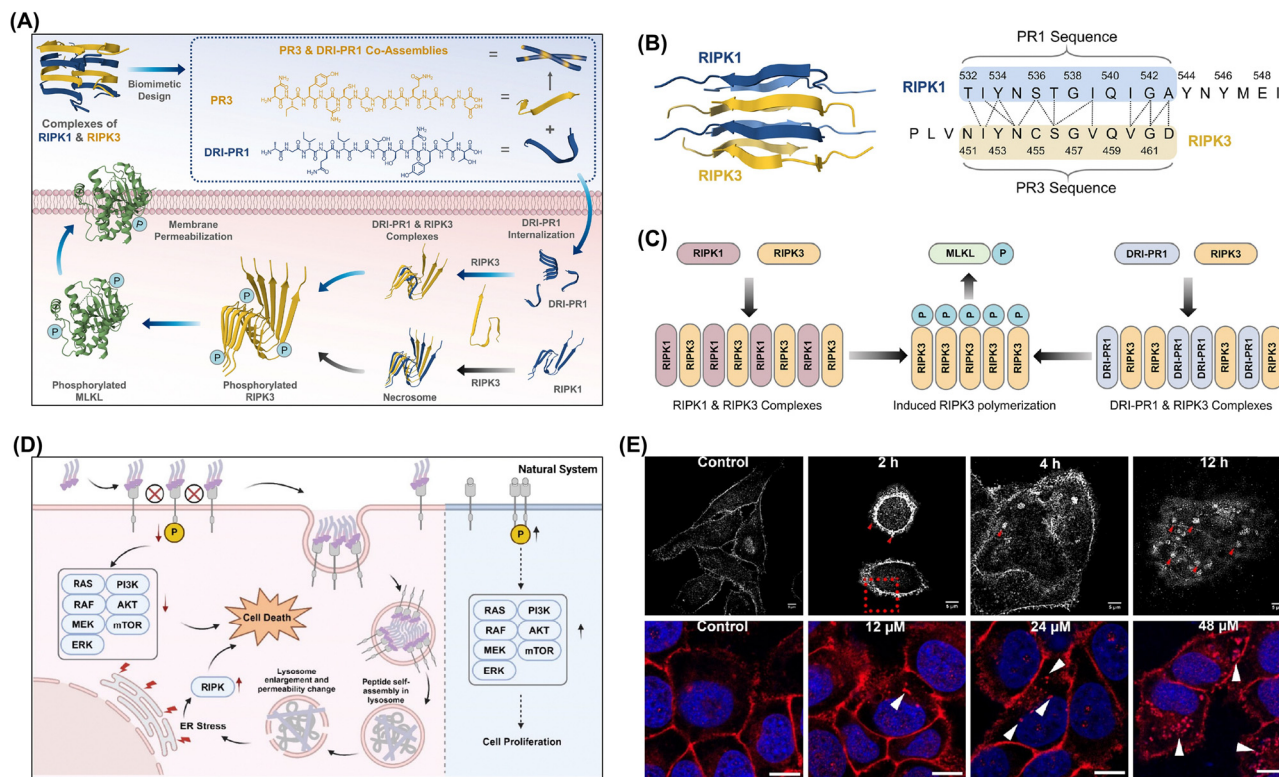


**Fig. 2** (A) Design of kinase-mimetic peptides PR3 and DRI-PR1 and role of DRI-PR1 in promoting RIPK3 aggregation to activate the necroptotic signaling pathway and induce cell necroptosis. (B) Design principle of RIPK1-mimetic peptide PR1 and RIPK3-mimetic peptide PR3 showcasing the truncation of the RIHM motifs from RIPK1 and RIPK3, respectively. (C) Natural necroptosis induced by RIPK1-RIPK3 complexes compared with necroptosis induced by RIPK1-mimetic peptides; DRI-PR1-RIPK3 complexes act as artificial necrosomes, inducing RIPK3 aggregation and phosphorylation and thus activating the necroptotic signaling pathway and promoting cell death. Adapted with permission from ref. 263. Copyright 2023 Wiley-VCH. (D) Peptide assemblies aimed at modulating the clustering of the membrane protein EGFR to inhibit cancer cells. (E) Structured illumination microscopy images showing EGFR clusters on the cell membrane and aggregates in the cytoplasm of HeLa cells treated with varying concentrations of PAD-1 (12, 24, and 48  $\mu$ M) for 24 h and revealing the concentration-dependent formation of EGFR aggregates. Adapted with permission from ref. 264. Copyright 2024 American Chemical Society.

reactions or immune escape phenomena caused by overactivation. Xing *et al.* developed lysosomal-targeting aggregated nanoparticles (LTANPs) for cancer treatment inspired by lysosomal swelling caused by the excessive accumulation of nondegraded substances. These nanoparticles were engineered with a specific surface composition, properties, and interparticle interactions to facilitate accumulation in tumors and selective aggregation within cancer cell lysosomes (Fig. 23B).<sup>274</sup> This aggregation resulted in irreversible lysosomal swelling and induced LMP in cancer cells (Fig. 23C). LMP triggered by nanoparticle aggregation effectively initiated immunogenic cell death by disrupting the autophagy-lysosome pathway, leading to robust antitumor immune responses and converting tumor immunogenicity from cold to hot in a melanoma model. Additionally, the LTANPs could be combined with clinically approved programmed death ligand-1 antibodies to enhance T cell-mediated antitumor immunity, which notably improved antitumor efficacy and reduced tumor recurrence and metastasis.

#### 4.2.5. Photodynamic therapy (PDT) and PTT promotion.

The intracellular aggregation induction of exogenous molecules has great potential for enhancing the efficiency of PDT and PTT.<sup>175,275-277</sup> The intracellular aggregation of photosensitizer

molecules increases their local concentration, thereby enhancing the probability of interaction between the photosensitizer and light and increasing the effectiveness of PDT.<sup>278-280</sup> Some photosensitizers may be unstable when present alone and are prone to degradation or inactivation. However, in the form of aggregates, they may form more stable structures, which helps extend their retention time within cells and enhance therapeutic efficacy.<sup>281</sup> In PDT, photosensitizers absorb light to generate cytotoxic ROS. When photosensitizer molecules aggregate, they may more effectively absorb light and produce more ROS, which enhances the efficacy of PDT. Wang *et al.* devised a nanosystem (TPFcNP) using a hydrophobic photosensitizer (TMPP) featuring multiple C=C bonds (Fig. 24A).<sup>282</sup> This photosensitizer was integrated with a ferrocene-containing amphiphilic block copolymer (PEG-*b*-PMAEFC). In the tumor microenvironment, this combination catalyzed H<sub>2</sub>O<sub>2</sub> decomposition *via* the Fenton reaction, producing hydroxyl radicals ( $\cdot$ OH). These radicals promoted an addition reaction between the abundant water-soluble GSH in tumor cells and C=C bonds of TMPP, improving the hydrophilicity of the photosensitizer and reducing aggregation. *In vitro* and *in vivo* studies showed that this approach considerably enhances the therapeutic efficacy of PDT.



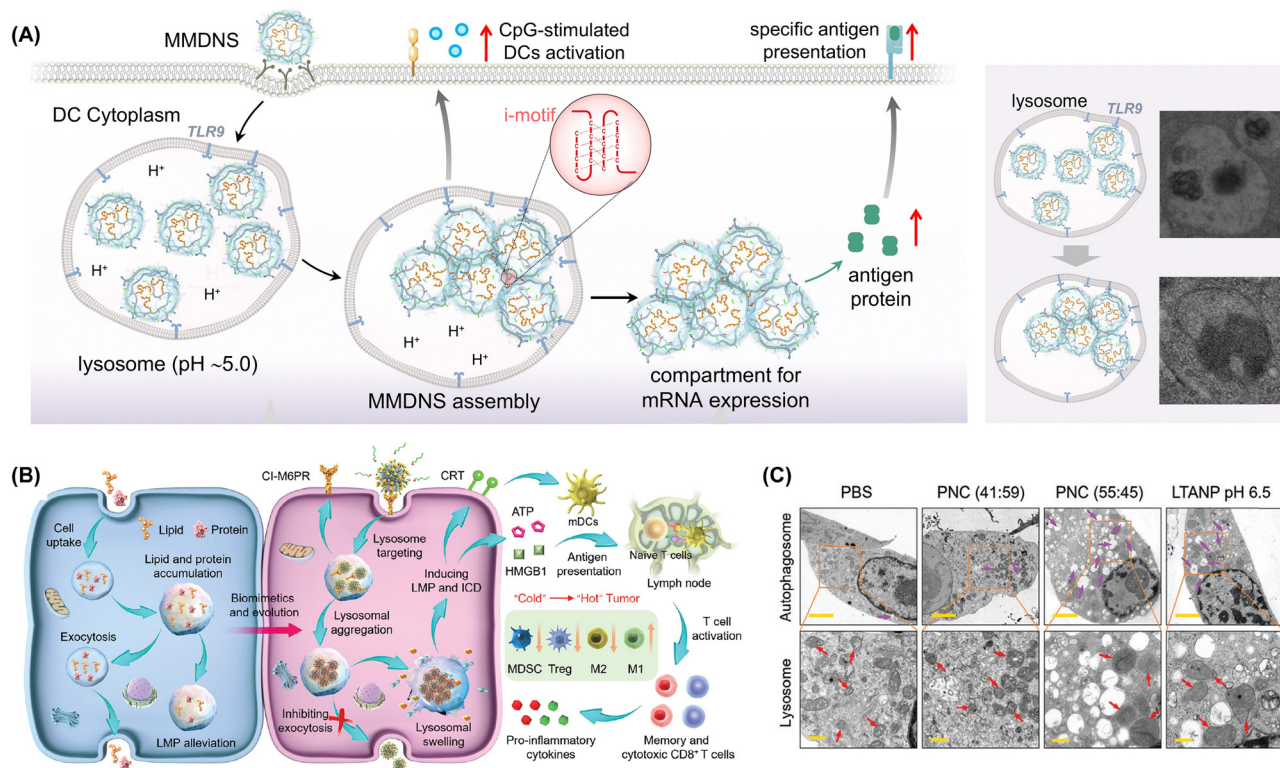


**Fig. 23** (A) Intracellular acidic environments induce the assembly of MMDNS in lysosomes, allowing the assembled aggregates to escape into the cytoplasm and create compartments for mRNA expression. Adapted with permission from ref. 273. Copyright 2024 American Association for the Advancement of Science. (B) LTANP-targeted aggregation in lysosomes inducing lysosomal membrane permeabilization and immunogenic cell death for cancer immunotherapy via a biomimetic strategy. (C) Bio-TEM images of B16F10 cells treated with various formations (scale bar: 2  $\mu\text{m}$ ). Regions of interest are highlighted with orange rectangles (scale bar: 0.5  $\mu\text{m}$ ), with purple and red arrows indicating autophagosomes and lysosomes, respectively. Adapted with permission from ref. 274. Copyright 2024 Wiley-VCH.

Photothermal conversion efficiency is a key factor determining PTT efficacy.<sup>283,284</sup> When exogenous molecules (such as photothermal agents) aggregate within cells, they may form more effective photothermal conversion structures, which helps increase the photothermal conversion efficiency and generate higher temperatures to enhance the therapeutic effect of PTT.<sup>285,286</sup> Aggregated exogenous molecules within cells can form hotspot regions with temperatures markedly exceeding those in the surrounding tissues. This localized hyperthermia can effectively kill tumor cells while reducing damage to normal tissues.<sup>287,288</sup> By designing exogenous molecules as nanoparticles or utilizing other delivery systems, one can achieve their effective accumulation within and penetration into tumor tissues. These nanoparticles or delivery systems can release exogenous molecules within cells and promote their aggregation to further enhance the therapeutic effect of PTT. Zhang *et al.* developed a molecular switch comprising a triple-helix probe (THP) and MUC1 aptamer-functionalized AuNPs for fluorescence imaging and PTT (Fig. 24B).<sup>289</sup> The MUC1 aptamer directed the THP-AuNP conjugates to tumor cells. At high levels of ATP, the triple-helix probes underwent structural changes, causing the intracellular aggregation of AuNPs. These aggregates remained trapped at the tumor site, enabling concurrent tumor imaging and PTT (Fig. 24C).

**4.2.6. Ferroptosis induction.** Ferroptosis is a cell death mode characterized by iron-dependent lipid peroxidation and ROS buildup. The corresponding mechanism involves the regulation of various cellular metabolic pathways,<sup>290</sup> including redox homeostasis and the metabolism of iron, amino acids, lipids, and glucose.<sup>291–293</sup> The aggregation of exogenous molecules can disrupt these metabolic pathways, leading to imbalances in ROS generation and degradation, which can trigger ferroptosis.<sup>294,295</sup> Additionally, such aggregates may directly damage cellular membranes and organelles, increasing membrane permeability and causing organelle dysfunction and thus promoting ROS accumulation and lipid peroxidation. The cellular antioxidant system, particularly GSH peroxidase GPX4, is vital for maintaining redox homeostasis. Tang's group developed a tumor-targeted aggregation-induced emission photosensitizer denoted as TBmA and activated by the tumor-overexpressed GGT (Fig. 25A).<sup>296</sup> TBmA was released through the GGT-mediated cleavage of the  $\gamma$ -glutamyl bond in its precursor, TBmA-Glu. The poor water solubility of TBmA led to its aggregation, enhancing its emission and photodynamic activity. Importantly, TBmA-Glu depleted GSH levels *via* GGT-driven photodegradation, promoting lipid peroxidation and initiating ferroptosis in cancer cells.

The aggregation of exogenous molecules may inhibit the antioxidant system, reducing the cellular antioxidant capacity



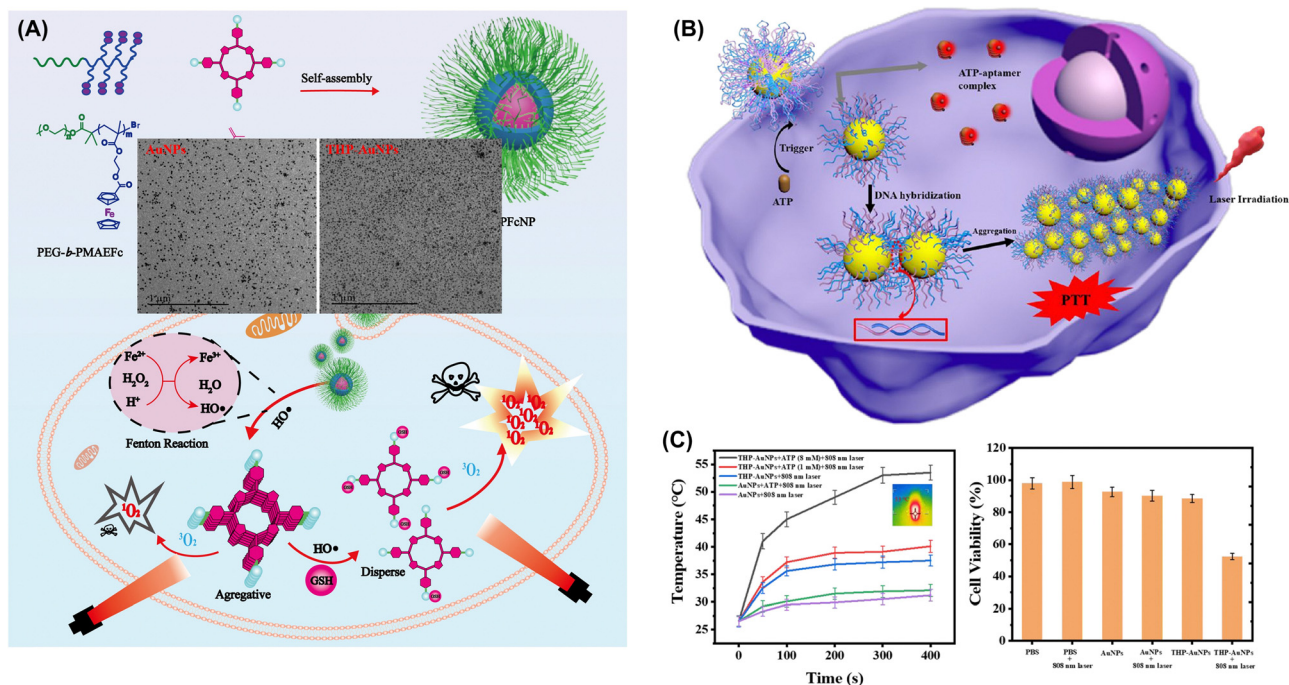


Fig. 24 (A) In the acidic microenvironment of tumors, TPFCNP catalyzes  $H_2O_2$  decomposition to generate hydroxyl radicals ( $HO^\bullet$ ), which break down TPFCNP and release aggregated TMPP. The hydroxyl radicals can further react with overexpressed hydrophilic glutathione and aggregative TMPP to enhance the hydrophilicity of the latter and reduce its aggregation. Under light exposure, the porphyrin dispersion generates large amounts of highly toxic singlet oxygen to kill tumor cells. Adapted with permission from ref. 282. Copyright 2020 American Chemical Society. (B) Design and construction of THP-AuNPs and the ATP-triggered aggregation of THP-AuNPs for the imaging and photothermal therapy of tumors. (C) Time-dependent heat generation by AuNPs and THP-AuNPs and illustration of the photothermal effect of THP-AuNPs exposed to an 808 nm laser in the presence of ATP, along with the viability of MCF-7 cells after treatment and irradiation. Adapted with permission from ref. 289. Copyright 2022 American Chemical Society.

and ROS accumulation and ultimately triggering ferroptosis. Additionally, exogenous molecules may possess iron-chelating abilities or affect the functions of iron metabolism-related proteins, resulting in intracellular iron overload.<sup>297–299</sup> This overload can initiate the Fenton reaction, generating a large amount of ROS, further exacerbating lipid peroxidation and cellular damage, and promoting ferroptosis. Luo *et al.* developed a nanoreactor (1-NBS@CeO<sub>2</sub>) integrating type I PDT with CeO<sub>2</sub> nanozymes. This system comprised spherical nanoparticles containing a peptide amphiphile (1-NBS) and CeO<sub>2</sub> and exhibited enhanced SOD- and POD-like activities (Fig. 25B).<sup>300</sup> Under light irradiation, 1-NBS@CeO<sub>2</sub> generated superoxide radicals ( $O_2^{\bullet-}$ ) that were converted into toxic hydroxyl radicals. This led to increased ROS and decreased GSH levels in A375 tumor cells, causing mitochondrial dysfunction and promoting apoptosis and ferroptosis (Fig. 25C).

## Conclusions

Although the intracellular aggregation of exogenous molecules has promising biomedical applications, it faces several challenges and limitations.<sup>301,302</sup> One critical concern lies in ensuring that polymer molecules are accurately synthesized and folded within the cellular environment.<sup>303</sup> This process requires meticulous control over the chemical and biological conditions

to prevent misfolding or aggregation in unintended ways, which could lead to cellular dysfunction or toxicity. Moreover, the need to avoid adverse effects on the cell is another hurdle. The introduction of exogenous molecules into cells must be carefully managed to prevent the disruption of normal cellular processes and induction of unwanted immune responses. Thus, a deep understanding of cell biology and the mechanisms by which these molecules interact with cellular components is required.

Effective delivery systems and precise regulatory mechanisms are also areas of considerable concern.<sup>304</sup> Developing robust and efficient methods for delivering exogenous molecules into cells while ensuring precise control over their aggregation and activity is crucial for the success of numerous biomedical applications. This includes the design of novel carriers, such as liposomes, nanoparticles, or viral vectors, capable of protecting the molecules during delivery and releasing them at the desired location within the cell. Recent advances in the intracellular aggregation of exogenous molecules have considerably contributed to gene therapy, drug delivery, and metabolic engineering.<sup>305</sup> The self-assembly properties of certain molecules within cells have been used to develop novel therapeutic agents that demonstrate improved efficacy and reduced toxicity compared with traditional treatments. This progress opens up new avenues for more effective therapeutic strategies.

In recent years, coacervates-dynamic liquid-liquid phase-separated droplets-have emerged as cornerstone models for



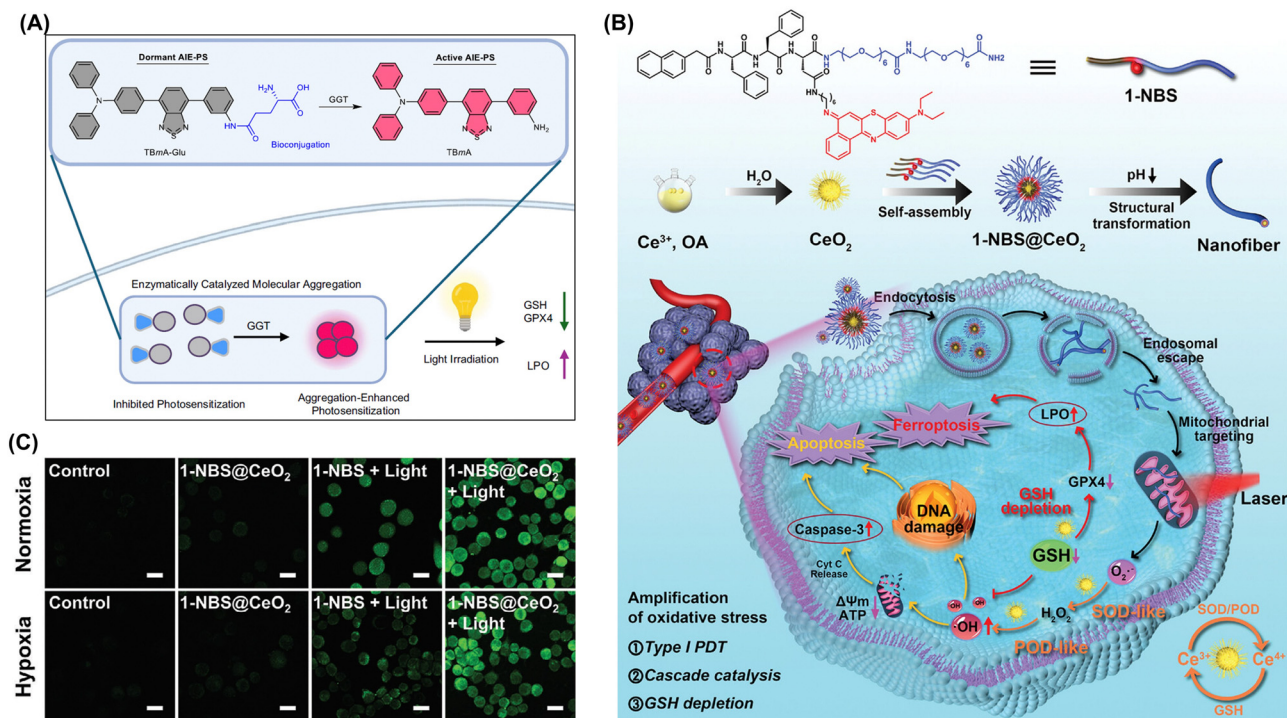


Fig. 25 (A) Aggregation-enhanced photodynamic therapy mechanism mediated by TBmA-Glu. GGT activation of TBmA-Glu leads to the formation of TBmA aggregates, which induce ferroptosis in cancer cells. Adapted with permission from ref. 296. Copyright 2024 Springer Nature. (B) Mechanisms of apoptosis and ferroptosis induced by 1-NBS@CeO<sub>2</sub> in tumor cells under light irradiation. (C) CLSM images depicting ROS levels in A375 cells following various treatments under normoxic and hypoxic conditions (scale bar: 20 μm). Adapted with permission from ref. 300. Copyright 2024 Wiley-VCH.

unraveling the formation and functions of membraneless organelles, which lack lipid membranes yet orchestrate critical cellular processes. These droplets hold transformative potential across three fronts: macromolecular drug delivery, biomimetic reaction chambers, and minimal cellular mimics. While exogenous molecule-induced coacervate formation within living cells remains underexplored due to technical hurdles, their advantages over rigid aggregates are striking. Unlike static aggregation, coacervates act as membraneless compartments that enhance enzyme activity by concentrating substrates up to 100-fold while preserving protein flexibility—a dual benefit that rigid aggregates lack. Moreover, these droplets can reprogram cellular workflows by sequestering or releasing regulatory factors, effectively altering metabolic pathways without genetic modification. Thus, engineering biologically active coacervates *via* exogenous molecules represents one of most promising directions in intracellular molecular aggregation, bridging the gap between synthetic chemistry and cell biology.

As interdisciplinary research and technological convergence accelerate, the intracellular aggregation of exogenous molecules is emerging as a cornerstone of next-generation biomedical innovation. In our view, this field is transitioning from a tool-driven paradigm to a programmable therapeutic platform, where controlled molecular self-assembly enables real-time modulation of cellular behavior with subcellular precision. For instance, integrating stimuli-responsive polymers (*e.g.*, light- or pH-sensitive materials) could allow clinicians to dynamically trigger aggregation dynamics within tumor microenvironments

or diseased compartments, minimizing off-target toxicity and maximizing therapeutic efficacy. A parallel frontier lies in co-opting endogenous cellular machinery—such as chaperone proteins or autophagy pathways—to regulate synthetic aggregate formation and clearance, transforming these constructs into transient, self-correcting therapeutic entities. This synergy between synthetic biology and cellular physiology may also revolutionize regenerative medicine, enabling *in situ* tissue engineering by directing stem cell differentiation or extracellular matrix remodeling through programmable aggregation of bioactive molecules.

Yet realizing this vision demands rigorous scrutiny of long-term safety and scalability. While preclinical studies underscore the promise of engineered aggregates, critical questions persist regarding their biodegradability, immunogenicity, and inter-patient variability. The intracellular aggregation of exogenous molecules represents a paradigm shift: a move from static drugs to adaptive, biology-integrated tools capable of tackling intractable diseases (*e.g.*, neurodegeneration, genetic disorders) where traditional approaches have stalled. Ascribing to the unique properties of AIE molecules, which may be poised to exert a significant translational impact within the next few years, which holds substantial promise for precise disease diagnosis and therapy. Ultimately, with the advances in technology and research, the intracellular aggregation of exogenous molecules will play an increasingly important role in biomedicine, holding promise for revolutionizing our approach to treating diseases and improving human health.



## Author contributions

Da-Yong Hou and Haoran Wang contribute equally to this work. D.-Y. Hou: conceptualization; writing – original draft; data curation; project administration. Y.-Z. Wang: conceptualization; data curation. H.-R. Wang, D.-B. Cheng, B.-Z. Tang and W.-H. Xu: supervision; validation; funding acquisition; writing – review & editing. All authors have read and approved the final version of the manuscript.

## Data availability

All data are obtained from peer-reviewed articles, books, and patents as reported in the references list. No other datasets have been used.

## Conflicts of interest

There are no conflicts to declare.

## Acknowledgements

This work was supported by the National Key R&D Program of China (2021YFB3801000), National Natural Science Foundation of China (82427806, 82302266, 52173138, and 22375155), Hong Kong Scholar Project (XJ2024052), Key Research and Development Program of Heilongjiang Province (2022ZX06004), Heilongjiang Provincial Natural Science Foundation of China (PL2024H159), Harbin Medical University Cancer Hospital Haiyan Foundation (JJYQ2024-03 and JJZD2024-17), the Open Fund of Guangdong Provincial Key Laboratory of Luminescence from Molecular Aggregates, Guangzhou 510640, China (South China University of Technology) (2023B1212060003) and Nn10 program of Harbin Medical University Cancer Hospital (Nn102024-01).

## Notes and references

- Z. Liu, J. Guo, Y. Qiao and B. Xu, *Acc. Chem. Res.*, 2023, **56**, 3076–3088.
- L. Shi, *Int. J. Biol. Macromol.*, 2016, **92**, 37–48.
- Y. M. Zhang, Y. H. Liu and Y. Liu, *Adv. Mater.*, 2020, **32**, e1806158.
- K. Liu, D. Zheng, H. Lei, J. Liu, J. Lei, L. Wang and X. Ma, *ACS Biomater. Sci. Eng.*, 2018, **5**, 1730–1737.
- M. Rinaudo, *Polym. Int.*, 2008, **57**, 397–430.
- R. Kalluri and V. S. LeBleu, *Science*, 2020, **367**, eaau6977.
- H. V. Goodson and E. M. Jonasson, *Cold Spring Harbor Perspect. Biol.*, 2018, **10**, a022608.
- M. Grasso, P. Piscopo, A. Confaloni and M. Denti, *Molecules*, 2014, **19**, 6891–6910.
- F. Ding, S. Zhang, Q. Chen, H. Feng, Z. Ge, X. Zuo, C. Fan, Q. Li and Q. Xia, *Small*, 2023, **19**, e2206228.
- Z. Zhang, J. Coniot, J. Amorim, Y. Jin, R. Prasad, X. Yan, K. Fan and J. Conde, *J. Controlled Release*, 2022, **350**, 80–92.
- Y. Zhao, X. Zuo, Q. Li, F. Chen, Y. Chen, J. Deng, D. Han, C. Hao, F. Huang, Y. Huang, G. Ke, H. Kuang, F. Li, J. Li, M. Li, N. Li, Z. Lin, D. Liu, J. Liu, L. Liu, X. Liu, C. Lu, F. Luo, X. Mao, J. Sun, B. Tang, F. Wang, J. Wang, L. Wang, S. Wang, L. Wu, Z. Wu, F. Xia, C. Xu, Y. Yang, B. Yuan, Q. Yuan, C. Zhang, Z. Zhu, C. Yang, X. Zhang, H. Yang, W. Tan and C. Fan, *Sci. China Chem.*, 2021, **64**, 171–203.
- W. Yi, P. Xiao, X. Liu, Z. Zhao, X. Sun, J. Wang, L. Zhou, G. Wang, H. Cao, D. Wang and Y. Li, *Signal Transduction Targeted Ther.*, 2022, **7**, 386.
- Y. Luo, X. He, Q. Du, L. Xu, J. Xu, J. Wang, W. Zhang, Y. Zhong, D. Guo, Y. Liu and X. Chen, *Exploration*, 2024, **4**, 20230134.
- F. Li, X. Lan and X. Liang, *Aggregate*, 2021, **2**, e27.
- W. Du, X. Hu, W. Wei and G. Liang, *Bioconjugate Chem.*, 2018, **29**, 826–837.
- M. Dergham, S. Lin and J. Geng, *Angew. Chem., Int. Ed.*, 2022, **61**, e202114267.
- W. Wang, Z. Xin, D. Liu, Q. Liu, Y. Liu, Z. Qiu, J. Zhang, P. Alam, X. Cai, Z. Zhao and B. Z. Tang, *Biosens. Bioelectron.*, 2025, **267**, 116800.
- H. Wang, W. Ouyang and H. Liu, *Nano TransMed*, 2024, **3**, 100032.
- W. Zhu, X. Zhang and W. Hu, *Sci. Bull.*, 2021, **66**, 512–520.
- H. Jiang, S. Zhu, Z. Cui, Z. Li, Y. Liang, J. Zhu, P. Hu, H. Zhang and W. Hu, *Chem. Soc. Rev.*, 2022, **51**, 3071–3122.
- X. Feng, X. Wang, C. Redshaw and B. Z. Tang, *Chem. Soc. Rev.*, 2023, **52**, 6715–6753.
- J. A. Finbloom, F. Sousa, M. M. Stevens and T. A. Desai, *Adv. Drug Delivery Rev.*, 2020, **167**, 89–108.
- U. E. Ewii, A. L. Onugwu, V. C. Nwokpor, I. Akpas, T. E. Ogbulie, B. Aharanwa, C. Chijioko, N. Verla, C. IHEME, C. Ujowundu, C. Anyiam and A. A. Attama, *Nano TransMed*, 2024, **3**, 100042.
- Z. Zhou, K. Maxeiner, D. Y. W. Ng and T. Weil, *Acc. Chem. Res.*, 2022, **55**, 2998–3009.
- D. Wu, J. Lei, Z. Zhang, F. Huang, M. Buljan and G. Yu, *Chem. Soc. Rev.*, 2023, **52**, 2911–2945.
- J. An, H. Hong, M. Won, H. Rha, Q. Ding, N. Kang, H. Kang and J. S. Kim, *Chem. Soc. Rev.*, 2023, **52**, 30–46.
- S. Chagri, D. Y. W. Ng and T. Weil, *Nat. Rev. Chem.*, 2022, **6**, 320–338.
- X. Zhang, J. Wang, Y. Zhang, Z. Yang, J. Gao and Z. Gu, *Chem. Soc. Rev.*, 2023, **52**, 8126–8164.
- J. Liu and B. Liu, *Prog. Polym. Sci.*, 2022, **129**, 101545.
- N. Song, F. Tian, Y. Zou and Z. Yu, *ACS Appl. Mater. Interfaces*, 2024, **16**, 45821–45829.
- F. Tian, R. Guo, C. Wu, X. Liu, Z. Zhang, Y. Wang, H. Wang, G. Li and Z. Yu, *Angew. Chem., Int. Ed.*, 2024, **63**, e202404703.
- W. Wang and S. Wang, *Lab Chip*, 2022, **22**, 1042–1067.
- P. Cen, J. Huang, C. Jin, J. Wang, Y. Wei, H. Zhang and M. Tian, *Aggregate*, 2023, **4**, e352.
- X. Mo, Z. Zhang, J. Song, Y. Wang and Z. Yu, *J. Mater. Chem. B*, 2024, **12**, 4289–4306.
- X. Liang, Y. Zhang, J. Zhou, Z. Bu, J. Liu and K. Zhang, *Coord. Chem. Rev.*, 2022, **473**, 214824.
- Y. Z. Yang, N. Xiao, S. G. Liu, L. Han, N. B. Li and H. Q. Luo, *Mater. Sci. Eng., C*, 2020, **108**, 110401.



- 37 S. Yang, Y. Cheng, M. Liu, J. Tang, S. Li, Y. Huang, X. Kou, C. Yao and D. Yang, *Nano Today*, 2024, **56**, 102224.
- 38 J. Wang, L. Zhou and H. Wang, *Nano Today*, 2024, **57**, 102317.
- 39 S. Yamamoto, K. Nishimura, K. Morita, S. Kanemitsu, Y. Nishida, T. Morimoto, T. Aoi, A. Tamura and T. Maruyama, *Biomacromolecules*, 2021, **22**, 2524–2531.
- 40 M. Waqas, W. Jeong, Y. Lee, D. Kim, C. Ryou and Y. Lim, *Biomacromolecules*, 2017, **18**, 943–950.
- 41 D. Cheng, G. Qi, J. Wang, Y. Cong, F. Liu, H. Yu, Z. Qiao and H. Wang, *Biomacromolecules*, 2017, **18**, 1249–1258.
- 42 D. Zhong, X. Hou, D. Pan, Z. Li, Q. Gong and K. Luo, *Adv. Mater.*, 2024, **36**, e2403588.
- 43 L. Huang, X. Mao, B. Liu, Z. Fan, J. Li, C. Fan, Y. Tian, S. Luo and M. Liu, *ACS Nano*, 2024, **18**, 8051–8061.
- 44 Q. Bai, M. Wang, K. Wang, J. Liu, F. Qu and H. Lin, *J. Colloid Interface Sci.*, 2024, **671**, 577–588.
- 45 M. Borkowska, M. Siek, D. V. Kolygina, Y. I. Sobolev, S. Lach, S. Kumar, Y. Cho, K. Kandere-Grzybowska and B. A. Grzybowski, *Nat. Nanotechnol.*, 2020, **15**, 331–341.
- 46 J. Zhang, Y. Cui, X. Feng, M. Cheng, A. Tang and D. Kong, *ACS Appl. Mater. Interfaces*, 2019, **11**, 39624–39632.
- 47 D. Cheng, X. Zhang, Y. Gao, L. Ji, D. Hou, Z. Wang, W. Xu, Z. Qiao and H. Wang, *J. Am. Chem. Soc.*, 2019, **141**, 7235–7239.
- 48 Y. Dai, T. Li, Z. Zhang, Y. Tan, S. Pan, L. Zhang and H. Xu, *J. Am. Chem. Soc.*, 2021, **143**, 10709–10717.
- 49 C. Liu, B. Xianyu, Y. Dai, S. Pan, T. Li and H. Xu, *ACS Nano*, 2023, **17**, 11905–11913.
- 50 A. Wang, H. Li, H. Feng, H. Qiu, R. Huang, Y. Wang, S. Ji, H. Liang, X. Shen and B. Jiang, *ACS Appl. Mater. Interfaces*, 2023, **15**, 5870–5882.
- 51 N. Lv, T. Ma, H. Qin, Z. Yang, Y. Wu, D. Li, J. Tao, H. Jiang and J. Zhu, *Sci. China Mater.*, 2022, **65**, 2861–2870.
- 52 Y. Di, E. Zhang, Z. Yang, Q. Shen, X. Fu, G. Song, C. Zhu, H. Bai, Y. Huang, F. Lv, L. Liu and S. Wang, *Angew. Chem., Int. Ed.*, 2022, **61**, e202116457.
- 53 H. Wang, Y. Song, W. Wang, N. Chen, B. Hu, X. Liu, Z. Zhang and Z. Yu, *J. Am. Chem. Soc.*, 2024, **146**, 330–341.
- 54 L. Zhou, F. Lv, L. Liu and S. Wang, *CCS Chem.*, 2019, **1**, 97–105.
- 55 Y. Zhao, Q. Yao, J. Chen, R. Zhang, J. Song and Y. Gao, *Biomater. Sci.*, 2022, **10**, 5662–5668.
- 56 J. Zhan, Y. Wang, S. Ma, Q. Qin, L. Wang, Y. Cai and Z. Yang, *Bioact. Mater.*, 2022, **9**, 120–133.
- 57 Y. Yuan, H. Sun, S. Ge, M. Wang, H. Zhao, L. Wang, L. An, J. Zhang, H. Zhang, B. Hu, J. Wang and G. Liang, *ACS Nano*, 2015, **9**, 761–768.
- 58 D. Zheng, Y. Chen, S. Ai, R. Zhang, Z. Gao, C. Liang, L. Cao, Y. Chen, Z. Hong, Y. Shi, L. Wang, X. Li and Z. Yang, *Research*, 2019, **2019**, 4803624.
- 59 D. S. Yang, Y. H. Yang, Y. Zhou, L. L. Yu, R. H. Wang, B. Di and M. M. Niu, *Adv. Funct. Mater.*, 2020, **30**, 1904969.
- 60 J. Zhan, J. Huang, Q. Xiao, Z. Yu, Y. Wang, X. Wang, F. Liu, Y. Cai, Z. Yang and L. Zheng, *Anal. Chem.*, 2024, **96**, 12630–12639.
- 61 N. Y. Zhang, D. Y. Hou, X. J. Hu, J. X. Liang, M. D. Wang, Z. Z. Song, L. Yi, Z. J. Wang, H. W. An, W. Xu and H. Wang, *Angew. Chem., Int. Ed.*, 2023, **62**, e202308049.
- 62 A. Wang, Q. Mao, M. Zhao, S. Ye, J. Fang, C. Cui, Y. Zhao, Y. Zhang, Y. Zhang, F. Zhou and H. Shi, *Anal. Chem.*, 2020, **92**, 16113–16121.
- 63 Y. Gao, Y. Li, H. Cao, H. Jia, D. Wang, C. Ren, Z. Wang, C. Yang and J. Liu, *J. Nanobiotechnol.*, 2022, **20**, 390.
- 64 Z. Hai, Y. Ni, D. Saimi, H. Yang, H. Tong, K. Zhong and G. Liang, *Nano Lett.*, 2019, **19**, 2428–2433.
- 65 Q. Shen, Y. Huang, Y. Zeng, E. Zhang, F. Lv, L. Liu and S. Wang, *ACS Mater. Lett.*, 2021, **3**, 1307–1314.
- 66 L. Feng, Z. Chen, W. Dong, A. Xie, X. Zang and J. Li, *New J. Chem.*, 2023, **47**, 21960–21968.
- 67 Y. Gao, J. Gao, G. Mu, Y. Zhang, F. Huang, W. Zhang, C. Ren, C. Yang and J. Liu, *Acta Pharm. Sin. B*, 2020, **10**, 2374–2383.
- 68 J. Li, Y. Kuang, J. Shi, J. Zhou, J. E. Medina, R. Zhou, D. Yuan, C. Yang, H. Wang, Z. Yang, J. Liu, D. M. Dinulescu and B. Xu, *Angew. Chem., Int. Ed.*, 2015, **54**, 13307–13311.
- 69 C. Wu, R. Zhang, W. Du, L. Cheng and G. Liang, *Nano Lett.*, 2018, **18**, 7749–7754.
- 70 Y. Zhao, X. Zhang, Z. Li, S. Huo, K. Zhang, J. Gao, H. Wang and X. J. Liang, *Adv. Mater.*, 2017, **29**, 1601128.
- 71 D. Liu, Z. Miao, C. Wu, F. He, P. Ren, S. Bai, X. Jiang and Y. Gao, *Chem. Sci.*, 2020, **11**, 1132–1139.
- 72 A. Tanaka, Y. Fukuoka, Y. Morimoto, T. Honjo, D. Koda, M. Goto and T. Maruyama, *J. Am. Chem. Soc.*, 2015, **137**, 770–775.
- 73 Q. Zhang, D. Zheng, X. Dong, P. Pan, S. Zeng, F. Gao, S. Cheng and X. Zhang, *J. Am. Chem. Soc.*, 2021, **143**, 5127–5140.
- 74 H. An, L. Li, Y. Wang, Z. Wang, D. Hou, Y. Lin, S. Qiao, M. Wang, C. Yang, Y. Cong, Y. Ma, X. Zhao, Q. Cai, W. Chen, C. Lu, W. Xu, H. Wang and Y. Zhao, *Nat. Commun.*, 2019, **10**, 4861.
- 75 Z. Chen, M. Chen, K. Zhou and J. Rao, *Angew. Chem., Int. Ed.*, 2020, **59**, 7864–7870.
- 76 L. L. Li, H. L. Ma, G. B. Qi, D. Zhang, F. Yu, Z. Hu and H. Wang, *Adv. Mater.*, 2016, **28**, 254–262.
- 77 P. Chen, H. Wang, H. Wu, P. Zou, C. Wang, X. Liu, Y. Pan, Y. Liu and G. Liang, *Anal. Chem.*, 2021, **93**, 6329–6334.
- 78 Y. Yuan, L. Wang, W. Du, Z. Ding, J. Zhang, T. Han, L. An, H. Zhang and G. Liang, *Angew. Chem., Int. Ed.*, 2015, **54**, 9700–9704.
- 79 G. B. Qi, F. Hu, Kenry, L. L. Shi, M. Wu and B. Liu, *Angew. Chem., Int. Ed.*, 2019, **58**, 16229–16235.
- 80 G. Qi, X. Liu, L. Shi, M. Wu, J. Liu and B. Liu, *Adv. Mater.*, 2022, **34**, e2106885.
- 81 L. Yang, R. Peltier, M. Zhang, D. Song, H. Huang, G. Chen, Y. Chen, F. Zhou, Q. Hao, L. Bian, M. He, Z. Wang, Y. Hu and H. Sun, *J. Am. Chem. Soc.*, 2020, **142**, 18150–18159.
- 82 T. Xu, Y. Cai, X. Zhong, L. Zhang, D. Zheng, Z. Gao, X. Pan, F. Wang, M. Chen and Z. Yang, *Chem. Commun.*, 2019, **55**, 7175–7178.
- 83 Y. M. Zhang, N. Y. Zhang, K. Xiao, Q. Yu and Y. Liu, *Angew. Chem., Int. Ed.*, 2018, **57**, 8649–8653.
- 84 J. Geng, W. Li, Y. Zhang, N. Thottappillil, J. Clavadetscher, A. Lilienkamp and M. Bradley, *Nat. Chem.*, 2019, **11**, 578–586.



- 85 M. Zhu, S. Wang, Z. Li, J. Li, Z. Xu, X. Liu and X. Huang, *Nat. Commun.*, 2023, **14**, 3598.
- 86 Y. Zhang, Q. Gao, W. Li, R. He, L. Zhu, Q. Lian, L. Wang, Y. Li, M. Bradley and J. Geng, *JACS Au*, 2022, **2**, 579–589.
- 87 J. C. Lin, C. Y. Hsu, J. Y. Chen, Z. S. Fang, H. W. Chen, B. Y. Yao, G. H. M. Shiau, J. S. Tsai, M. Gu, M. Jung, T. Y. Lee and C. M. J. Hu, *Adv. Mater.*, 2021, **33**, e2101190.
- 88 N. Yin, X. Wang, Y. Shu and J. Wang, *J. Colloid Interface Sci.*, 2025, **679**, 519–528.
- 89 J. Qiao, L. Qi, Y. Shen, L. Zhao, C. Qi, D. Shangguan, L. Mao and Y. Chen, *J. Mater. Chem.*, 2012, **22**, 11543.
- 90 J. Wang, Y. Wang, S. Qiao, M. Mamuti, H. An and H. Wang, *Natl. Sci. Rev.*, 2022, **9**, nwab159.
- 91 R. Sharma, N. Vijay, B. J. Kim and H. Lee, *Eur. Polym. J.*, 2023, **201**, 112545.
- 92 R. S. Fernandes and N. Dey, *ACS Appl. Nano Mater.*, 2023, **6**, 5168–5176.
- 93 T. Wu, X. Chen, Z. Gong, J. Yan, J. Guo, Y. Zhang, Y. Li and B. Li, *Adv. Sci.*, 2022, **9**, e2103354.
- 94 B. Saha, B. Ruidas, S. Mete, C. D. Mukhopadhyay, K. Bauri and P. De, *Chem. Sci.*, 2020, **11**, 141–147.
- 95 F. Liu, Y. Cong, G. Qi, L. Ji, Z. Qiao and H. Wang, *Nano Lett.*, 2018, **18**, 6577–6584.
- 96 S. Qiao, Y. Ma, Y. Wang, Y. Lin, H. An, L. Li and H. Wang, *ACS Nano*, 2017, **11**, 7301–7311.
- 97 Q. Zhang, Q. Zhang, Y. Sun, X. Tao, Y. Zhao, F. Guo, Z. Li, Z. Wang, Z. Liang and C. Yi, *ACS Biomater. Sci. Eng.*, 2024, **10**, 7167–7175.
- 98 T. Yin, T. Yang, L. Chen, R. Tian, C. Cheng, L. Weng, Y. Zhang and X. Chen, *Acta Biomater.*, 2023, **166**, 485–495.
- 99 R. Hu, X. Chen, T. Zhou, H. Si, B. He, R. T. K. Kwok, A. Qin and B. Z. Tang, *Sci. China Chem.*, 2019, **62**, 1198–1203.
- 100 M. Deng, R. Guo, S. Zang, J. Rao, M. Li, X. Tang, C. Xia, M. Li, Z. Zhang and Q. He, *ACS Appl. Mater. Interfaces*, 2021, **13**, 18033–18046.
- 101 X. Q. Li, Y. L. Jia, Z. X. Wang, Y. W. Zhang, H. Y. Chen and J. J. Xu, *Adv. Funct. Mater.*, 2024, **34**, 2401711.
- 102 J. Shi, W. Nie, X. Zhao, X. Yang, H. Cheng, T. Zhou, Y. Zhang, K. Zhang and J. Liu, *Adv. Mater.*, 2022, **34**, e2201049.
- 103 M. Wang, L. Yi, Y. Li, R. Xu, J. Hu, D. Hou, C. Liu and H. Wang, *J. Am. Chem. Soc.*, 2024, **146**, 28669–28676.
- 104 S. Qi, P. Zhang, M. Ma, M. Yao, J. Wu, E. Mäkilä, J. Salonen, H. Ruskoaho, Y. Xu, H. A. Santos and H. Zhang, *Small*, 2019, **15**, e1804332.
- 105 J. V. Jokerst, C. Khademi and S. S. Gambhir, *Sci. Transl. Med.*, 2013, **5**, 177ra35.
- 106 X. Zhao, F. Wang, C. Kam, M. Wu, J. Zhang, C. Xu, K. Bao, Q. He, R. Ye, B. Z. Tang and S. Chen, *ACS Nano*, 2024, **18**, 21447–21458.
- 107 Y. Liu, Y. Wang, C. Wang, T. Dong, H. Xu, Y. Guo, X. Zhao, Y. Hu and J. Wu, *Adv. Sci.*, 2022, **9**, e2203027.
- 108 X. Q. Zhou, M. Mytiliniou, J. Hilgendorf, Y. Zeng, P. Papadopoulou, Y. Shao, M. P. Dominguez, L. Zhang, M. B. S. Hesselberth, E. Bos, M. A. Siegler, F. Buda, A. M. Brouwer, A. Kros, R. I. Koning, D. Heinrich and S. Bonnet, *Adv. Mater.*, 2021, **33**, e2008613.
- 109 N. Chu, L. Cong, J. Yue, W. Xu and S. Xu, *ACS Omega*, 2022, **7**, 34268–34277.
- 110 M. T. Jeena, S. Lee, A. K. Barui, S. Jin, Y. Cho, S. Hwang, S. Kim and J. Ryu, *Chem. Commun.*, 2020, **56**, 6265–6268.
- 111 S. Kim, B. Jana, E. M. Go, J. E. Lee, S. Jin, E. An, J. Hwang, Y. Sim, S. Son, D. Kim, C. Kim, J. Jin, S. K. Kwak and J. Ryu, *ACS Nano*, 2021, **15**, 14492–14508.
- 112 S. Kim, J. Chae, D. Kim, C. Park, Y. Sim, H. Lee, G. Park, J. Lee, S. Hong, B. Jana, C. Kim, H. Chung and J. Ryu, *J. Am. Chem. Soc.*, 2023, **145**, 21991–22008.
- 113 X. Yang, B. Wu, J. Zhou, H. Lu, H. Zhang, F. Huang and H. Wang, *Nano Lett.*, 2022, **22**, 7588–7596.
- 114 Y. Guo, S. Li, Z. Tong, J. Tang, R. Zhang, Z. Lv, N. Song, D. Yang and C. Yao, *J. Am. Chem. Soc.*, 2023, **145**, 23859–23873.
- 115 F. Li, Y. Liu, Y. Dong, Y. Chu, N. Song and D. Yang, *J. Am. Chem. Soc.*, 2022, **144**, 4667–4677.
- 116 S. Jin, M. T. Jeena, B. Jana, M. Moon, H. Choi, E. Lee and J. Ryu, *Biomacromolecules*, 2020, **21**, 4806–4813.
- 117 M. T. Jeena, L. Palanikumar, E. M. Go, I. Kim, M. G. Kang, S. Lee, S. Park, H. Choi, C. Kim, S. Jin, S. C. Bae, H. W. Rhee, E. Lee, S. K. Kwak and J. Ryu, *Nat. Commun.*, 2017, **8**, 26.
- 118 H. Choi, G. Park, E. Shin, S. W. Shin, B. Jana, S. Jin, S. Kim, H. Wang, S. K. Kwak, B. Xu and J. Ryu, *Chem. Sci.*, 2022, **13**, 6197–6204.
- 119 C. Yao, Y. Xu, J. Tang, P. Hu, H. Qi and D. Yang, *Nat. Commun.*, 2022, **13**, 7739.
- 120 X. Ge, Y. Cao, X. Zhu, B. Yuan, L. He, A. Wu and J. Li, *Adv. Healthcare Mater.*, 2023, **12**, e2300265.
- 121 J. Wang, L. Hu, H. Zhang, Y. Fang, T. Wang and H. Wang, *Adv. Mater.*, 2022, **34**, e2104704.
- 122 S. Ji, J. Li, X. Duan, J. Zhang, Y. Zhang, M. Song, S. Li, H. Chen and D. Ding, *Angew. Chem., Int. Ed.*, 2021, **60**, 26994–27004.
- 123 X. Ouyang, N. Jia, J. Luo, L. Li, J. Xue, H. Bu, G. Xie and Y. Wan, *JACS Au*, 2023, **3**, 2566–2577.
- 124 M. Pileni, *J. Phys. Chem. C*, 2021, **125**, 20143–20156.
- 125 D. Hou, M. Wang, N. Zhang, S. Xu, Z. Wang, X. Hu, G. Lv, J. Wang, M. Lv, L. Yi, L. Wang, D. Cheng, T. Sun, H. Wang and W. Xu, *Nano Lett.*, 2022, **22**, 3983–3992.
- 126 D. Y. Hou, N. Y. Zhang, M. D. Wang, S. X. Xu, Z. J. Wang, X. J. Hu, G. T. Lv, J. Q. Wang, X. H. Wu, L. Wang, D. B. Cheng, H. Wang and W. Xu, *Angew. Chem., Int. Ed.*, 2022, **61**, e202116893.
- 127 X. Zhao, K. Zhang, Y. Wang, W. Jiang, H. Cheng, Q. Wang, T. Xiang, Z. Zhang, J. Liu and J. Shi, *Adv. Funct. Mater.*, 2022, **32**, 2108883.
- 128 S. Liu, Q. Zhang, H. He, M. Yi, W. Tan, J. Guo and B. Xu, *Angew. Chem., Int. Ed.*, 2022, **61**, e202210568.
- 129 S. Liu, Q. Zhang, A. N. Shy, M. Yi, H. He, S. Lu and B. Xu, *J. Am. Chem. Soc.*, 2021, **143**, 15852–15862.
- 130 P. J. Pacheco-Liñán, C. Alonso-Moreno, A. Ocaña, C. Ripoll, E. García-Gil, A. Garzón-Ruiz, D. Herrera-Ochoa, S. Blas-Gómez, B. Cohen and I. Bravo, *ACS Appl. Mater. Interfaces*, 2023, **15**, 44786–44795.
- 131 D. Eisenberg and M. Jucker, *Cell*, 2012, **148**, 1188–1203.



- 132 J. L. Silva, E. A. Cino, I. N. Soares, V. F. Ferreira and G. A. P. De Oliveira, *Acc. Chem. Res.*, 2018, **51**, 181–190.
- 133 K. Bae, S. Ng, L. Li and M. Kurisawa, *Biofunct. Mater.*, 2023, **1**, 2.
- 134 Y. Deng, W. Zhan and G. Liang, *Adv. Healthcare Mater.*, 2021, **10**, e2001211.
- 135 Y. Chen, B. S. N. Tan, Y. Cheng and Y. Zhao, *Angew. Chem., Int. Ed.*, 2024, **63**, e202410579.
- 136 W. Poon, B. R. Kingston, B. Ouyang, W. Ngo and W. C. W. Chan, *Nat. Nanotechnol.*, 2020, **15**, 819–829.
- 137 W. C. W. Chan, *BME Front.*, 2023, **4**, 16.
- 138 Y. Guo, P. Li, X. Guo, C. Yao and D. Yang, *ACS Nano*, 2024, **18**, 30224–30246.
- 139 H. Cui, A. Glidle and J. M. Cooper, *ACS Appl. Mater. Interfaces*, 2022, **14**, 31586–31593.
- 140 Y. Gao, J. Shi, D. Yuan and B. Xu, *Nat. Commun.*, 2012, **3**, 1033.
- 141 L. Li, S. Qiao, W. Liu, Y. Ma, D. Wan, J. Pan and H. Wang, *Nat. Commun.*, 2017, **8**, 1276.
- 142 J. J. Rennick, A. P. R. Johnston and R. G. Parton, *Nat. Nanotechnol.*, 2021, **16**, 266–276.
- 143 V. L. Shepherd, *Trends Pharmacol. Sci.*, 1989, **10**, 458–462.
- 144 H. He, J. Wang, H. Wang, N. Zhou, D. Yang, D. R. Green and B. Xu, *J. Am. Chem. Soc.*, 2018, **140**, 1215–1218.
- 145 J. Zhou, X. Du, C. Berciu, S. J. Del Signore, X. Chen, N. Yamagata, A. A. Rodal, D. Nicastro and B. Xu, *Mol. Ther.*, 2018, **26**, 648–658.
- 146 Y. Huang, L. Ning, X. Zhang, Q. Zhou, Q. Gong and Q. Zhang, *Chem. Soc. Rev.*, 2024, **53**, 1090–1166.
- 147 P. She, Y. Qin, X. Wang and Q. Zhang, *Adv. Mater.*, 2022, **34**, e2101175.
- 148 J. Ochi, K. Tanaka and Y. Chujo, *Angew. Chem., Int. Ed.*, 2020, **59**, 9841–9855.
- 149 D. P. Karothu, J. Mahmoud Halabi, E. Ahmed, R. Ferreira, P. R. Spackman, M. A. Spackman and P. Naumov, *Angew. Chem., Int. Ed.*, 2022, **61**, e202113988.
- 150 Y. Liu, L. Wang, L. Zhao, Y. Zhang, Z. Li and F. Huang, *Chem. Soc. Rev.*, 2024, **53**, 1592–1623.
- 151 J. Zhang, K. Liu, K. Mullen and M. Yin, *Chem. Commun.*, 2015, **51**, 11541–11555.
- 152 L. Zhang, J. Huang, D. Buratto, P. Han, Z. Yang and R. Zhou, *Aggregate*, 2024, **5**, e434.
- 153 N. Lin, X. Chen, S. Yan, H. Wang, Z. Lu, X. Xia, M. Liang, Y. Wu, L. Zheng, Q. Cao and Z. Ding, *RSC Adv.*, 2016, **6**, 25416–25419.
- 154 Z. Cao, D. Li, L. Zhao, M. Liu, P. Ma, Y. Luo and X. Yang, *Nat. Commun.*, 2022, **13**, 2038.
- 155 Y. Cote, I. W. Fu, E. T. Dobson, J. E. Goldberger, H. D. Nguyen and J. K. Shen, *J. Phys. Chem. C*, 2014, **118**, 16272–16278.
- 156 Z. Cheng, Y. Cheng, Q. Chen, M. Li, J. Wang, H. Liu, M. Li, Y. Ning, Z. Yu, Y. Wang and H. Wang, *Nano Today*, 2020, **33**, 100878.
- 157 A. Nicolas Boluda, Z. Yang, I. Dobryden, F. Carn, N. Winckelmans, C. P echoux, P. Bonville, S. Bals, P. M. Claesson, F. Gazeau and M. P. Pileni, *Adv. Funct. Mater.*, 2020, **30**, 2004274.
- 158 H. Wu, Z. Zhang, Y. Cao, Y. Hu, Y. Li, L. Zhang, X. Cao, H. Wen, Y. Zhang, H. Lv and X. Jin, *Adv. Sci.*, 2024, **11**, e2401047.
- 159 M. Pieszka, S. Han, C. Volkmann, R. Graf, I. Lieberwirth, K. Landfester, D. Y. W. Ng and T. Weil, *J. Am. Chem. Soc.*, 2020, **142**, 15780–15789.
- 160 D. Wei, Y. Sun, H. Zhu and Q. Fu, *ACS Nano*, 2023, **17**, 23223–23261.
- 161 Z. Zheng, P. Chen, M. Xie, C. Wu, Y. Luo, W. Wang, J. Jiang and G. Liang, *J. Am. Chem. Soc.*, 2016, **138**, 11128–11131.
- 162 H. Fan, Y. Li, J. Yang and X. Ye, *J. Phys. Chem. B*, 2017, **121**, 9708–9717.
- 163 J. Zhan, Y. Cai, S. He, L. Wang and Z. Yang, *Angew. Chem., Int. Ed.*, 2018, **57**, 1813–1816.
- 164 M. Shahriari, M. Zahiri, K. Abnous, S. M. Taghdisi, M. Ramezani and M. Alibolandi, *J. Controlled Release*, 2019, **308**, 172–189.
- 165 C. Wang, W. Du, C. Wu, S. Dan, M. Sun, T. Zhang, B. Wang, Y. Yuan and G. Liang, *Angew. Chem., Int. Ed.*, 2022, **61**, e202114766.
- 166 Y. Zhang, C. Xu, X. Yang and K. Pu, *Adv. Mater.*, 2020, **32**, e2002661.
- 167 X. Zhang, D. Cheng, L. Ji, H. An, D. Wang, Z. Yang, H. Chen, Z. Qiao and H. Wang, *Nano Lett.*, 2020, **20**, 1286–1295.
- 168 M. K. Pastuszka, S. M. Janib, I. Weitzhandler, C. T. Okamoto, S. Hamm-Alvarez and J. A. MacKay, *Biomacromolecules*, 2012, **13**, 3439–3444.
- 169 W. Li, Y. Zhou, S. He, T. Tong, C. Wang, P. Shi, S. Li, X. Wang, L. Yang, X. Cao and Z. Tian, *Aggregate*, 2024, **5**, e496.
- 170 F. Liu, Y. Guo, Y. Hu, X. Zhang and X. Zheng, *Anal. Bioanal. Chem.*, 2019, **411**, 5845–5854.
- 171 M. Giel and Y. Hong, *Aggregate*, 2023, **4**, e336.
- 172 T. Miki, K. Kajiwara, S. Nakayama, M. Hashimoto and H. Mihara, *ACS Synth. Biol.*, 2022, **11**, 2144–2153.
- 173 H. Liu and H. Wang, *Adv. Drug Delivery Rev.*, 2024, **209**, 115327.
- 174 K. Qian, S. Gao, Z. Jiang, Q. Ding and Z. Cheng, *Exploration*, 2024, **4**, 20230063.
- 175 F. Wang, Q. Zhang, M. Yang, B. Yin and S. H. D. Wong, *Biomed. Eng. Commun.*, 2024, **3**, 12–16.
- 176 Y. Li, X. He, P. Wang, B. Yuan, Y. Pan, X. Hu, L. Lu, A. Wu and J. Li, *Small*, 2024, **20**, e2308621.
- 177 X. Yang, H. Lu, Y. Tao, L. Zhou and H. Wang, *Angew. Chem., Int. Ed.*, 2021, **60**, 23797–23804.
- 178 B. Jana, S. Jin, E. M. Go, Y. Cho, D. Kim, S. Kim, S. K. Kwak and J. Ryu, *J. Am. Chem. Soc.*, 2023, **145**, 18414–18431.
- 179 C. P. Brangwynne, *Soft Matter*, 2011, **7**, 3052.
- 180 L. He, D. Lu, H. Liang, S. Xie, C. Luo, M. Hu, L. Xu, X. Zhang and W. Tan, *ACS Nano*, 2017, **11**, 4060–4066.
- 181 Q. Huang, P. Ma, H. Li, B. Yin and B. Ye, *ACS Appl. Bio Mater.*, 2020, **3**, 2861–2866.
- 182 J. Li, D. Li, R. Yuan and Y. Xiang, *ACS Appl. Mater. Interfaces*, 2017, **9**, 5717–5724.
- 183 Z. Yang, S. Zhang, H. Zhao, H. Niu, Z. Wu and H. Chang, *Anal. Chem.*, 2018, **90**, 13891–13899.
- 184 X. Li, F. Yang, C. Gan, R. Yuan and Y. Xiang, *Biosens. Bioelectron.*, 2022, **197**, 113809.



- 185 Z. Zhang, R. T. K. Kwok, Y. Yu, B. Z. Tang and K. M. Ng, *J. Mater. Chem. B*, 2018, **6**, 4575–4578.
- 186 H. Xu, X. Cheng, X. Sun, P. Chen, W. Zhan, X. Liu, X. Wang, B. Hu and G. Liang, *Nano Lett.*, 2023, **23**, 6178–6183.
- 187 B. Dong, S. Du, C. Wang, H. Fu, Q. Li, N. Xiao, J. Yang, X. Xue, W. Cai and D. Liu, *ACS Nano*, 2019, **13**, 1421–1432.
- 188 H. A. Ki, P. K. Naoghare, B. Oh, J. Choi and J. M. Song, *Anal. Biochem.*, 2009, **388**, 23–27.
- 189 L. Li, X. Fang, J. Le, Y. Zheng, X. Tan, Z. Jiang, H. Li, J. Xu and H. Xu, *Talanta*, 2022, **250**, 123753.
- 190 L. Wen, Y. Lin, Z. Zhang, W. Lu, C. Lv, Z. Chen, H. Wang and D. Pang, *Biomaterials*, 2016, **99**, 24–33.
- 191 L. Dai, W. Mao, L. Hu, J. Song, Y. Zhang, T. Huang and M. Wang, *Dyes Pigm.*, 2022, **204**, 110436.
- 192 D. Ye, G. Liang, M. L. Ma and J. Rao, *Angew. Chem., Int. Ed.*, 2011, **50**, 2275–2279.
- 193 R. Liu, S. Zhang, T. Zheng, Y. Chen, J. Wu and Z. Wu, *ACS Nano*, 2020, **14**, 9572–9584.
- 194 J. Xu, Z. Wu, Z. Wang, J. Le, T. Zheng and L. Jia, *Biomaterials*, 2017, **120**, 57–65.
- 195 Y. Yuan, R. T. K. Kwok, G. Feng, J. Liang, J. Geng, B. Z. Tang and B. Liu, *Chem. Commun.*, 2014, **50**, 295–297.
- 196 N. Singha, P. Gupta, B. Pramanik, S. Ahmed, A. Dasgupta, A. Ukil and D. Das, *Biomacromolecules*, 2017, **18**, 3630–3641.
- 197 F. Sun, G. Zhang, D. Zhang, L. Xue and H. Jiang, *Org. Lett.*, 2011, **13**, 6378–6381.
- 198 J. Wang, S. Ma, K. Ge, R. Xu, F. Shen, X. Gao, Y. Yao, Y. Chen, Y. Chen, F. Gao and G. Wu, *Anal. Chem.*, 2024, **96**, 8922–8931.
- 199 L. Yang, Q. Wu, Y. Chen, X. Liu, F. Wang and X. Zhou, *ACS Sens.*, 2019, **4**, 110–117.
- 200 S. Zhou, Y. Xia, Y. Liu, Q. He and B. Song, *Langmuir*, 2017, **33**, 5947–5956.
- 201 J. Tavakoli, Q. Hu, J. L. Tipper and Y. Tang, *Aggregate*, 2024, **5**, e645.
- 202 X. Wei, Y. Wang, J. Shen, X. Chi, J. Xu, L. Jia, H. Xu and W. Liu, *Sens. Actuators, B*, 2025, **424**, 136919.
- 203 W. Lv, M. Lin, R. Li, Q. Zhang, H. Liu, J. Wang and C. Huang, *Chin. Chem. Lett.*, 2019, **30**, 1410–1414.
- 204 X. Gong, R. Li, J. Zhang, P. Zhang, Z. Jiang, L. Hu, X. Liu, Y. Wang and F. Wang, *Adv. Sci.*, 2024, **11**, e2400517.
- 205 J. Liu, P. Du, J. Zhang, H. Shen and J. Lei, *Chem. Commun.*, 2018, **54**, 2550–2553.
- 206 D. Li, Y. Wu, C. Gan, R. Yuan and Y. Xiang, *Nanoscale*, 2018, **10**, 17623–17628.
- 207 Y. Wu, Y. Gao, J. Su, Z. Chen and S. Liu, *Chem. Commun.*, 2020, **56**, 9008–9011.
- 208 L. Dong, M. Zhang, H. Han, Y. Zang, G. Chen, J. Li, X. He and S. Vidal, *Chem. Sci.*, 2021, **13**, 247–256.
- 209 S. Yang, H. Yu, X. Xu, T. Yang, Y. Wei, R. Zan, X. Zhang, Q. Ma, H. C. Shum and Y. Song, *ACS Nano*, 2023, **17**, 8195–8203.
- 210 X. Sun, L. Xu, H. D. Xu, L. Xie, R. Wang, Z. Yang, W. Zhan, S. Shen and G. Liang, *Adv. Healthcare Mater.*, 2024, **13**, e2303472.
- 211 Y. Yuan, S. Ge, H. Sun, X. Dong, H. Zhao, L. An, J. Zhang, J. Wang, B. Hu and G. Liang, *ACS Nano*, 2015, **9**, 5117–5124.
- 212 Y. Yuan, F. Wang, W. Tang, Z. Ding, L. Wang, L. Liang, Z. Zheng, H. Zhang and G. Liang, *ACS Nano*, 2016, **10**, 7147–7153.
- 213 M. Su, J. Ye, Q. Li, W. Ge, Y. Zhang, H. Jiang, C. Amatore and X. Wang, *RSC Adv.*, 2015, **5**, 74844–74849.
- 214 M. Madhu, W. Tseng, Y. Chou, A. S. Krishna Kumar, C. Lu, P. Chang and W. Tseng, *Anal. Chem.*, 2024, **96**, 9007–9015.
- 215 A. Dutta, U. Goswami and A. Chattopadhyay, *ACS Appl. Mater. Interfaces*, 2018, **10**, 19459–19472.
- 216 S. Kim, J. Kim, B. Jana and J. Ryu, *RSC Adv.*, 2020, **10**, 43383–43388.
- 217 K. Gong, Q. Wu, H. Wang, S. He, J. Shang and F. Wang, *Chem. Commun.*, 2020, **56**, 1141–11413.
- 218 Y. Yuan, Z. Ding, J. Qian, J. Zhang, J. Xu, X. Dong, T. Han, S. Ge, Y. Luo, Y. Wang, K. Zhong and G. Liang, *Nano Lett.*, 2016, **16**, 2686–2691.
- 219 Y. Wang, X. Li, P. Chen, Y. Dong, G. Liang and Y. Yu, *Nanoscale*, 2020, **12**, 1886–1893.
- 220 R. Zhang, R. Zhang, C. Zhao and X. Xu, *Anal. Chim. Acta*, 2022, **1193**, 339395.
- 221 L. Qiu, K. Li, W. Dong, Y. Seimille, Q. Liu, F. Gao and J. Lin, *ACS Nano*, 2021, **15**, 18250–18259.
- 222 S. Liu, S. Fang, W. J. Jang, J. Yoon and L. Zhang, *Anal. Chem.*, 2024, **96**, 12794–12800.
- 223 J. Wang, M. Liu, X. Zhang, X. Wang, M. Xiong and D. Luo, *Exploration*, 2024, **4**, 20230027.
- 224 S. Sun, H. Xu, Y. Yang, L. Wang, L. Ye, H. Jiang, C. Xue, Z. Shen and Z. Wu, *Chem. Eng. J.*, 2022, **428**, 131150.
- 225 Y. Jiang and K. Pu, *Chem. Rev.*, 2021, **121**, 13086–13131.
- 226 J. Li, Z. Hai, H. Xiao, X. Yi and G. Liang, *Chem. Commun.*, 2018, **54**, 3460–3463.
- 227 M. Wei, L. Wang, Y. Wang, T. Zhang, C. Wang, C. Wu, C. Tian, G. Liang and Y. Yuan, *Small*, 2023, **19**, e2300015.
- 228 S. Ye, S. Wang, D. Gao, K. Li, Q. Liu, B. Feng, L. Qiu and J. Lin, *Bioconjugate Chem.*, 2020, **31**, 174–181.
- 229 L. Xu, H. Gao, W. Zhan, Y. Deng, X. Liu, Q. Jiang, X. Sun, J. Xu and G. Liang, *J. Am. Chem. Soc.*, 2023, **145**, 27748–27756.
- 230 W. Fu, C. Yan, Z. Guo, J. Zhang, H. Zhang, H. Tian and W. Zhu, *J. Am. Chem. Soc.*, 2019, **141**, 3171–3177.
- 231 J. Zhang, H. Guo, M. Liu, K. Tang, S. Li, Q. Fang, H. Du, X. Zhou, X. Lin, Y. Yang, B. Huang and D. Yang, *Exploration*, 2024, **4**, 20230087.
- 232 M. Jiang, J. Kang and A. Dong, *Biosens. Bioelectron.*, 2025, **267**, 116873.
- 233 F. Hu, G. Qi, Kenry, D. Mao, S. Zhou, M. Wu, W. Wu and B. Liu, *Angew. Chem., Int. Ed.*, 2020, **59**, 9288–9292.
- 234 C. Yang, F. Hu, X. Zhang, C. Ren, F. Huang, J. Liu, Y. Zhang, L. Yang, Y. Gao, B. Liu and J. Liu, *Biomaterials*, 2020, **244**, 119972.
- 235 G. Dai, Y. Luo, M. Liao, P. Zhang, H. Pan, T. Yin, Q. Yang, S. Zheng, J. Liao, D. Liu, Z. He, W. Zhao, L. Song, P. Zhao, L. Cai, Z. Zhang and M. Zheng, *Cell Rep. Phys. Sci.*, 2023, **4**, 101238.



- 236 Q. Cai, Y. Fei, L. Hu, Z. Huang, L. Li and H. Wang, *Nano Lett.*, 2018, **18**, 6229–6236.
- 237 Q. Cai, Y. Fei, H. W. An, X. X. Zhao, Y. Ma, Y. Cong, L. Hu, L. L. Li and H. Wang, *ACS Appl. Mater. Interfaces*, 2018, **10**, 9197–9202.
- 238 J. Zhou, X. Du, J. Li, N. Yamagata and B. Xu, *J. Am. Chem. Soc.*, 2015, **137**, 10040–10043.
- 239 D. Hou, W. Xiao, J. Wang, M. Yaseen, Z. Wang, Y. Fei, M. Wang, L. Wang, H. Wang, X. Shi, M. Cai, H. Feng, W. Xu and L. Li, *Biomaterials*, 2022, **284**, 121523.
- 240 L. Wang, B. Fu, D. Hou, Y. Lv, G. Yang, C. Li, J. Shen, B. Kong, L. Zheng, Y. Qiu, H. Wang, C. Liu, J. Zhang, S. Bai, L. Li, H. Wang and W. Xu, *Biomaterials*, 2023, **296**, 122060.
- 241 M. Sun, C. Wang, M. Lv, Z. Fan and J. Du, *J. Am. Chem. Soc.*, 2022, **144**, 7337–7345.
- 242 H. Wang, Z. Feng, Y. Qin, J. Wang and B. Xu, *Angew. Chem., Int. Ed.*, 2018, **57**, 4931–4935.
- 243 J. Deng, W. Wan, M. Wang, R. Sun, W. Jin, D. Shen, Q. Xia, Z. Zhang, X. Dong, X. Sun and Y. Liu, *Sens. Actuators, B*, 2024, **413**, 135891.
- 244 C. Wu, C. Wang, Y. Zheng, Y. Zheng, Z. Liu, K. Xu and W. Zhong, *Adv. Funct. Mater.*, 2021, **31**, 2104418.
- 245 Y. L. Fan, N. Y. Zhang, D. Y. Hou, Y. Hao, R. Zheng, J. Yang, Z. Fan, H. W. An and H. Wang, *Adv. Healthcare Mater.*, 2023, **12**, e2301162.
- 246 Y. Wang, H. Li, Q. Jin and J. Ji, *Chem. Commun.*, 2016, **52**, 582–585.
- 247 J. Song, C. Wu, Y. Zhao, M. Yang, Q. Yao and Y. Gao, *Small*, 2022, **18**, e2104772.
- 248 N. Chen, Z. Zhang, X. Liu, H. Wang, R. Guo, H. Wang, B. Hu, Y. Shi, P. Zhang, Z. Liu and Z. Yu, *J. Am. Chem. Soc.*, 2024, **146**, 10753–10766.
- 249 W. Ji, G. Liu, F. Wang, Z. Zhu and C. Feng, *Chem. Commun.*, 2016, **52**, 12574–12577.
- 250 W. Tan, Q. Zhang, M. C. Quiñones-Frías, A. Y. Hsu, Y. Zhang, A. Rodal, P. Hong, H. R. Luo and B. Xu, *J. Am. Chem. Soc.*, 2022, **144**, 6709–6713.
- 251 J. Fan, Y. Li, Z. Wei, Y. Fan, X. Li, Z. Chen, D. Hou, W. Xiao, M. Ding, H. Wang and L. Wang, *Nano Lett.*, 2021, **21**, 6202–6210.
- 252 S. Zhang and Y. Zhang, *ACS Appl. Mater. Interfaces*, 2020, **12**, 41105–41112.
- 253 S. Ruan, C. Hu, X. Tang, X. Cun, W. Xiao, K. Shi, Q. He and H. Gao, *ACS Nano*, 2016, **10**, 10086–10098.
- 254 E. Du, Y. Tang, Q. Zhang, Z. Song, Y. Tao and Y. Zhang, *Langmuir*, 2022, **38**, 4364–4370.
- 255 X. Liu, F. Tian, Z. Zhang, J. Liu, S. Wang, R. Guo, B. Hu, H. Wang, H. Zhu, A. Liu, L. Shi and Z. Yu, *J. Am. Chem. Soc.*, 2024, **146**, 24177–24187.
- 256 J. Li, D. Bullara, X. Du, H. He, S. Sofou, I. G. Kevrekidis, I. R. Epstein and B. Xu, *ACS Nano*, 2018, **12**, 3804–3815.
- 257 E. Muro, A. Fragola, T. Pons, N. Lequeux, A. Ioannou, P. Skourides and B. Dubertret, *Small*, 2012, **8**, 1029–1037.
- 258 W. Sun, J. Yin, L. Liu, Z. Wu, Y. Wang, T. Liu, H. Xiong, X. Liu, X. Wang and H. Jiang, *Anal. Chem.*, 2023, **95**, 14101–14110.
- 259 X. Liu, M. Li, J. Liu, Y. Song, B. Hu, C. Wu, A. Liu, H. Zhou, J. Long, L. Shi and Z. Yu, *J. Am. Chem. Soc.*, 2022, **144**, 9312–9323.
- 260 X. Lin, W. Li, Y. Wen, L. Su and X. Zhang, *Biomaterials*, 2022, **287**, 121603.
- 261 J. Zhou, X. Du, X. Chen, J. Wang, N. Zhou, D. Wu and B. Xu, *J. Am. Chem. Soc.*, 2018, **140**, 2301–2308.
- 262 C. Gao, Q. Wang, J. Li, C. H. T. Kwong, J. Wei, B. Xie, S. Lu, S. M. Y. Lee and R. Wang, *Sci. Adv.*, 2022, **8**, eabn1805.
- 263 R. C. Guo, N. Wang, W. Wang, Z. Zhang, W. Luo, Y. Wang, H. Du, Y. Xu, G. Li and Z. Yu, *Angew. Chem., Int. Ed.*, 2023, **62**, e202314578.
- 264 Y. Li, L. Hu, J. Wang and H. Wang, *Nano Lett.*, 2024, **24**, 10681–10690.
- 265 X. Peng, J. Hao, W. Tao, D. Guo, T. Liang, X. Hu, H. Xu, X. Fan and C. Chen, *J. Colloid Interface Sci.*, 2023, **640**, 498–509.
- 266 Y. M. Zhang, J. H. Liu, Q. Yu, X. Wen and Y. Liu, *Angew. Chem., Int. Ed.*, 2019, **58**, 10553–10557.
- 267 B. Xie, H. Zhao, Y. Ding, Z. Wang, Y. Wang, C. Gao and R. Wang, *J. Controlled Release*, 2023, **357**, 572–579.
- 268 P. Chandra Saha, R. S. Das, T. Chatterjee, M. Bhattacharyya and S. Guha, *Bioconjugate Chem.*, 2020, **31**, 1301–1306.
- 269 A. Hu, Y. Pu, N. Xu, Z. Cai, R. Sun, S. Fu, R. Jin, Y. Guo, H. Ai, Y. Nie and X. Shuai, *Theranostics*, 2023, **13**, 1454–1469.
- 270 J. Lin, C. Chien, C. Lin, B. Yao, Y. Chen, Y. Liu, Z. Fang, J. Chen, W. Chen, N. Lee, H. Chen and C. J. Hu, *Nat. Commun.*, 2019, **10**, 1057.
- 271 K. Morihito, H. Osumi, S. Morita, T. Hattori, M. Baba, N. Harada, R. Ohashi and A. Okamoto, *J. Am. Chem. Soc.*, 2023, **145**, 135–142.
- 272 J. Peng, Y. Xiao, Q. Yang, Q. Liu, Y. Chen, K. Shi, Y. Hao, R. Han and Z. Qian, *Acta Pharm. Sin. B*, 2021, **11**, 1069–1082.
- 273 X. Guo, M. Guo, R. Cai, M. Hu, L. Rao, W. Su, H. Liu, F. Gao, X. Zhang, J. Liu and C. Chen, *Sci. Adv.*, 2024, **10**, eadp3680.
- 274 Y. Xing, J. Yang, A. Peng, Y. Qian, Y. Liu, P. Pan and Q. Liu, *Adv. Mater.*, 2024, **36**, e2412730.
- 275 R. Wang, X. Li and J. Yoon, *ACS Appl. Mater. Interfaces*, 2021, **13**, 19543–19571.
- 276 X. Li, N. Kwon, T. Guo, Z. Liu and J. Yoon, *Angew. Chem., Int. Ed.*, 2018, **57**, 11522–11531.
- 277 Y. Zhao, X. Zhang, Z. Chen, Y. Xu, H. Kim, H. Jeong, Y. R. Lee, J. Lee, X. Li and J. Yoon, *Aggregate*, 2024, **5**, e514.
- 278 Y. Wang, W. Wu, D. Mao, C. Teh, B. Wang and B. Liu, *Adv. Funct. Mater.*, 2020, **30**, 2002431.
- 279 Y. C. Liu, G. J. Liu, W. Zhou, G. L. Feng, Q. Y. Ma, Y. Zhang and G. W. Xing, *Angew. Chem., Int. Ed.*, 2023, **62**, e202309786.
- 280 Y. Yang, Y. Hu, H. Du and H. Wang, *Chem. Commun.*, 2014, **50**, 7287–7290.
- 281 J. Shum, L. C. C. Lee, M. W. L. Chiang, Y. W. Lam and K. K. W. Lo, *Angew. Chem., Int. Ed.*, 2023, **62**, e202303931.
- 282 C. Wang, P. Zhao, D. Jiang, G. Yang, Y. Xue, Z. Tang, M. Zhang, H. Wang, X. Jiang, Y. Wu, Y. Liu, W. Zhang and W. Bu, *ACS Appl. Mater. Interfaces*, 2020, **12**, 5624–5632.



- 283 J. Yang, L. Wu, L. Wang, R. Ren, P. Chen, C. Qi, H. Feng and B. Z. Tang, *Aggregate*, 2024, **5**, e535.
- 284 M. Wang, H. Yi, Z. Zhan, Z. Feng, G. Yang, Y. Zheng and D. Zhang, *Aggregate*, 2024, **5**, e622.
- 285 T. Du, Z. Shi, X. Mou and Y. Zhu, *Colloids Surf., B*, 2024, **234**, 113706.
- 286 J. Chen, Y. Ma, W. Du, T. Dai, Y. Wang, W. Jiang, Y. Wan, Y. Wang, G. Liang and G. Wang, *Adv. Funct. Mater.*, 2020, **30**, 2001566.
- 287 N. Li, F. Shen, Z. Cai, W. Pan, Y. Yin, X. Deng, X. Zhang, J. O. Machuki, Y. Yu, D. Yang, Y. Yang, M. Guan and F. Gao, *Small*, 2020, **16**, e2005511.
- 288 W. Ye, H. Li, X. Li, X. Fan, Q. Jin and J. Ji, *Bioconjugate Chem.*, 2019, **30**, 1763–1772.
- 289 Y. Jiang, W. Zhao, H. Zhou, Q. Zhang and S. Zhang, *Langmuir*, 2022, **38**, 3755–3764.
- 290 N. Kang, S. Son, S. Min, H. Hong, C. Kim, J. An, J. S. Kim and H. Kang, *Chem. Soc. Rev.*, 2023, **52**, 3955–3972.
- 291 W. Kong, Q. Meng, R. M. Kong, Y. Zhao and F. Qu, *Adv. Healthcare Mater.*, 2024, **13**, e2402899.
- 292 M. T. Jeena, J. Link, J. Zhang, I. Harley, P. Turunen, R. Graf, M. Wagner, L. A. Baptista, H. R. A. Jonker, L. Cui, I. Lieberwirth, K. Landfester, J. Rao, D. Y. W. Ng and T. Weil, *Angew. Chem., Int. Ed.*, 2024, **63**, e202412477.
- 293 X. Zhang, B. Zhang, Y. Zhang, Y. Ding, Z. Zhang, Q. Liu, Z. Yang, L. Wang and J. Gao, *Angew. Chem., Int. Ed.*, 2024, **63**, e202406602.
- 294 B. Wang, C. Li, D. He, K. Ding, Q. Tian, G. Feng, A. Qin and B. Z. Tang, *Small*, 2024, **20**, e2307309.
- 295 H. Wang, D. Jiao, D. Feng, Q. Liu, Y. Huang, J. Hou, D. Ding and W. Zhang, *Adv. Mater.*, 2024, **36**, e2311733.
- 296 W. Wang, R. Zhang, L. Zhang, L. Hao, X. Cai, Q. Wu, Z. Qiu, R. Han, J. Feng, S. Wang, P. Alam, G. Zhang, Z. Zhao and B. Z. Tang, *Nat. Commun.*, 2024, **15**, 9999.
- 297 X. Wu, T. Zhuang, M. Liu, X. Sun, L. Zhu, Q. Zhang, J. Han, L. Wang and R. Guo, *Org. Chem. Front.*, 2024, **11**, 6055–6063.
- 298 Z. Zhang, B. Xie, X. Lu, L. Xiong, X. Li, Y. Zhang, C. Li and C. Wang, *Nanoscale*, 2024, **16**, 903–912.
- 299 M. Rong, J. Liu and L. Lu, *Adv. Healthcare Mater.*, 2024, **13**, e2400325.
- 300 X. Luo, Q. Jiao, S. Pei, S. Zhou, Y. Zheng, W. Shao, K. Xu and W. Zhong, *Adv. Healthcare Mater.*, 2024, **13**, e2401787.
- 301 Y. Li, R. Tian, H. Shi, J. Xu, T. Wang and J. Liu, *Aggregate*, 2023, **4**, e317.
- 302 Q. Xu, Y. Ma, Y. Sun, D. Li, X. Zhang and C. Liu, *Aggregate*, 2023, **4**, e333.
- 303 W. Li, Y. Zhou, S. He, T. Tong, C. Wang, P. Shi, S. Li, X. Wang, L. Yang, X. Cao and Z. Tian, *Aggregate*, 2024, **5**, e496.
- 304 Z. Haidar, *Biofunct. Mater.*, 2023, **1**, 3.
- 305 B. Lin, A. Hung, W. Singleton, K. K. Darmawan, R. Moses, B. Yao, H. Wu, A. Barlow, M. Sani, A. J. Sloan, M. A. Hossain, J. D. Wade, Y. Hong, N. M. O'Brien-Simpson and W. Li, *Aggregate*, 2023, **4**, e329.

